Stratigraphy and geochemistry of the 1745–1700 Ma Peter Pan Supersuite

Claire E Wade and Stacey O McAvaney

Report Book
2016/00026

SOUTH AUSTRALIA

Government of South Australia
Department of State Development

Stratigraphy and geochemistry of the 1745–1700 Ma Peter Pan Supersuite

Claire E Wade and Stacey O McAvaney

**Geological Survey of South Australia,
Resources and Energy Group, DSD**

March 2017

Report Book 2016/00026

Resources and Energy
Department of State Development
Level 7, 101 Grenfell Street, Adelaide
GPO Box 320, Adelaide SA 5001
Phone +61 8 8463 3037
Email dsd.minerals@sa.gov.au
www.minerals.statedevelopment.sa.gov.au

South Australian Resources Information Geoserver (SARIG)
SARIG provides up-to-date views of mineral, petroleum and geothermal tenements and other geoscientific data. You can search, view and download information relating to minerals and mining in South Australia including tenement details, mines and mineral deposits, geological and geophysical data, publications and reports (including company reports).
www.statedevelopment.sa.gov.au/sarig

Preferred way to cite this publication
Wade CE and McAvaney SO 2017. *Stratigraphy and geochemistry of the 1745–1700 Ma Peter Pan Supersuite*, Report Book 2016/00026. Department of State Development, South Australia, Adelaide.

CONTENTS

TABLES

FIGURES

Stratigraphy and geochemistry of the 1745–1700 Ma Peter Pan Supersuite

Claire E Wade and Stacey O McAvaney

ABSTRACT

During the period 1745–1700 Ma felsic and mafic rocks were intruded throughout the Gawler Craton broadly coeval with the 1740–1690 Ma Kimban Orogeny. These rocks were previously considered part of the Lincoln Complex, a stratigraphic term defined by Thomson (1980) to describe the igneous rocks intruding the Archean to Paleoproterozoic basement of the Eyre Peninsula during the later Paleoproterozoic. However, this term is now in disuse due to the fact that more recent U-Pb geochronology has revealed that units included within the Lincoln Complex range in age from the Mesoarchaean to the Paleoproterozoic, and the term thus groups together units which are not genetically related. The term Peter Pan Supersuite has been defined to describe those parts of the Lincoln Complex which are synchronous with the Kimban Orogeny. The supersuite contains three suites: the Moola Suite (1745–1735 Ma), the Pinbong Suite (1735–1700 Ma) and the Moody Suite (1720–1700 Ma).

The Moola Suite is best exposed on north-eastern Eyre Peninsula, but also occurs in the eastern Gawler Craton beneath the Stuart Shelf, the Peake and Denison Inliers and Yoolperlunna Inlier in the northern Gawler Craton, and the Fowler Domain in the western Gawler Craton. It contains unfoliated to weakly foliated mica-poor granites as well as diorite, dolerite and amphibolite. Granites of the Moola Suite are classified as magnesian, alkalic to calc-alkalic and metaluminous, and represent melts of heterogeneous crustal source regions, demonstrated by broad Sm-Nd isotopic signatures ($\varepsilon_{Nd(1740\ Ma)}$ = -17.1 to -2.4). The mafic rocks of the Moola Suite consist of two geochemical groups: a tholeiitic and LREE-depleted group and a calc-alkaline, LREE-enriched group. The depleted, tholeiitic mafic rocks are characterised by low $[La/Yb]_N$ ratios (1.4–3.6) and juvenile Sm-Nd signatures ($\varepsilon_{Nd(1740\ Ma)}$ = -1.2 to 0.4). In contrast, the enriched, calc-alkaline mafic rocks are characterised by high $[La/Yb]_N$ ratios (10.8–66.4) and evolved Sm-Nd signatures ($\varepsilon_{Nd(1740\ Ma)}$ = ~-8.8).

The Pinbong Suite is the most widespread suite in the Peter Pan Supersuite, occurring on central and southern Eyre Peninsula in the southern Gawler Craton, the Olympic Domain in the eastern Gawler Craton, Coober Pedy Ridge in the northern Gawler Craton and in the central Gawler Craton. It includes foliated to migmatitic biotite-rich granites, dolerites and gabbros. Granitic rocks are mostly peraluminous or metaluminous and largely magnesian and alkali-calcic, while the gabbroic rocks are metaluminous and enriched in alkalis. Pinbong Suite granites have $\varepsilon_{Nd(1730\ Ma)}$ values that range from -11.7 to -4.3. Two geochemical groups are also observed in the Pinbong Suite gabbros: tholeiitic and LREE-depleted ($[La/Yb]_N$ = 3–8) and calc-akaline, LREE-enriched ($[La/Yb]_N$ = 12.9–36.2). Less distinction, however, is observed in the Sm-Nd composition, with the tholeiitic and LREE-depleted gabbros displaying slightly more evolved Nd signatures ($\varepsilon_{Nd(1730\ Ma)}$ = -5.3 and -4.6) than the calc-akaline, LREE-enriched gabbros ($\varepsilon_{Nd(1730\ Ma)}$ = -3.8 and -3.4). Isotopic signatures of the Pinbong Suite gabbros suggest an enriched mantle source region.

Comparable geochemical characteristics of the Moola Suite and the Pinbong Suite suggest similar crustal and mantle source regions were melting during their genesis. Signatures for the Moola and Pinbong Suite granites are consistent with granites generated in orogenic settings from a lower- to mid-crustal c. 2565–2410 Ma Sleaford Complex or c. 3150 Ma Cooyerdoo Granite source region. The geochemical characteristics of the mafic rocks of the Peter Pan Supersuite are indicative of extensional-related melting events by lithospheric extension or thinning. The mafic rocks represent a heterogeneous mantle source region

that comprises an older, enriched lithospheric mantle reservoir, enriched in incompatible elements and relatively depleted in compatible elements, and a younger, juvenile mantle.

The Moody Suite is restricted to the Tumby Bay area on central-eastern Eyre Peninsula, and includes unfoliated leucogranite, monzogranite and monzonite which commonly contains metasedimentary xenoliths derived from the Paleoproterozoic Hutchison Group country rock. The Moody Suite intrusives are ferroan, calc-alkalic to alkali-calcic and peraluminous, and has moderately evolved Sm-Nd isotopic signatures ($\varepsilon_{Nd(1700\ Ma)}$ = -10.2 to -4.5), consistent with derivation from the Hutchison Group. The geochemical signature of the Moody Suite is typical of A-type post-orogenic granites derived from continental crust or underplated crust that has been through a cycle of continent-continent collision.

INTRODUCTION

Early frameworks of the stratigraphy of the southern Gawler Craton recognised an Archean to Paleoproterozoic basement, comprising the Sleaford Complex and Hutchison Group, which was intruded by a series of magmatic rocks known as the Lincoln Complex during a younger Paleoproterozoic tectonothermal event, the Kimban Orogeny (Thomson, 1980, Parker *et al.*, 1985). Thus, deformed intrusive igneous rocks in the southern Gawler Craton were either mapped as part of the Archean Sleaford Complex or Paleoproterozoic Lincoln Complex, with the division into these two units assisted in part by Rb-Sr isotopic data (Webb *et al.*, 1986). The Lincoln Complex comprised a number of suites and intrusions spanning the time period c. 1850–1690 Ma, including the Donington Suite, Colbert Granite, Moody Suite, Wertigo Granite, Middle Camp Granite Carappee Granite, Minbrie Gneiss, Carpa Granite, Tournefort Dykes and Coolanie Gneiss (Parker, 1993).

However, subsequent U-Pb zircon geochronology has redefined the duration of the Kimban Orogeny to 1730–1690 Ma (Hoek and Schaefer, 1998), and has shown that the Lincoln Complex encompasses a number of units outside of this time period unrelated to the Kimban Orogeny, ranging from Mesoarchaean to Paleoproterozoic (Fraser *et al.*, 2010, Fraser and Neumann, 2010, McAvaney *et al.*, 2016a). Therefore, it is necessary to discontinue use of the term Lincoln Complex, and a new stratigraphic nomenclature is being developed for the rocks which were formerly part of the Lincoln Complex (Cowley *et al.*, 2017). These include the c. 3150 Ma Cooyerdoo Granite (Fraser *et al.*, 2010, McAvaney, 2012), the c. 2820 Ma Coolanie Gneiss (Fraser and Neumann, 2010), the c. 2520 Ma Carpa Granite (Fraser and Neumann, 2010, Wade and McAvaney, 2017), the c. 2520–2420 Ma Minbrie Gneiss (Fraser and Neumann, 2010), the c. 1850 Ma Donington Suite (Hoek and Schaefer, 1998, Reid *et al.*, 2008a), the c. 1790–1770 Ma Wertigo Granite and the c. 1775 Ma Tip Top Granite (McAvaney *et al.*, 2016a).

The new term Peter Pan Supersuite has been created to comprise the igneous rocks which intruded broadly synchronous with the 1740–1690 Ma Kimban Orogeny. This report contains a description of the age range, distribution, lithologies and stratigraphy of the Peter Pan Supersuite. It also presents new whole rock geochemical and Sm-Nd isotopic data for the supersuite, and characterises its geochemical signatures to provide constraints on the melting source region. A formal stratigraphic definition of the Peter Pan Supersuite and its subunits is provided in Appendix I.

GEOLOGICAL SETTING

The Gawler Craton, South Australia (Fig. 1), comprises a Mesoarchaean and Neoarchaean to earliest Paleoproterozoic basement overlain and intruded by Paleoproterozoic to Mesoproterozoic volcanosedimentary basins and igneous suites (Hand *et al.*, 2007, Reid and Hand, 2012).

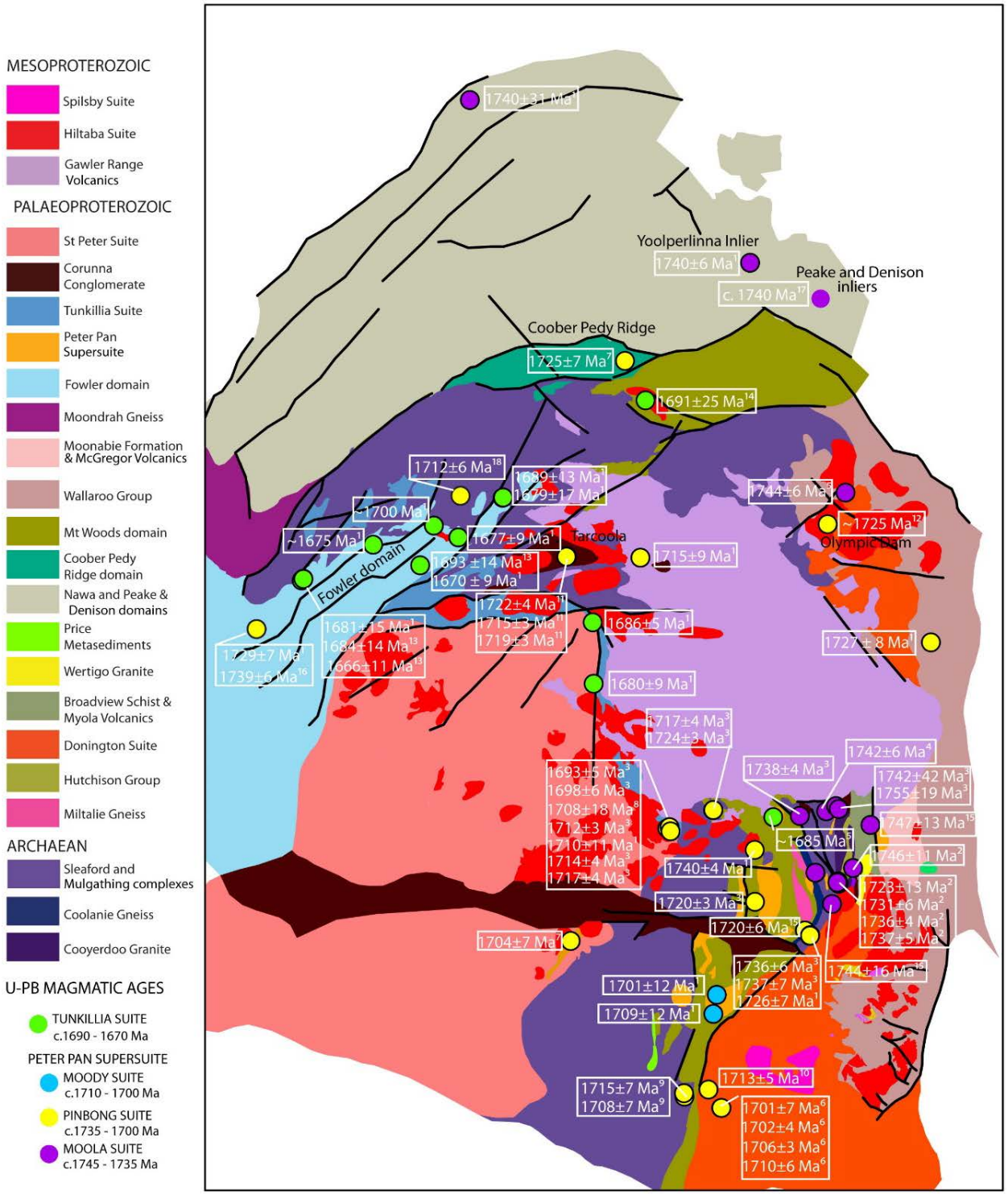

Figure 1. Interpreted solid geology of the Gawler Craton, showing magmatic ages of the Peter Pan Supersuite and post-orogenic Tunkillia Suite. Age data derived from [1]Fanning *et al.* (2007), [2] Reid and Jagodzinski (2011), [3]Fraser and Neumann (2010), [4]McAvaney and Jagodzinski (2012), [5]Reid and Jagodzinski (2012), [6]Reid *et al.* (2007), [7]Jagodzinski *et al.* (2007), [8]Fraser *et al.* (2007), [9]Fanning (1997), [10]Jagodzinski *et al.* (2006), [11]Budd (2006), [12]Reid (2007), [13]Teasdale (1997), [14]Finlay (1993), [15]Jagodzinski and McAvaney (2017), [16]Reid (2015), Hopper [17](2001) and [18]Dawson (2016).

The oldest exposed basement of the Gawler Craton is the c. 3150 Ma Cooyerdoo Granite, which is the product of melting of an older (c. 3400 Ma) tonalite-trondhjemite-granodiorite crust (Fraser *et al.*, 2010). The Cooyerdoo Granite is exposed only on northeastern Eyre Peninsula, but inherited zircons and Nd isotope values of younger igneous units indicate that it extends in the mid to lower crust to the central part of the Gawler Craton (Fraser *et al.*, 2010, McAvaney, 2012). The next event recorded in the Gawler Craton is the intrusion of the protolith of the c. 2820 Ma Coolanie Gneiss, an S-type granite which occurs on northeastern Eyre Peninsula (Fraser and Neumann, 2010).

Overlying and intruding this Mesoarchaean basement are deformed and metamorphosed rocks of the Sleaford and Mulgathing complexes, in the southern and northern Gawler Craton respectively. These comprise felsic and ultramafic volcanics, sedimentary rocks and felsic and mafic intrusive rocks spanning the interval 2560–2475 Ma, metamorphosed from greenschist to granulite facies and intruded by syn-orogenic intrusives during the c. 2475–2410 Ma Sleafordian Orogeny (Daly and Fanning, 1993, Swain *et al.*, 2005b, McFarlane, 2006, Reid *et al.*, 2014, Halpin and Reid, 2016).

No geological activity was recorded in the Gawler Craton following the Sleafordian Orogeny until c. 2000 Ma, when the igneous precursor to the Miltalie Gneiss was emplaced (Fanning *et al.*, 2007). The intrusion of this granite heralds the beginning of prolonged basin formation and growth over the period c. 2000 to 1740 Ma, wherein large, lithologically complex shallow marine to continental basins were formed across the entire Gawler Craton (Cowley *et al.*, 2003, Payne *et al.*, 2006, Szpunar and Fraser, 2010, Szpunar *et al.*, 2011, Jagodzinski *et al.*, 2012, Lane *et al.*, 2015). Deposition during this phase of basin development was punctuated by the c. 1850 Ma Cornian Orogeny, comprising localised deformation and metamorphism and the emplacement of the Donington Suite along the eastern margin of the craton (Reid *et al.*, 2008a).

Sedimentation was terminated by the Kimban Orogeny (1740–1690 Ma), a major orogenic episode that affected the majority of the Gawler Craton (Parker, 1993, Dutch *et al.*, 2008). It resulted in greenschist to granulite facies metamorphism and high strain deformation largely partitioned into regional-scale transpressional belts, including the Kalinjala Mylonite Zone (Parker, 1980, Vassallo and Wilson, 2002). Widespread felsic and mafic magmatism of the Peter Pan Supersuite also accompanied deformation of the Kimban Orogeny (Hand *et al.*, 2007). Post-orogenic granite intrusions are represented by the c.1690–1670 Ma Tunkillia Suite (Payne *et al.*, 2010). The Kimban Orogeny and accompanying magmatism was synchronous with localised sedimentation in the Fowler Domain in the western Gawler Craton (c. 1740–1720 Ma; Howard *et al.*, 2011a) as well as clastic and bimodal volcanics of the Labyrinth Formation in the central Gawler Craton (c. 1715 Ma; Howard *et al.*, 2011b).

During the latest Paleoproterozoic (c. 1680–1640 Ma) localised sedimentation is recorded in the Gawler Craton. This includes fluvial and alluvial sediments of the Corunna Conglomerate on Eyre Peninsula (c. 1680 Ma; McAvaney and Reid, 2008), and sandstone, shale, dolomite and dacitic to andesitic volcanoclastic rocks of the c. 1655 Ma Tarcoola Formation in the central Gawler Craton (Daly, 1993). This was followed by an extended period of magmatism and volcanism from 1645–1570 Ma. In the southwestern part of the craton the felsic Nuyts Volcanics were extruded at c. 1630 Ma (Rankin *et al.*, 1990), temporally overlapping with felsic to mafic, juvenile intrusive rocks of the c. 1645–1610 Ma St Peter Suite (Swain *et al.*, 2008, Chalmers, 2009, Symington *et al.*, 2014, Reid *et al.*, 2016). This was followed by continued felsic volcanism in the central part of the craton, producing the c. 1595–1585 Ma Gawler Range Volcanics (Allen *et al.*, 2008, Jagodzinski *et al.*, 2016). The volcanics are comagmatic with high-temperature fractionated felsic and minor mafic intrusives of the c. 1595–1575 Ma Hiltaba Suite (Stewart and Foden, 2003).

Synchronous with extrusion of the Gawler Range Volcanics in the central part of the craton, deformation and metamorphism occurred in the northern and eastern parts of the craton during the c. 1600–1570 Ma Kararan Orogeny. This included amphibolite to granulite facies metamorphism in the Mount Woods Domain, Coober Pedy Ridge and Mabel Creek Ridge in the northern Gawler Craton (Hand *et al.*, 2007) and greenschist to lower amphibolite facies metamorphism on Yorke Peninsula in the eastern Gawler Craton (Conor, 1995). Deformation in the central Gawler Craton

was partitioned into shear zones, including the east-west-trending Yerda Shear Zone and north-south-trending Yarlbrinda Shear Zone in the central Gawler Craton (Stewart, 2010), and the northeast-southwest-trending Bulgunnia Shear Zone along the southern margin of the Mount Woods Domain (Fraser and Lyons, 2006).

At c. 1560 Ma granulite facies metamorphism is recorded in the Nundroo block of the Fowler Domain and may be linked with the reactivation of the shear zones (Fanning *et al.*, 2007, Jagodzinski and McAvaney, 2017). Minor localised magmatism also occurred at c. 1555–1530 Ma in the Peake and Denison inliers in the northern Gawler Craton and intrusion of the Spilsby Suite in the southern Gawler Craton (Fanning *et al.*, 2007). The youngest event recorded in the Gawler Craton consists of the reactivation of shear zones between c. 1470 and 1450 Ma at greenschist to amphibolite facies in the western Gawler Craton (Fraser and Lyons, 2006).

STRATIGRAPHY AND AGE RANGE OF THE PETER PAN SUPERSUITE

The Peter Pan Supersuite comprises felsic and lesser mafic intrusive rocks which were intruded during the Kimban Orogeny, a major tectonic event which affected the majority of the Gawler Craton, but excluding its eastern margin (Reid and Fabris, 2015). Although originally considered to span the time interval 1730–1690 Ma (Hoek and Schaefer, 1998), more recent data indicates that metamorphism during the Kimban Orogeny commenced at c. 1740 Ma (Fig. 2a). The Peter Pan Supersuite spans the entire length of the orogenic cycle, with the earliest magmatism commencing prior to metamorphism, and both magmatism and metamorphism were continuous throughout this period.

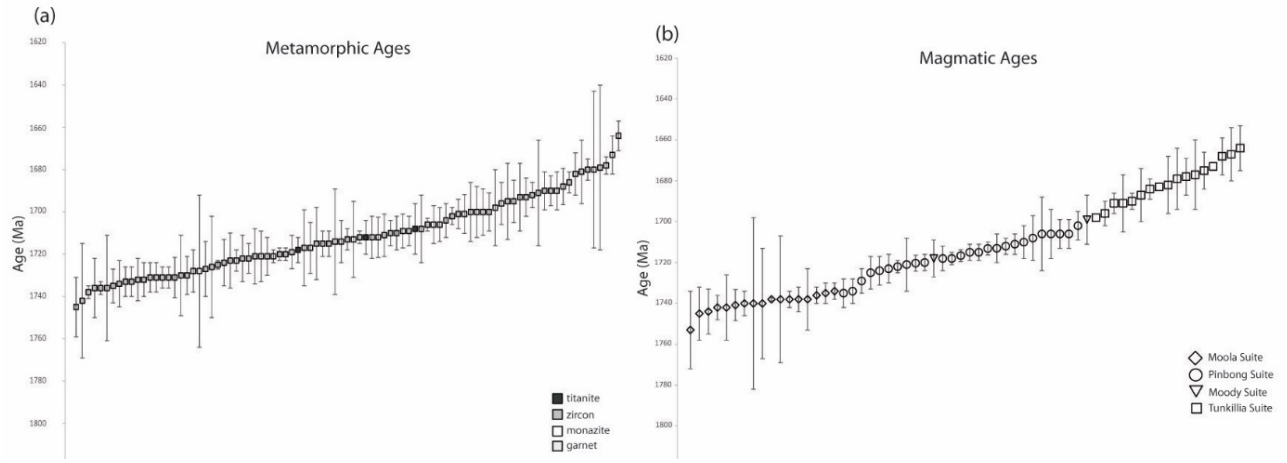

Figure 2. (a) Ages of metamorphism during the Kimban Orogeny and (b) ages of magmatism of the Peter Pan Supersuite (syn-orogenic) and Tunkillia Suite (post-orogenic). Age data derived from Budd (2006), Dutch *et al.* (2008), Dutch (2009), Fanning (1997), Fanning *et al.* (1988), Fanning *et al.* (2007), Finlay (1993), Fraser and Neumann (2010), Fraser *et al.* (2007), Fraser *et al.* (2012), Hopper (2001), Howard *et al.* (2011a), Howard *et al.* (2011b), Jagodzinski and Reid (2010), Jagodzinski *et al.* (2006), Jagodzinski *et al.* (2007), Jagodzinski *et al.* (2012), Jagodzinski and McAvaney (2017), Lane (2011), Lane *et al.* (2015), McAvaney and Jagodzinski (2012), Mortimer *et al.* (1988), Payne *et al.* (2008), Reid and Jagodzinski (2011), Reid and Jagodzinski (2012), Reid (2007), Reid *et al.* (2007), Swain *et al.* (2005a),Teasdale (1997).

Although the effects of high temperature metamorphism are recorded by zircon growth throughout the craton, the structural architecture of the Kimban Orogeny is best understood in the southern Gawler Craton where the Archean to Paleoproterozoic basement rocks deformed during the orogen are well-exposed. The earliest structures are tight to isoclinal folds originally shallowly inclined to recumbent and overturned to the west, with axial planar fabrics and elongation

lineations parallel to fold hinges formed at upper amphibolite to granulite facies (Parker, 1993). These tight to isoclinal folds are overprinted by major north-south-trending open to tight upright folds with a highly variable plunge (Parker, 1993). Metamorphic grade during open folding was retrograde, corresponding to the greenschist-amphibolite facies boundary. A schistosity axial planar to open folding is poorly developed to absent.

High strain was partitioned into a system of north- northeast- and northwest-trending transpressional mylonite zones contemporaneous both with the tight and open folding events (Parker, 1993). These mylonite zones have accommodated a component of vertical and lateral uplift, juxtaposing fault-bound blocks of varying lithostratigraphy and metamorphic grade. The most significant of these structures on Eyre Peninsula is the Kalinjala Shear Zone, a northeast-trending subvertical high strain shear zone between 4 and 6 km wide which extends for approximately 200 km along the eastern coast of Eyre Peninsula from Sleaford Bay along to Port Neill (Parker, 1980; Vassallo and Wilson, 2002). This shear zone juxtaposes the c. 1850 Ma Donington Suite on the east against the c. 2565–2410 Ma Sleaford Complex and c. 1790 Ma Hutchison Group on the west (Schwarz, 2003), and is interpreted to have accommodated c. 300 km of lateral movement (Hand *et al.*, 1995).

Magmatism of the Peter Pan Supersuite during the Kimban Orogeny is broadly distributed throughout the entire Gawler Craton (Fig. 1). The supersuite has been divided into three suites (Table 1), largely defined by mineralogy, geochronology and spatial distribution. The Moola Suite (1745–1735 Ma) comprises unfoliated to weakly foliated mica-poor granites, as well as minor diorite, dolerite and amphibolite, and is largely restricted to the eastern and western margins of the Gawler Craton (Fig. 1). The Pinbong Suite (1735–1700 Ma) comprises foliated to migmatitic mica-rich granites, as well as minor dolerite and gabbro, and occurred throughout the central part of the Gawler Craton (Fig. 1). The Moody Suite (1710–1700 Ma), an existing stratigraphic term defined by Schwarz (1999), comprises unfoliated leucogranite, monzogranite and monzonite, and is restricted to central-eastern Eyre Peninsula (Fig. 1). Some occurrences of the Peter Pan Supersuite without geochronology or detailed mineralogy remain undifferentiated into the suites.

Following intrusion of the Peter Pan Supersuite and the Kimban Orogeny, the post-orogenic Tunkillia Suite intruded in the western and central Gawler Craton (Fig. 1). A formal definition of the Peter Pan Supersuite and its subdivisions is provided in Appendix I.

MOOLA SUITE (1745–1735 Ma)

The Moola Suite occurs extensively across the Gawler Craton, on northeastern Eyre Peninsula in the southern Gawler Craton, the Olympic Domain in the eastern Gawler Craton, the Peake and Denison Inliers and Yoolperlunna Inlier in the northern Gawler Craton, and the Fowler Domain in the western Gawler Craton (Fig. 1). The suite is dominated by undeformed to weakly foliated granites, but also includes hornblende-bearing syenite, garnet-bearing leucogneiss, diorite, dolerite and amphibolite. The Moola Suite includes the Burkitt Granite, Wortham Granite, Gluepot Granite, Deuter Diorite and Wade Amphibolite (Table 1).

Outcrops of the Moola Suite are largely limited to northeastern Eyre Peninsula (Fig. 3), where the Burkitt Granite, Wortham Granite, Gluepot Granite and Wade Amphibolite are exposed. Notable outcrops of unnamed granite, dolerite and amphibolite belonging to the Moola Suite also occur on Eyre Peninsula west of Lake Gilles (Fraser and Neumann, 2010), at Refuge Rocks (Fanning *et al.*, 2007) and west of Iron Duke (Goodwin, 2010, Reid and Jagodzinski, 2011). The Deuter Diorite is intersected in drillhole LED001 east of Lake Gilles, and unnamed granites are intersected in drillhole at the Moola Prospect (Reid and Jagodzinski, 2011). In the eastern Gawler Craton an unnamed granite of the Moola Suite is intersected at the Vulcan Prospect (Reid and Jagodzinski, 2012). In the northern Gawler Craton a 1733 ± 13 Ma trondhjemite/tonalite cropping out at Lagoon Hills in the Peake and Denison inliers is assigned to the Moola Suite (Hopper, 2001), as well as a granite gneiss with a poorly constrained protolith age of 1740 ± 31 Ma in the Yoolperlunna Inlier. Intrusion of the Moola Suite is contemporaneous with c. 1745 Ma felsic volcanism and deposition

of clastic and iron-rich sediments at Spring Hill in the Peake and Denison inliers (Fanning *et al.*, 2007).

Table 1. Stratigraphy of the Peter Pan Supersuite.

Name			**Map symbol**	**Age** (Ma)
Supersuite	*Suite*	*Formation*		
Peter Pan Supersuite			Lz	c. 1745–1700
		undifferentiated felsic intrusives	Lz_{11}	—
		undifferentiated mafic intrusives	Lz_{12}	—
	Moola Suite		Lzm	c. 1745–1730
		Burkitt Granite	Lzmb	c. 1750
		Wortham Granite	Lzmw	c. 1745
		Gluepot Granite	Lzmg	c. 1740
		Deuter Diorite	Lzmd	c. 1740
		Wade Amphibolite	Lzma	c. 1735
	Pinbong Suite		Lzp	c. 1735–1700
		Middle Camp Granite	Lzpm	c. 1735–1725
		Carappee Granite	Lzpc	c. 1720
		Colona Gabbro	Lzpo	c. 1735
		Paxton Granite	Lzpp	c. 1720
		unnamed gabbro, metagabbro and dolerite	Lzp_1	c. 1725–1710
		unnamed cream-pink muscovite granite	Lzp_2	—
	Moody Suite		Lzo	c. 1720–1700
		Chinmina Monzonite	Lzoh	c. 1700
		Moreenia Monzogranite	Lzom	c. 1720
		Uranno Microgranite	Lzou	—
		Yunta Well Leucogranite	Lzoy	—

Burkitt Granite (c. 1745 Ma)

The Burkitt Granite is exposed on Corunna Station on northeastern Eyre Peninsula (Fig. 3), occurring as low hills, tors (Fig. 4a) and scattered small outcrops over an area of about 12 km in north-south direction and about 5 km in east-west direction. In the subsurface the Burkitt Granite extends c. 14 km to the south, evident in TMI imagery, and is intersected in diamond drillhole RDD002 (drillhole 229989) over the depth interval 15–481 m (Fig. 3).

The Burkitt Granite is a K-feldspar-quartz-plagioclase-hornblende-magnetite granite. Lath-shaped K-feldspar phenocrysts are up to 25 mm in length, and sit within an equigranular groundmass of medium- to coarse-grained K-feldspar, quartz and plagioclase, with hornblende and magnetite, and accessory sphene, monazite and zircon (Fig. 3b). The pluton is largely unfoliated, but locally contains a magmatic foliation orientated north-northwest, defined by the alignment of K-feldspar phenocrysts.

The Burkitt Granite is interpreted to intrude an Archean to earliest Paleoproterozoic basement comprising the Cooyerdoo Granite and Sleaford Complex, and is unconformably overlain by the c. 1680 Ma Corunna Conglomerate. The magmatic age of the Burkitt Granite is poorly constrained as zircons within the granite are metamict, due to its high U content (up to 60 ppm; Appendix I). Magmatic crystallisation ages for the Burkitt Granite include 1755 ± 19 Ma and 1742 ± 42 Ma (Fraser and Neumann, 2010).

Wortham Granite (c. 1745 Ma)

The Wortham Granite is exposed as low outcrops and subcrops in the vicinity of Wortham Dam on Roopena Station, north-eastern Eyre Peninsula (Fig. 3). In the subsurface the Wortham Granite may be defined by a magnetic high trending north-northwest ~750 m wide and with a linear extent of ~8 km, along the eastern side of the Roopena Fault. The Wortham Granite is a weakly foliated, orange-pink, medium-grained, equigranular granite (Fig. 4c) composed K-feldspar and quartz with

minor plagioclase and biotite and trace amounts of tourmaline, opaques and zircon (McAvaney *et al.*, 2016b). The gneissic fabric is defined by alternating quartz- and feldspar-rich layers and quartz ribbons. No contact relationships are observed for the Wortham Granite, but it is inferred to intrude the c. 1790 Ma Broadview Schist which crops out in close proximity to the granite. U-Pb SHRIMP dating of zircon from the Wortham Granite yielded a magmatic crystallisation age of 1747 ± 13 Ma (Jagodzinski and McAvaney, 2017).

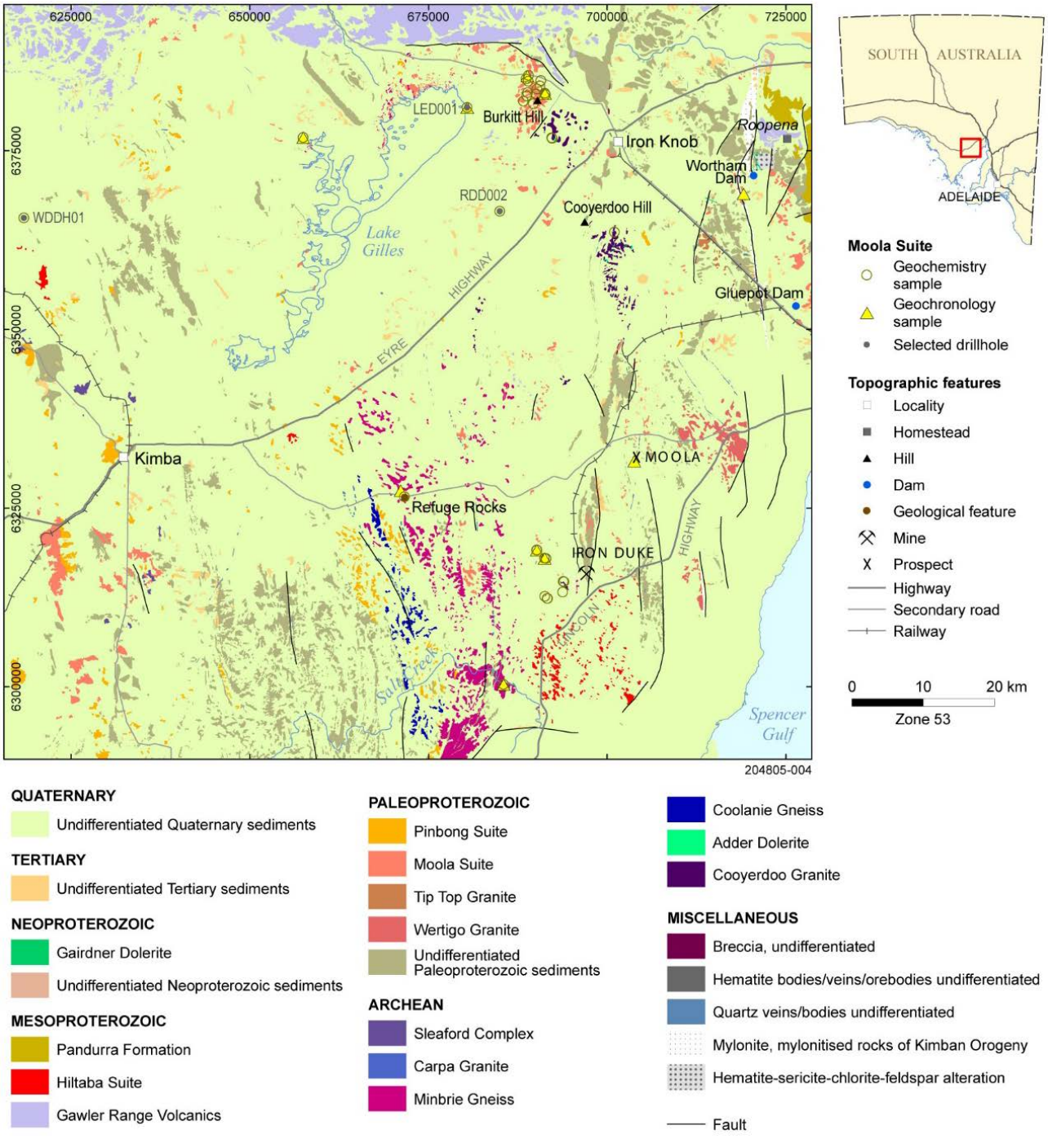

Figure 3. Distribution of the Moola Suite on north-eastern Eyre Peninsula, location of geochemistry samples presented in this report, and location of dated samples of the Moola Suite.

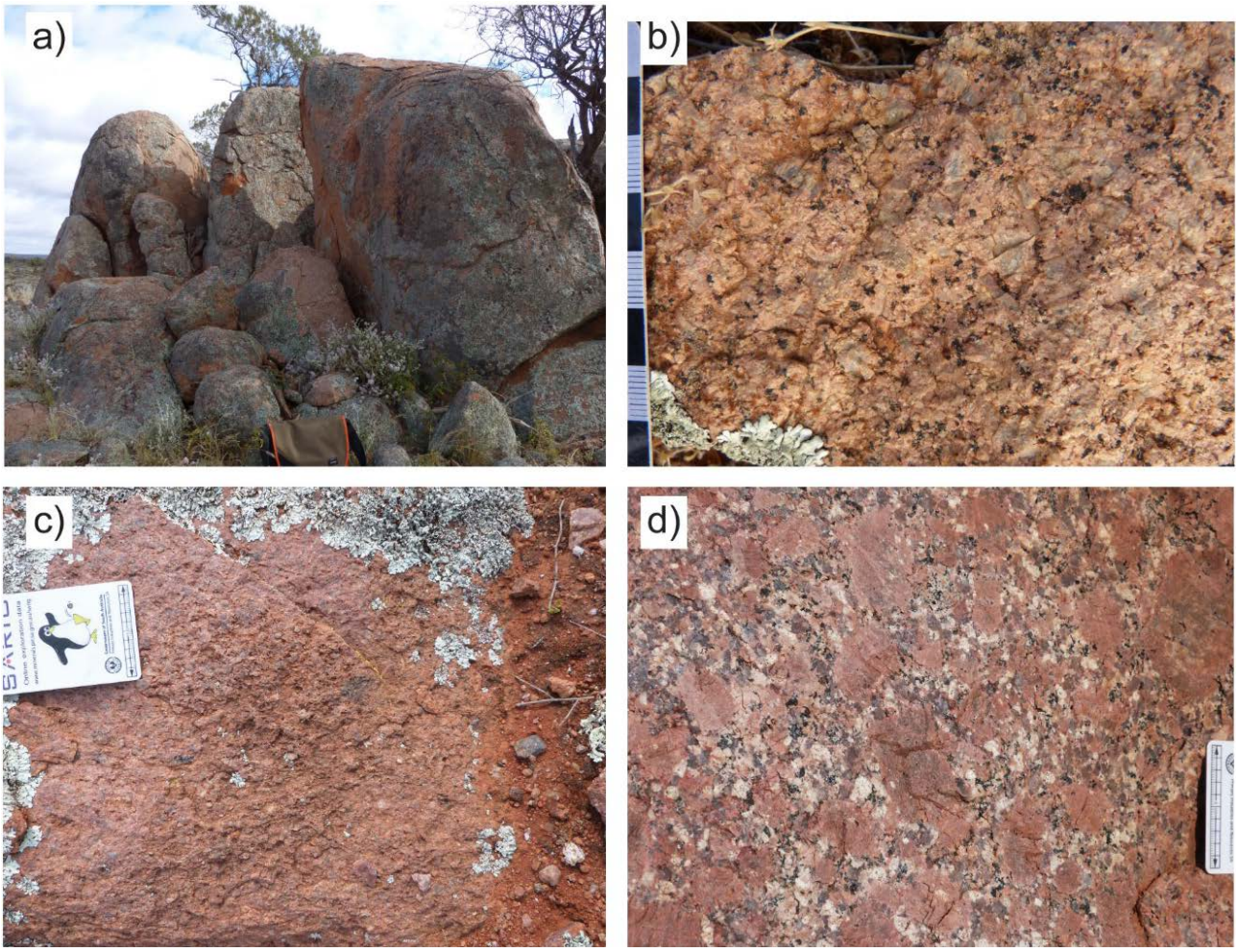

Figure 4. **Felsic units of the Moola Suite. (a)** Granite tors of the Burkitt Granite, Burkitt Hill (site 1906545). **(b)** Porphyritic K-feldspar-quartz-plagioclase-hornblende-biotite Burkitt Granite (site 1906545). **(c)** K-feldspar-quartz Wortham Granite (site 1906198). **(d)** K-feldspar megacrysts in porphyrtic Glue Pot Granite (site 1993614).

Gluepot Granite (c. 1740 Ma)

The Gluepot Granite is a north-northwest-trending pluton approximately 25 km long and up to 8 km wide, extending from Angle Dam near Roopena Homestead in the north to Wild Dog Hill near Whyalla in the south, on Roopena Station, north-eastern Eyre Peninsula (Fig. 3). The Gluepot Granite is poorly exposed and dominated by subcrop and saprolitic

granite, with isolated platform exposures and rare granite hills and tors. It is a heterogeneous granite comprising coarse-grained porphyritic granite, medium-grained equigranular granite, and late stage pegmatite and aplite phases (McAvaney *et al.*, 2016b). The pluton is dominated by the coarse-grained porphyritic phase (Fig. 4d) composed of large pink tabular to rounded K-feldspar phenocrysts up to 60 mm in diameter, often with Rapakivi rims, in a groundmass of medium- to coarse-grained plagioclase and potassium feldspar, subround quartz, biotite, and minor tourmaline. Locally it displays a tectonic fabric defined by aligned ovoid quartz crystals.

Pegmatitic and aplitic phases of the Gluepot Granite are observed to intrude the c. 1755 Ma Moonabie Formation along its eastern margin. The Gluepot Granite yielded a CA-TIMS age of 1740 ± 0.6 Ma (McAvaney *et al.*, 2017); prior to this dating, it was interpreted as Hiltaba Suite. A quartz-phyric rhyolite plug intruding the Moonabie Formation at SE Mount Whyalla is interpreted to be genetically related to the Gluepot Granite and has a magmatic age of 1752 ± 10 Ma (Fraser and Neumann, 2010).

Deuter Diorite (c. 1740 Ma)

The Deuter Diorite does not crop out, but is intersected in drillhole DDH LED001 (drill hole number 229988), at the northeastern margin of Lake Gilles (Fig. 3). It comprises an elliptical magnetic pluton which can be traced on magnetic imagery spanning 9 x 2.5 km orientated in a north-south direction. The Deuter Diorite (Fig. 5b) is medium- to coarse-grained and composed of plagioclase and hornblende crystals in a groundmass of biotite, pyroxene, K-feldspar and minor quartz with trace titanite, magnetite, apatite and zircon (McAvaney and Jagodzinski, 2012).

In DDH LED001 the Deuter Diorite contains xenoliths of amphibolite schist at 83.3–85.0 m, c. 1855 Ma quartzofeldspathic metasediment at 87.5–91.6 m and the Wade Amphibolite at 595–603 m (McAvaney and Jagodzinski, 2012). In TMI imagery the Deuter Diorite appears to cross-cut the magnetic fabric of the Archean to earliest Paleoproterozoic basement, which comprises the Cooyerdoo Granite and Sleaford Complex. The Deuter Diorite has a magmatic crystallisation age of 1742 ± 6 Ma (McAvaney and Jagodzinski, 2012).

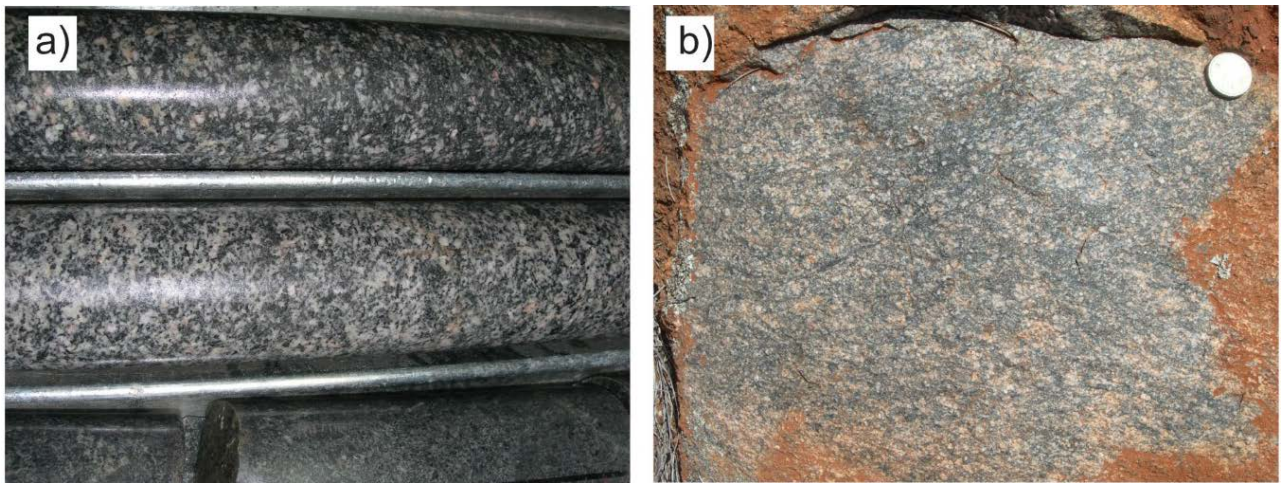

Figure 5. Intermediate and mafic units of the Moola Suite. (a) Medium-grained, equigranular Deuter Diorite LED001 (drillhole 229988). **(b)** Massive hornblende-plagioclase-clinopyroxene amphibolite of the Wade Amphibolite, west of Iron Duke.

Wade Amphibolite (c. 1735 Ma)

The Wade Amphibolite occurs as isolated outcrops and subcrops on northeastern Eyre Peninsula on Cooyerdoo, Shirrocoe and Gilles Downs and Corunna stations. Notable outcrops occur in on the northern shore of Lake Gilles and to the west of Iron Duke (Fig. 3). It also occurs in drillholes DDH LED001 (drillhole 229988) between the interval 595.0–603.0 m, and in RDD002 (drillhole 229989) at 308.2–316.4 m, 317.2–379.0 m and 413.0–417.5 m (Fig. 3).

The Wade Amphibolite is a fine- to coarse-grained amphibolite composed of hornblende, clinopyroxene, plagioclase, biotite ± K-feldspar ± quartz, with accessory apatite and titanite (Fig. 5b; Goodwin, 2010). The amphibolite ranges from massive recrystallised to gneissic, with alternating hornblende-rich and plagioclase-rich laminae.

On the northern shore of Lake Gilles, on Corunna Station, the Wade Amphibolite is observed to intrude c. 2520 Ma leucogranite gneiss of the Sleaford Complex as north-northwest-trending dykes parallel to the regional Kimban structural grain (Reid *et al.*, 2008b). In the vicinity of Iron Duke contact relationships are not exposed, but it is inferred to intrude the c. 3150 Ma Cooyerdoo Granite and Sleaford Complex. In LED001 the Wade Amphibolite occurs as a dolerite xenolith within the Deuter Diorite (McAvaney and Jagodzinski, 2012).

An amphibolite from the Wade Amphibolite from west of Iron Duke yielded a magmatic age of 1736 ± 4 Ma, within error of the age obtained for an unnamed granite of the Moola Suite cropping out within 2 km of the gabbro, which yielded an age of 1737±5 Ma (Reid and Jagodzinski, 2011).

PINBONG SUITE (1735–1700 Ma)

The Pinbong Suite is the most widespread suite in the Peter Pan Supersuite, occurring on central and southern Eyre Peninsula in the southern Gawler Craton, the Olympic Domain in the eastern Gawler Craton, Coober Pedy Ridge in the northern Gawler Craton and in the central Gawler Craton (Fig. 1). The Pinbong Suite is dominated by equigranular, foliated, gneissic and migmatitic quartz-feldspar-biotite granite which is generally more plagioclase-rich and biotite-rich compared to the Moola Suite. The suite also contains K-feldspar megacrystic granite, feldspar-quartz-muscovite granite, hornblende-biotite-titanite monzogranite, syenogranite, gabbro and dolerite. It includes four named formations; the Middle Camp Granite, Carappee Granite, Paxton Granite, and the Colona Gabbro (Table 1).

The most extensive outcrops of the Pinbong Suite are on central Eyre Peninsula, including the Middle Camp Granite in the Cleve Hills, the Carappee Granite ~35 km southwest of Kimba, and unnamed occurrences at Poverty Corner, Little Pinbong Rockhole, Peter Pan Platforms, Bascombe Rocks and Ferns Quarry (Fig. 6). In addition, an unnamed feldspar-quartz-muscovite granite crops out in the Cleve Hills 2.5 km north and 5 km west of Cleve (map symbol Lzp_2). In central Eyre Peninsula the Pinbong Suite is also intersected in drillholes at the Bungalow Prospect 15 km north-northwest of Cowell in drillholes DDH BUDD 23 (drillhole 255924), DDH BUDD 28 (drillhole 255925) and DDH BUDD 168 (drillhole 277601) (Reid and Jagodzinski, 2011), and in WDDH01 (drillhole 270096) between 649.91–734.40 m at Moseley Nobs, ~35 km north-northwest of Kimba (Sunthe Uranium Pty. Ltd., 2011). On southern Eyre Peninsula the Pinbong Suite occurs at Seal Point on Flinders Island, at Redbanks, and Cape Carnot (Fanning *et al.*, 2007, Jagodzinski *et al.*, 2007).

In the eastern Gawler Craton dolerites of the Pinbong Suite are intersected in drillhole DDH RD 160 (681735 mE 6630758 mN) in the Olympic Dam deposit. In the central Gawler Craton the Pinbong Suite is represented by the Paxton Granite, which crops out in the Tarcoola Goldfields, and is intersected in the subsurface at the Perserverance Deposit in drillholes GP078D (drillhole 235049), GP004D (drillhole 207047) and GP028RD (drillhole 235002) (Budd and Fraser, 2004). In the northern Gawler Craton gabbro of the Pinbong Suite is intersected in drillhole DD89LR 22 (drillhole 134168) at the Mount Brady Prospect, Coober Pedy Ridge. In the western Gawler Craton granite, granodiorite and diorite of the Pinbong Suite crops out on the shores of Lake Anthony (Dawson, 2016), and in the Fowler Domain the Colona Gabbro is intersected in drillholes in near Colona Homestead (Daly *et al.*, 1994).

Middle Camp Granite (c.1735–1725 Ma)

The Middle Camp Granite is exposed in the Cleve Hills, eastern Eyre Peninsula, approximately 9.5 km west of Cowell along the Lock-Cowell Road and directly north of Minbrie Homestead (Fig. 6). The pluton has a lateral extent of 3.5 km east-west and ~11 km north-south, aligned north-northeast with the dominant Kimban structural grain. It is well exposed as broad hill slope exposures and granite tors (Fig. 7a). The Middle Camp Granite is grey, moderately to strongly foliated, fine- to medium-grained, equigranular plagioclase-quartz- K-feldspar-biotite granite (Fig. 7b). The tectonic foliation in the Middle Camp Granite is isoclinally folded, and late-stage aplitic and pegmatitic veins and dykes intrude subparallel to the foliation or cut it at a low angle (Parker and Fanning, 1998). The Middle Camp Granite intrudes c. 2000 Ma Warrow Quartzite and the c. 2520–2420 Ma Minbrie Gneiss (Parker *et al.*, 1981), although contacts have been modified by deformation during the Kimban Orogeny. The Middle Camp Granite has yielded magmatic ages ranging from 1736 ± 6 Ma (Fraser and Neumann, 2010) to 1726 ± 7 Ma (Fanning *et al.* 2007).

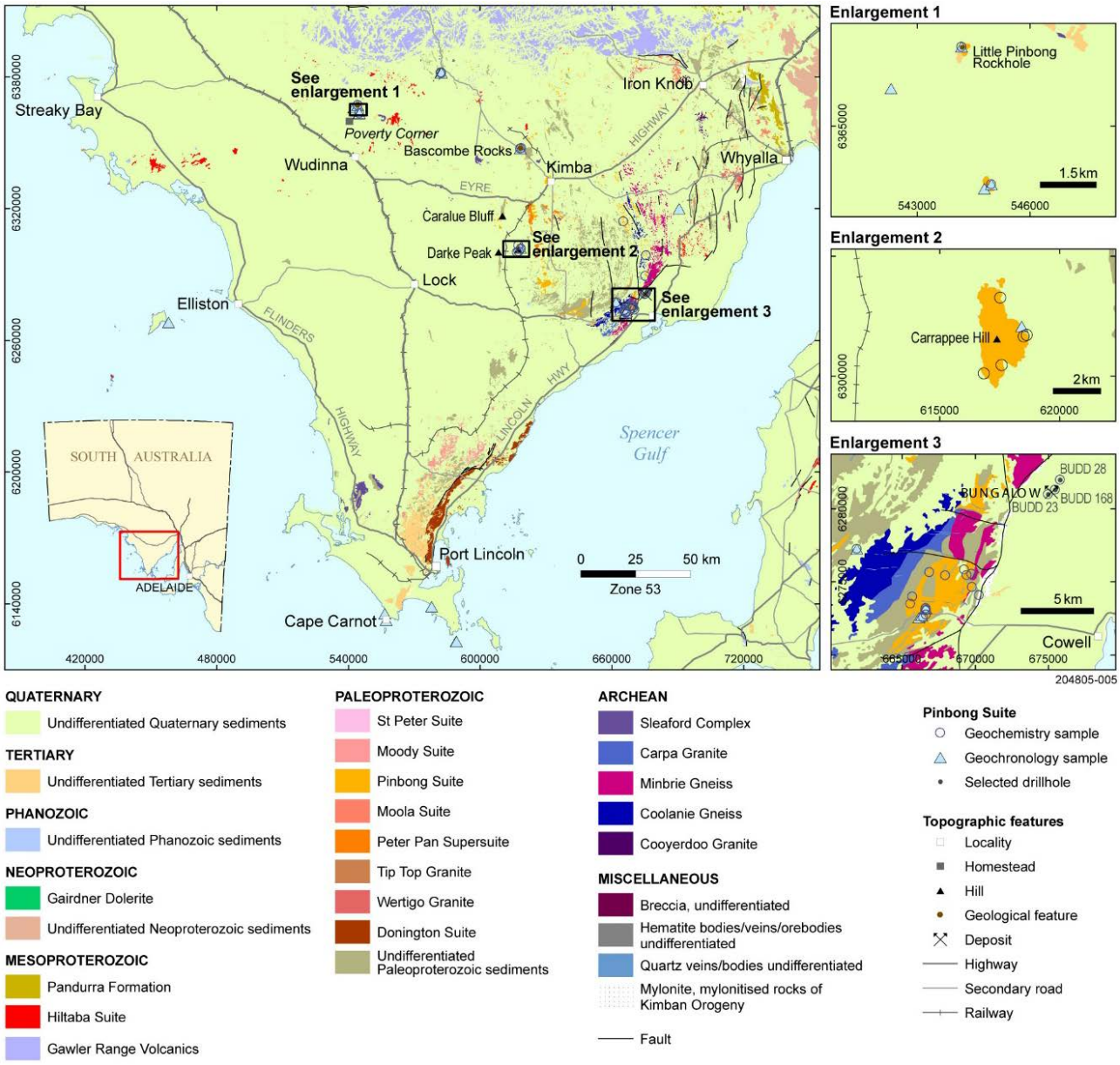

Figure 6. Distribution of the Pinbong Suite on Eyre Peninsula, location of geochemistry samples presented in this report, and location of dated samples of the Pinbong Suite.

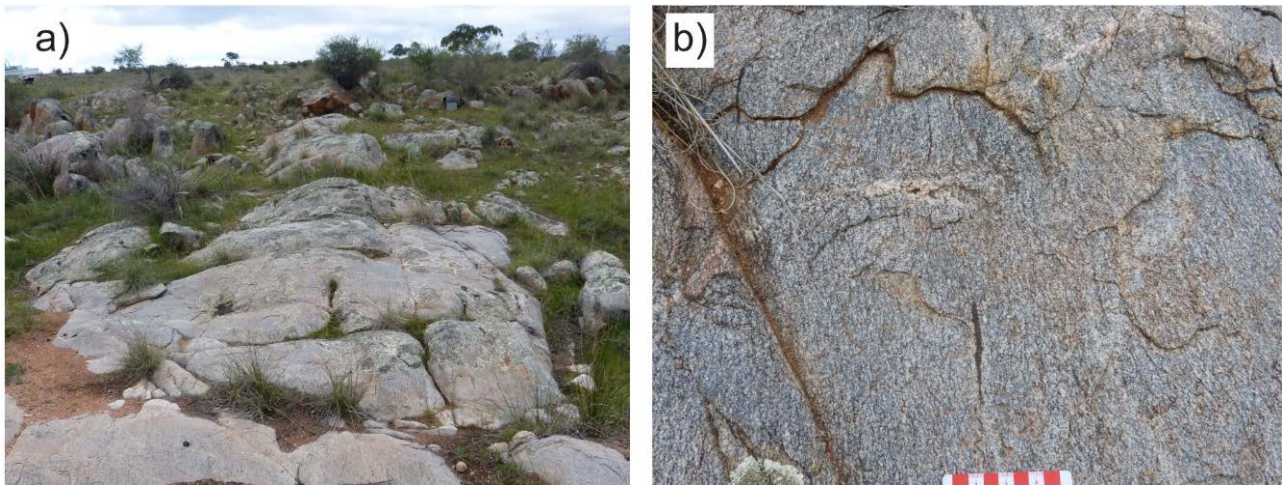

Figure 7. Middle Camp Granite. (a) Outcrop of Middle Camp Granite (site 1979781). **(b)** Medium-grained, foliated quartz-biotite-feldspar granite (site 1979781).

Carappee Granite (c. 1720 Ma)

The Carappee Granite is exposed at Carappee Hill (Fig. 8a), ~35 km northwest of Cleve, and on the western edge of Darke Peak Range on central Eyre Peninsula (Fig. 6). Contacts with the surrounding rocks are not exposed, but it is presumed to intrude the Hutchison Group. It is a medium- to coarse-grained megacrystic quartz-feldspar-biotite granite (Figs 8a-b). K-feldspar phenocrysts up to 3 cm in length sit within an equigranular medium- to coarse-grained groundmass of quartz, plagioclase and biotite (Flint *et al.*, 1988). The Carappee Granite contains a weak foliation defined by a preferred alignment of K-feldspar megacrysts trending north-south. It has yielded a magmatic crystallisation age of 1720 ± 3 Ma (Fraser and Neumann, 2010).

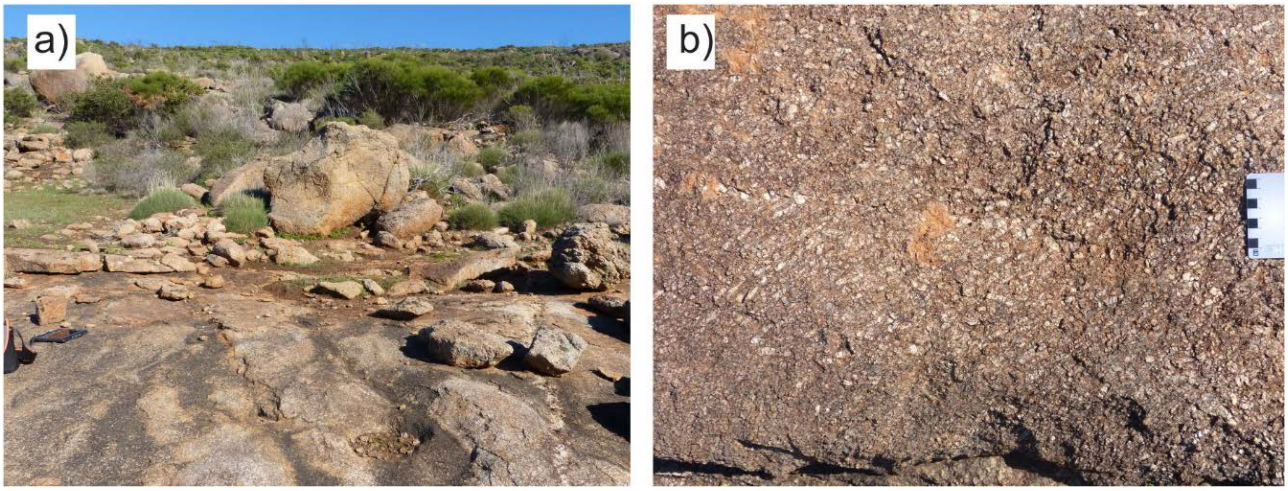

Figure 8. **Carappee Granite. (a)** Outcrop of Carappee Granite, Carappee Hill (site 1979767). **(b)** Weakly aligned megacrystic K-feldspar phenocrysts in Carappee Granite, Carappee Hill (site 1979767).

Paxton Granite (c. 1720 Ma)

The Paxton Granite occurs in the Tarcoola Goldfields in the central Gawler Craton (Fig. 1). It has limited outcrop extent, but is intersected in drillholes GP078D (drillhole 235049), GP004D (drillhole 207047) and GP028RD (drillhole 235002) at the Perseverence Prospect

The granite contains three phases comprising monzongranite, syenogranite and quartz monzonite (Budd and Fraser, 2004). The Paxton Granite is dominated by coarse-grained hornblende-biotite-titanite monzogranite with K-feldspar megacrysts (Fig. 9a). Late-stage finer-grained biotite-bearing syenogranite and hornblende-biotite-titanite quartz monzonite intrude the monzogranite (Fig. 9b).

The Paxton Granite is unconformably overlain by the c. 1680 Ma Tarcoola Formation and is intruded by the Lady Jane Diorite (Budd and Fraser, 2004). Magmatic crystallisation ages for the Paxton Granite are 1722 ± 4 Ma for the monzogranite, 1715 ± 3 Ma for the syenogranite and 1718 ± 3 Ma for the quartz monzonite (Budd, 2006).

Colona Gabbro (c. 1735 Ma)

The Colona Gabbro does not crop out, but is intersected in ~20 drillholes in the Colona Homestead area in the western Gawler Craton (Fig. 1). It comprises layered intermediate to mafic intrusive rocks including granodiorite, tonalite and hornblende gabbros (Fig. 10a-b). Complex intermingling and mixing textures between the intermediate to mafic rocks indicate that they are comagmatic (Teasdale, 1997). The body in drill holes Colona 43D and Colona 45D preserves apparent layered cumulate textures, with hornblende-rich gabbroic layers and plagioclase-rich dioritic layers (Daly *et al.*, 1994). The Colona Gabbro has been affected by amphibolite facies metamorphism and weak to strong tectonic fabrics (Daly *et al.*, 1994).

Host rocks to the Colona Gabbro has not been intersected in drillholes. The Colona Gabbro has yielded magmatic ages ranging from 1739 ± 6 Ma (Reid, 2015) to 1729 ± 7 Ma (Fanning *et al.*, 2007). Given that these two ages are within error they are interpreted to represent a single unimodal population, and the magmatic age of the Colona Gabbro is estimated at c. 1735 Ma.

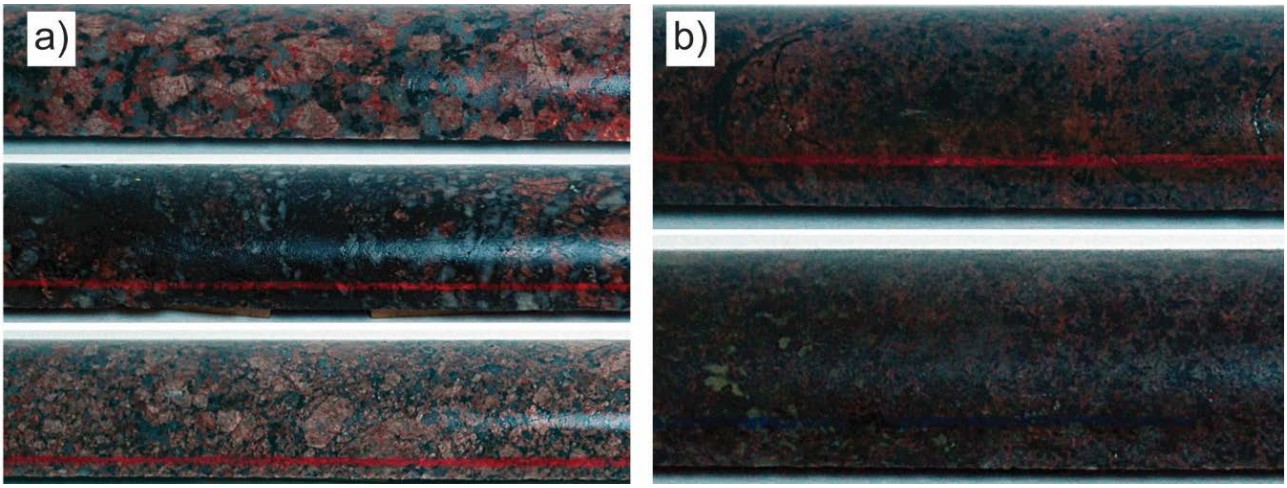

Figure 9. Paxton Granite (photos by B. Bendall). (a) K-feldspar megacrystic hornblende-biotite monzogranite, GP004D (drillhole 207047). Depth intervals are 389.26–389.58 m (top image), 320.42–320.62 m (middle image), 158.73–159 m (bottom image). **(b)** Fine-grained phases of the Paxton Granite, drillhole GP004D. Depth intervals are 146–146.3 m (top image), 116.01–116.24 m (bottom image).

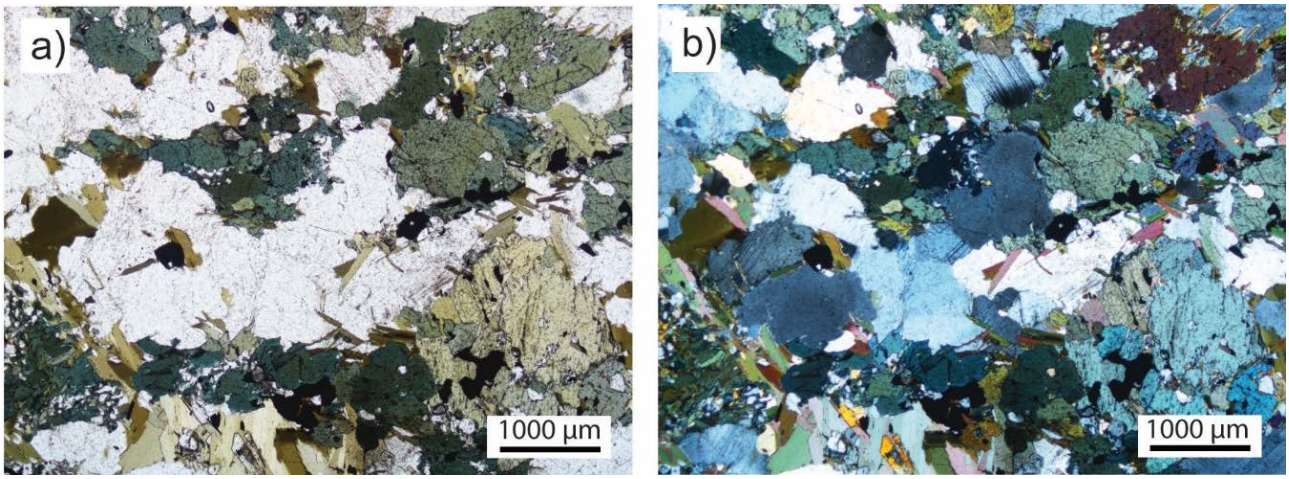

Figure 10. Colona Gabbro. Photomicrographs of the gabbroic phase of Colona Gabbro in **(a)** plain-polarised, and **(b)** cross-polarised light, Colona 43D (drillhole 137323), 53.6–54 m.

Unnamed mafic to intermediate rocks of the Pinbong Suite, Lzp_1 (c.1725–1710 Ma)

Lzp_1 comprises unnamed mafic to intermediate rocks belonging to the Pinbong Suite. It includes outcrops of diorite on the northern shores of Lake Anthony in the western Gawler Craton; gabbros intersected in DD89LR 22 (drillhole 134168) at Mount Brady Prospect, Coober Pedy Ridge, in the northern Gawler Craton; in WDDH01 (drillhole 270096) at Moseley Nobs, ~35 km north-northwest of Kimba on central Eyre Peninsula; and in DDH RD 160 (681735 mE 6630758 mN), at the Olympic Dam deposit in the eastern Gawler Craton (Fig. 1).

At Lake Anthony, diorites are massive and equigranular to porphyritic, fine- to medium-grained and composed of quartz, biotite and plagioclase (Benbow, 1993). The diorite is intruded by

granodiorite, monzogranite and granite which is interpreted to also be part of the Pinbong Suite. Lzp_1 in drillhole DD89LR 22 is grey-green, very fine- to medium-grained, crystalline, plagioclase-hornblende-biotite gabbro (Figs 11a-b). Lzp_1 from drillhole RD 160 is a dolerite with randomly oriented plagioclase laths in a groundmass of pyroxene, plagioclase, iron oxides and quartz (Jagodzinski, 2005). In WDDH01 the Wade Amphibolite intrudes grey-green fine-grained quartz-biotite-feldspar-garnet schist and quartzite of the c. 1790 Ma Hutchison Group (Sunthe Uranium Pty Ltd, 2011).

The mafic and intermediate rocks of the Pinbong Suite have yielded a range of magmatic ages, from 1725 ± 7 Ma in DD89LR 22 (Fanning *et al.*, 2007), c. 1725 Ma in DDH RD 160 (Jagodzinski, 2005) and 1712 ± 6 Ma at Lake Anthony (Dawson, 2016).

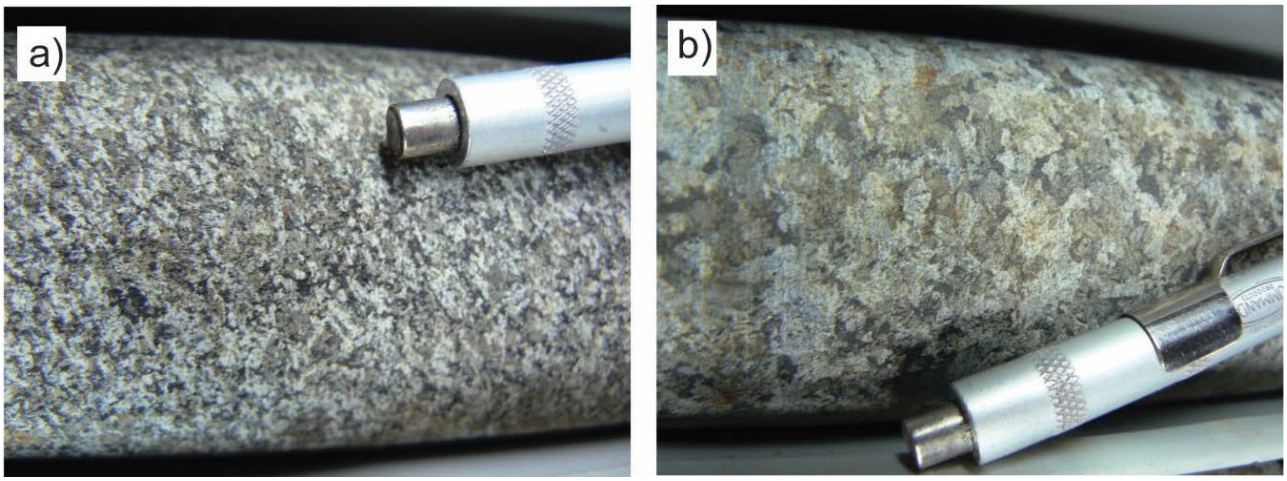

Figure 11. Unnamed gabbro of the Pinbong Suite (Lzp_1) in DD89LR22 (drillhole 134168). (a) Fine-grained hornblende-plagioclase-biotite gabbro at ~152 m. **(b)** Coarse-grained hornblende-plagioclase-biotite gabbro at ~120 m. Photos courtesy of Adrian Fabris.

MOODY SUITE (1720–1700 Ma)

The Moody Suite occurs 10 km northwest of Tumby Bay on central Eyre Peninsula (Fig. 12). The term was first used by Parker *et al.* (1981) to describe igneous rocks of the former Lincoln Complex which were weakly deformed to unfoliated, and interpreted to have intruded in the late stages of the Kimban Orogeny. It originally included the Burkitt Granite, Carpa Granite, Wertigo Granite, Yunta Well Leucogranite, Uranno Microgranite and Bungalow Granodiorite (Parker, 1993). More recently, the Moody Suite has been formally defined and described by Schwarz (1999) to include the Yunta Well Leucogranite, the Moreenia Adamellite, the Chinmina Syenite and the Uranno Microgranite. Some of these names have been modified in this report (see Appendix I).

The Moody Suite comprises granite, monzogranite, monzonite and garnet- and muscovite-bearing leucogranite, which intrude the c. 1790 Ma Hutchison Group and c. 2570–2410 Ma Sleaford Complex. Magmatic ages of the Moody Suite range from 1710 to 1700 Ma (Fanning *et al.*, 2007).

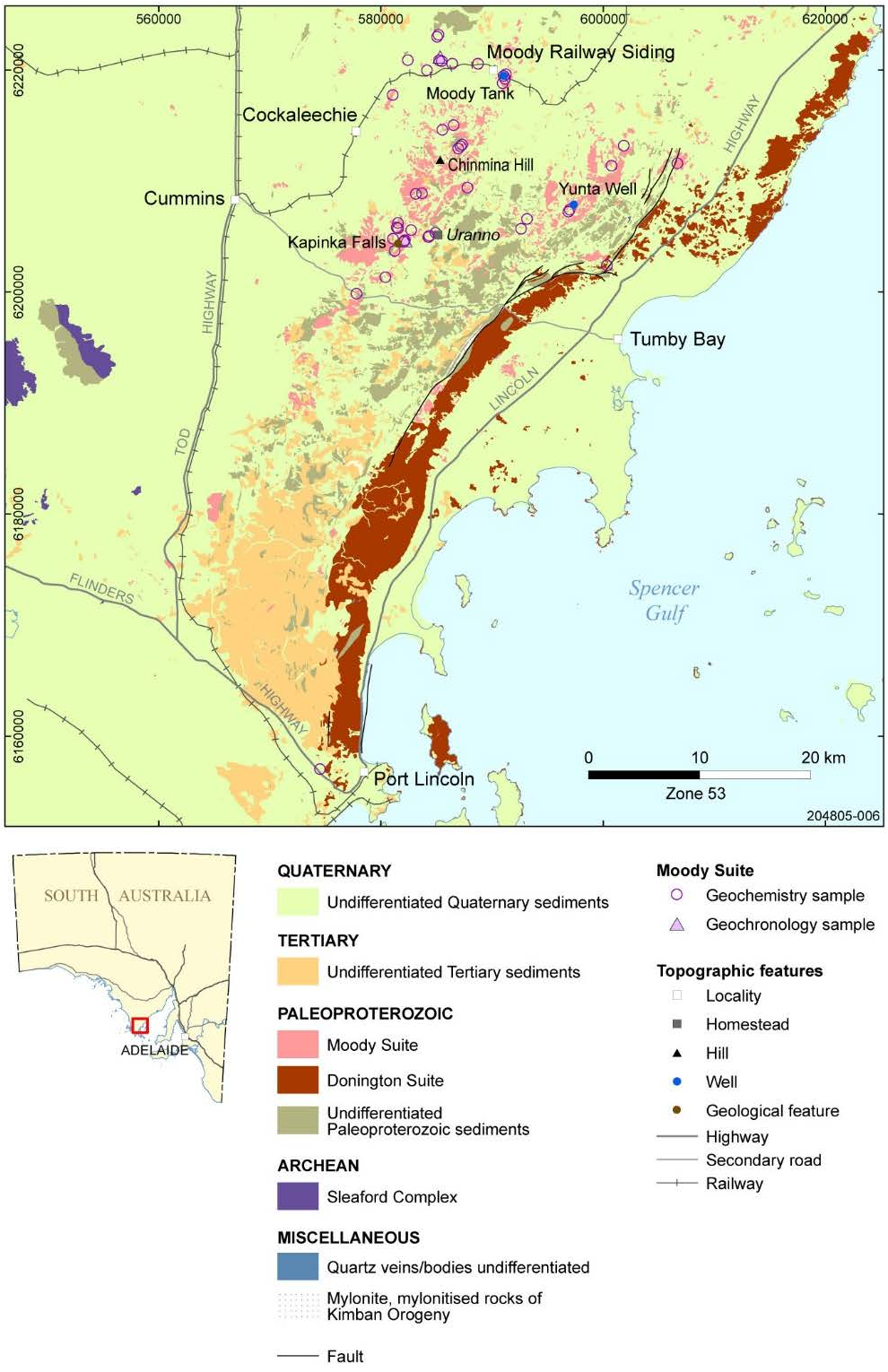

Figure 12. Distribution of the Moody Suite on Eyre Peninsula, location of geochemistry samples presented in this report, and location of dated samples of the Pinbong Suite.

Yunta Well Leucrogranite

The Yunta Well Leucogranite forms a discrete, elliptical pluton 10 km northwest of Tumby Bay (Fig. 12). It is a medium- to coarse-grained quartz-K feldspar-plagioclase-muscovite-garnet-biotite-tourmaline granite (Fig. 13a-b) (Schwarz, 1999). The leucogranite has a weak foliation in the centre of the intrusion that grades to moderate around the margins of the intrusion, suggesting a late tectonic emplacement (Coin, 1976). The leucogranite contains the most abundant sedimentary xenoliths of the Moody Suite units, including schist and layered amphibolite of the Hutchison Group (Schwarz, 1999). Contact relationships of the Yunta Well Leucogranite are not well exposed, but it is interpreted to intrude the Hutchison Group. No geochronological constraints exist for the Yunta Well Leucogranite.

Figure 13. Yunta Well Leucogranite. (a) Outcrop of leucogranite on roadside (site 2012256). **(b)** Equigranular, quartz-K-feldspar-plagioclase-garnet-bearing leucogranite (site 2138800).

Moreenia Monzogranite

The Moreenia Monzogranite (originally Moreenia Adamellite) is found in the Moody Tank area and near the Cummins-Buckleboo railway between Cockaleechie and Moody Railway siding (Fig. 12). The monzogranite is lithologically variable but is dominated by a medium-grained porphyritic monzogranite composed of K-feldspar megacrysts in an equigranular matrix of plagioclase, quartz, biotite with minor muscovite (Fig. 14a-b) (Schwarz, 1999). The Moreenia Monzogranite contains abundant xenoliths of variable monzogranite phases (Fig. 14c), as well as metasedimentary xenoliths (Fig. 14d; Schwarz, 1999). It contains a foliation with a highly variable orientation, interpreted to be a flow foliation produced by plastic flow of a magma (Coin, 1976). No contact relationships between the Moreenia Monzogranite and surrounding rocks are exposed, but it is inferred to intrude the Hutchison Group. The magmatic crystallisation age of the Moreenia Monzogranite is 1720 ± 9 Ma (Fanning *et al.*, 2007).

Uranno Microgranite

The Uranno Microgranite crops out in the vicinity of Uranno Homestead and west of Kapinka Falls, 25 km west-northwest from Tumby Bay (Fig. 12). The Uranno Microgranite is a light pink to grey, fine- to medium-grained microgranite composed of porphyritic pink K-feldspar in a matrix of plagioclase, quartz and minor biotite (Fig. 15a-b). It is in faulted contact with the Chinmina Monzonite, with the contact trending northeast-southwest, and well-developed foliation sub-parallel to the adjacent faulted contact with the Chinmina Monzonite is observed (Schwarz, 1999). The microgranite becomes undeformed, massive and equigranular to the south. The Uranno Microgranite is observed to intrude the Hutchison Group east of Cummins (Parker 1993). No geochronological constraints exist for the Uranno Microgranite.

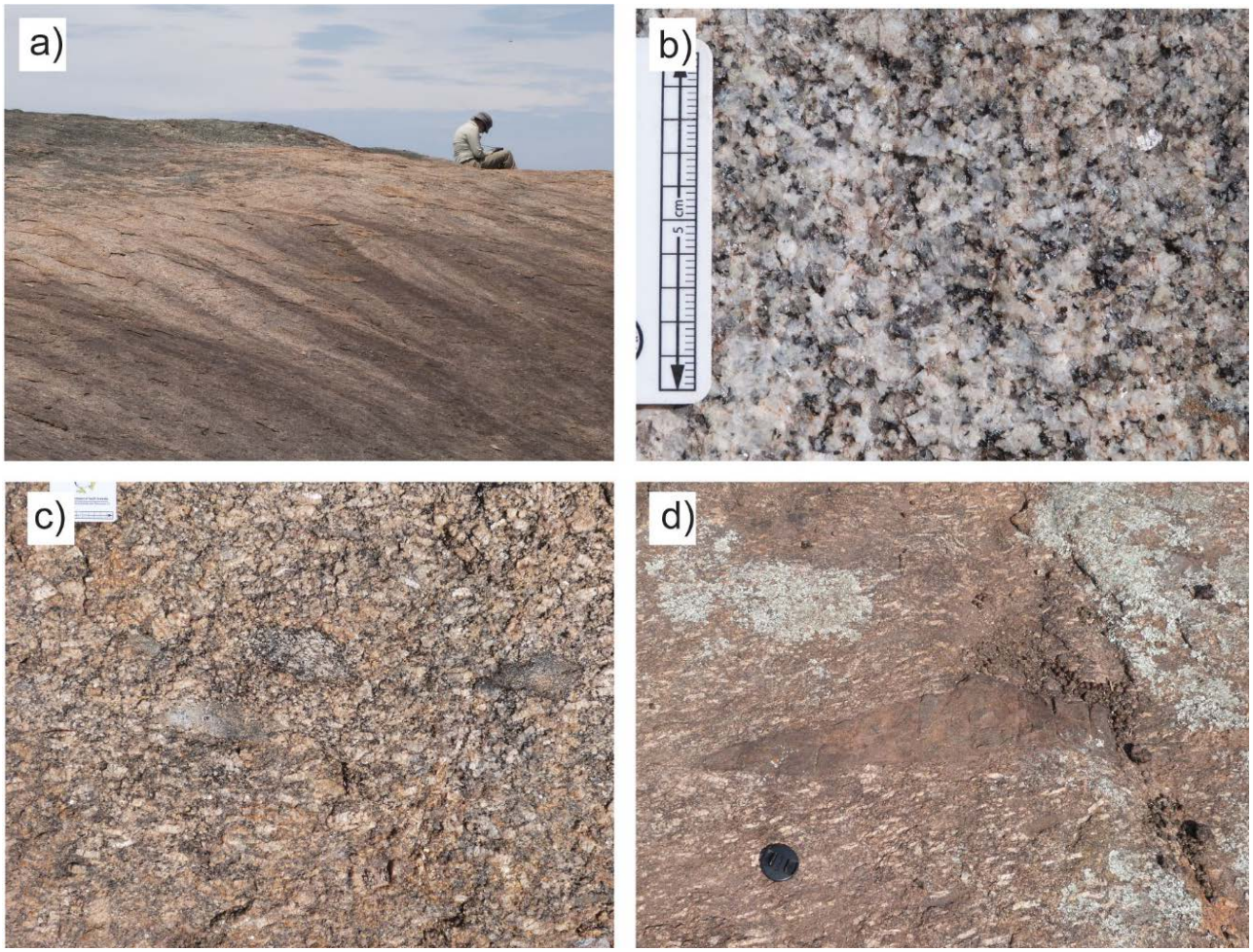

Figure 14. Moreenia Monzogranite. (a) Outcrop of Moreenia Monzogranite at Moody Tank (site 2012257). **(b)** Equigranular, quartz-feldspar-biotite Moreenia Monzogranite, Moody Tank, (site 2012257). **(c)** Biotite-rich microgranite xenoliths in Moreenia Monzogranite. **(d)** Metasedimentary xenolith aligned with magmatic layering in Moreenia Monzogranite (site 2012261).

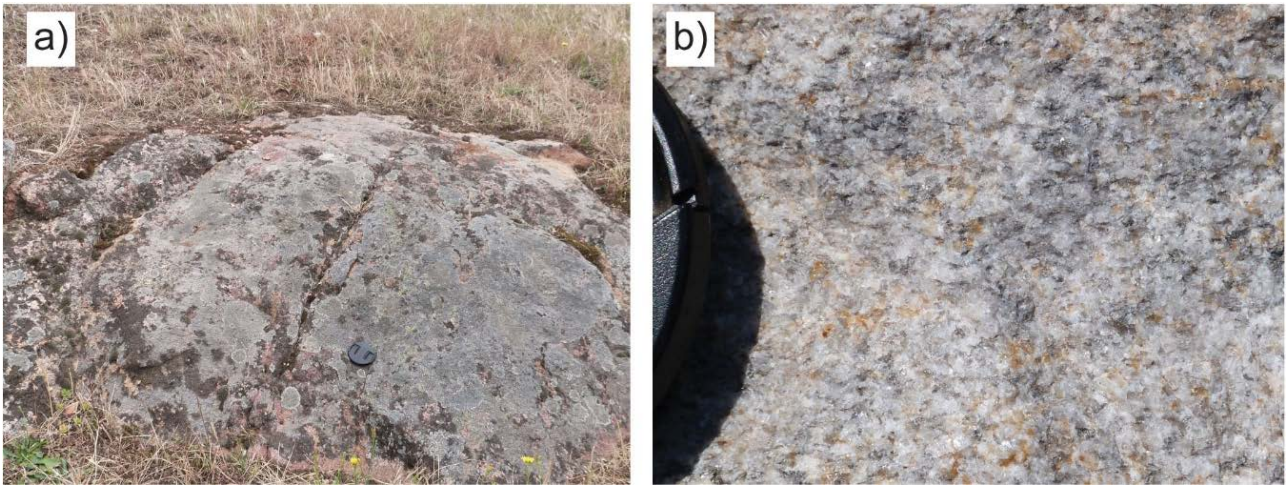

Figure 15. Uranno Microgranite. (a) Outcrop of Uranno Microgranite, Uranno Homestead ruins (site 2012250). **(b)** Grey, fine-grained, quartz-plagioclase-biotite microgranite (site 2012240).

Chinmina Monzonite

The Chinmina Monzonite is exposed at Chinmina Hill and a road metal quarry near Kapinka Falls, 25 km west-northwest from Tumby Bay (Fig. 12). Outcrop is dominated by a homogenous medium- to coarse-grained hornblende monzonite (Fig. 16a) with euhedral phenocrysts to megacrysts of K-feldspar in a groundmass of feldspar, hornblende, biotite and quartz (Schwarz, 1999). At its contact with Uranno Microgranite, the Chinmina Monzonite is undeformed suggesting it postdates the microgranite (Coin, 1976). At least three other lithologies/phases are associated with the Chinmina Monzonite. At the type locality of the Chinmina Monzonite, the quarry near Kapinka Falls, the monzonite is cross-cut by coarse-grained pegmatite (Fig. 16b) and fine-grained granitic dykes (Fig. 16c-d). A coarse-grained granodiorite to diorite composed of biotite, feldspar and quartz (Fig. 16e) also occurs in close vicinity to the monzonite, and is often foliated (Fig. 16f).

Contact relationships between the Chinmina Monzonite and host rocks are not exposed, but it is interpreted to intrude the Hutchison Group. It shares a faulted contact with the Uranno Microgranite, and unlike the Uranno Granite has not been affected by deformation at this contact, suggesting it may be younger in age (Coin, 1976). The magmatic crystallisation age of the Chinmina Monzonite is 1701 ± 12 Ma (Fanning *et al.*, 2007).

GEOCHEMISTRY OF THE PETER PAN SUPERSUITE

ANALYTICAL METHODS

Major and trace elements

119 samples were collected from outcrop and diamond drillholes for whole rock geochemistry between 2006 and 2015 (Fig. 17). Major and trace element analyses were performed at a two commercial geochemical laboratories in Adelaide (Amdel Laboratories and ALS Global). Major elements were analysed by Inductively Coupled Plasma with Optical Emission Spectroscopy (ICP-OES) at Amdel Laboratories and Inductively Coupled Plasma-Mass Spectrometry (ICP-MS) at ALS Laboratories. All trace-elements were analysed by ICP-MS. Geochemical data for an additional 26 samples of the Wade Amphibolite were provided by Investigator Resources and only includes trace and rare earth element analyses (Sunthe Uranium Pty Ltd, 2011). The whole rock geochemistry results for the Peter Pan Supersuite are presented in Appendix II.

Sm-Nd isotopes

A subset of 38 samples were analysed for whole-rock Sm–Nd isotope geochemistry. Thirty-eight samples were analysed for whole-rock Sm–Nd isotope compositions including 12 Moola Suite, 16 Pinbong Suite and 10 Moody Suite samples, presented in Tables 2–4.

Sm–Nd isotope analyses were performed at the University of Adelaide following the method of Wade *et al.* (Wade *et al.*, 2006). Nd analyses were conducted using a Finnigan MAT 262 thermal ionisation mass spectrometer, in static and quadruple-cup dynamic measurement modes, normalised to $^{146}/^{144}Nd = 0.7219$ and Nd concentrations corrected for 100 pg blank. Sm analyses were carried out on a Finnigan MAT 261 thermal ionisation mass spectrometer, in single-cup dynamic mode, and Sm concentrations were corrected for 50 pg blank.

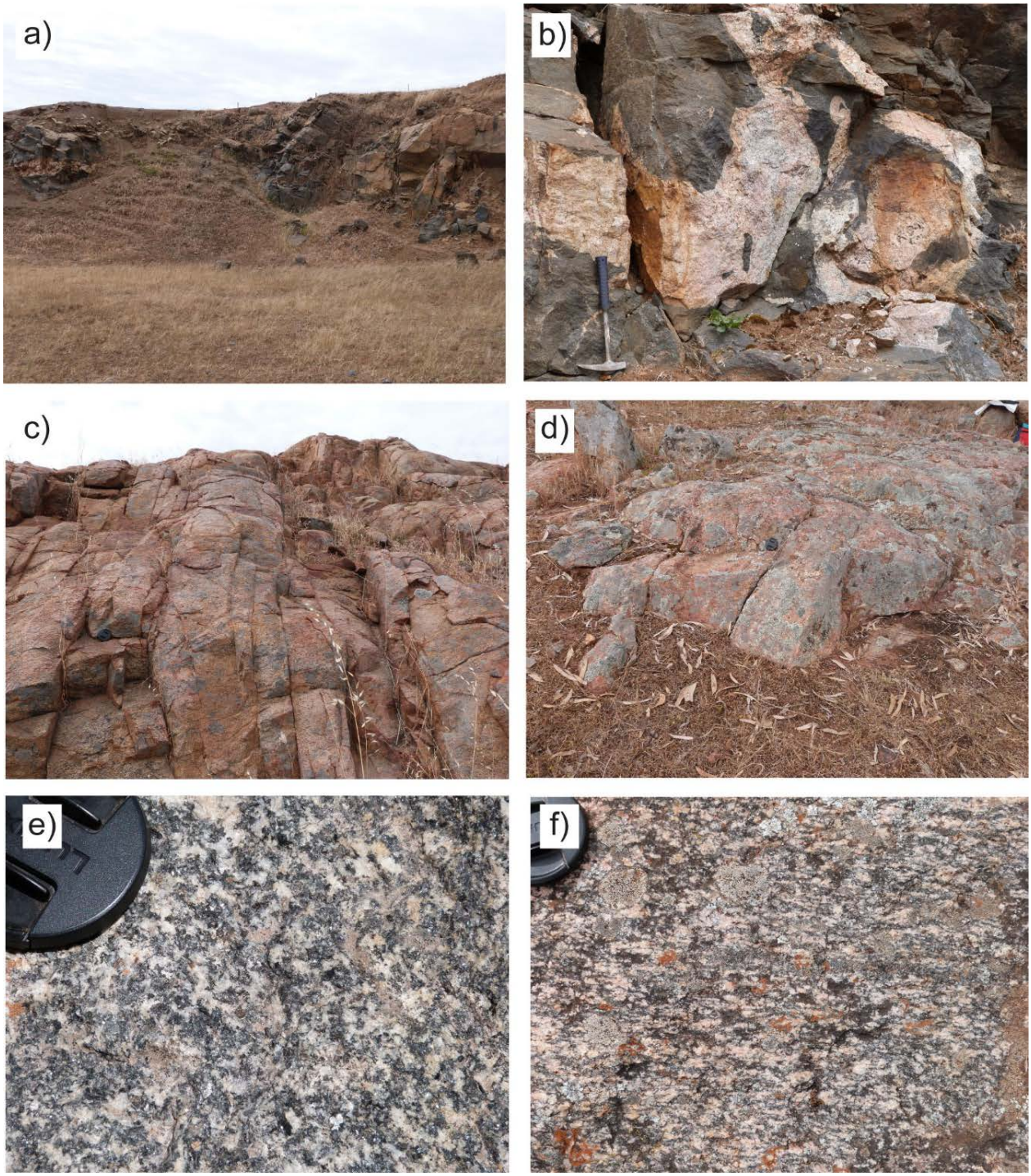

Figure 16. Chinmina Monzogranite. (a) Exposure of the Chinmina Monzonite at the road metal quarry, Kapinka Falls, (site 2012249). The dark grey monzonite is crosscut by pink pegmatite veins. **(b)** Pegmatite cross-cutting Chinmina Monzonite at quarry, Kapinka Falls, (site 2012249). **(c)** Fine- to medium-grained, -feldspar- quartz-biotite granite dyke associated with the Chinmina Monzonite, (site 2012248). **(d)** Outcrop of fine-grained granite dyke phase associated with Chinmina Monzonite (site 2012246). **(e)** Medium- to coarse-grained, equigranular, plagioclase-biotite-quartz granodiorite associated with the Chinmina Monzonite (site 2012242). **(f)** Gneissic fabric in plagioclase-biotite-quartz granite associated with Chinmina Monzonite (site 2012247).

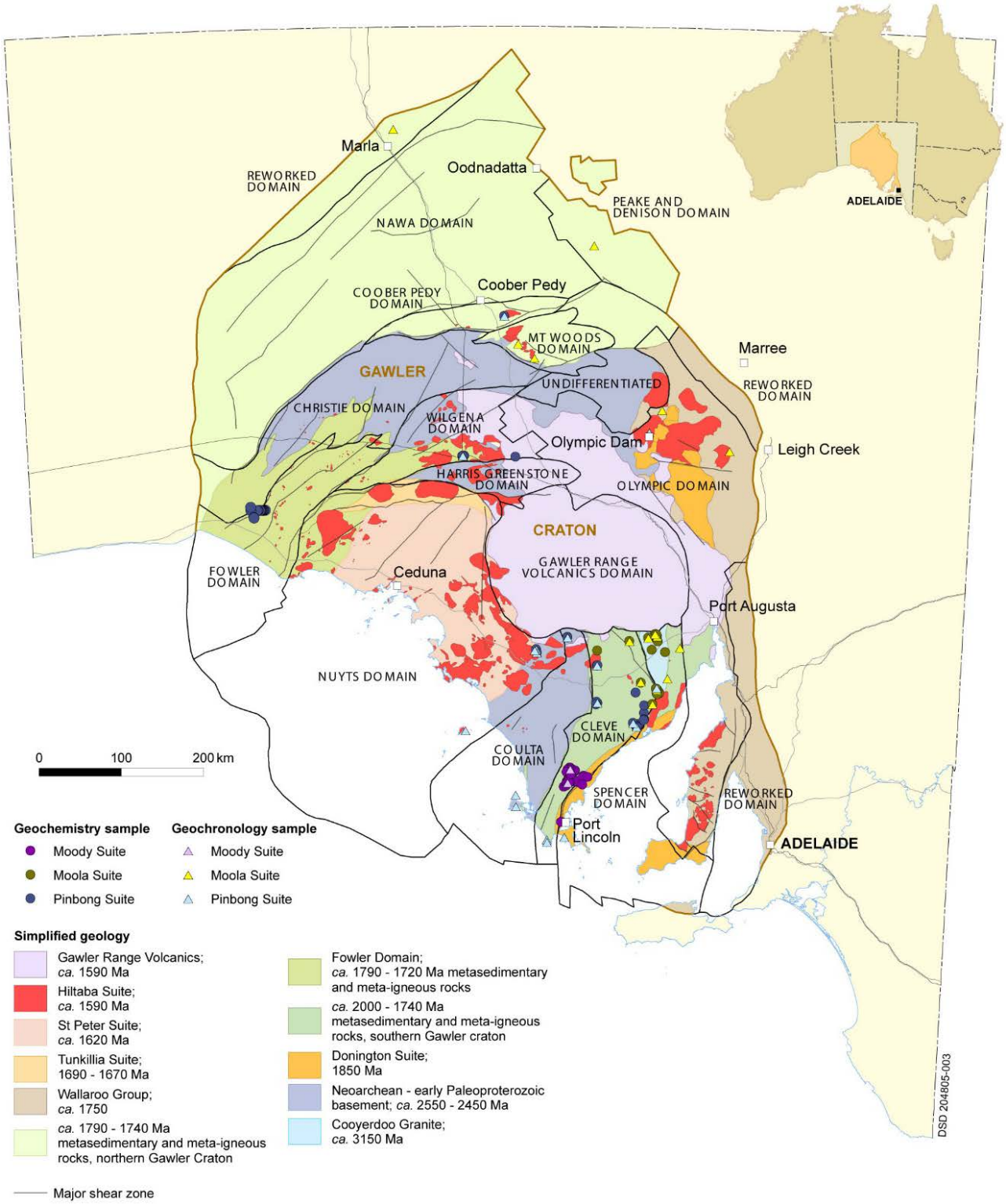

Figure 17. Simplified solid geology map of the Gawler Craton, showing the location of geochemistry samples of the Peter Pan Supersuite presented in this report, as well as dated samples of Peter Pan Supersuite. Samples of the Moola, Pinbong and Moody suites from Eyre Peninsula are also shown in Figures 3, 6 and 12 respectively.

Table 2. Sm-Nd data for the Moola Suite.

Sample	Unit	Lithology	E	N	Zone	Age (Ma)	Nd (ppm)	Sm (ppm)	$^{147}Sm/^{144}Nd$	$^{143}Nd/^{144}Nd$	$\varepsilon_{Nd(0)}$[a]	$\varepsilon_{Nd(t)}$[b]	$T_{(DM)}$	Reference
2014267	Moola Suite	granite	685536	6300283	53	1745	3.39	1.25	0.2232	0.512621	-0.3	-6.3	2.6^	This study
884-B11	Burkitt Granite	granite	689000	6384700	53	1740	65.43	10.02	0.0927	0.511019	-31.6	-8.4	2.7	Stewart (1994)
884-B3	Burkitt Granite	granite	691400	6382800	53	1740	69.49	10.7	0.0932	0.511063	-30.7	-7.7	2.6	Stewart (1994)
884-B5	Burkitt Granite	granite	690200	6383600	53	1740	43.99	6.17	0.0849	0.510485	-42	-17.1	3.1	Stewart (1994)
884-B7	Burkitt Granite	granite	688300	6381900	53	1740	66.88	10.1	0.0914	0.511029	-31.4	-7.9	2.6	Stewart. (1994)
884-B9	Burkitt Granite	granite	688900	6383100	53	1740	53.86	7.64	0.0858	0.51091	-33.7	-9	2.7	Stewart. (1994)
1708863	Deuter Diorite	diorite	680450	6381003	53	1740	37.21	6.3	0.1024	0.511307	-26	-4.9	2.5	This study
2017712	Wortham Granite	granite	719075	6368946	53	1740	20.42	3.84	0.1136	0.511565	-20.9	-2.4	2.4	This study
1657899	Wade Amphibolite	amphibolite	701049	6363554	53	1740	20.48	5.66	0.1671	0.51232	-6.2	0.4	2.7	This study
1657921	Wade Amphibolite	amphibolite	692299	6376765	53	1740	20.23	5.44	0.1627	0.512242	-7.7	-0.1	2.7	This study
1657954	Wade Amphibolite	amphibolite	692345	6376682	53	1740	18.87	4.8	0.1537	0.512086	-10.8	-1.2	2.7	This study
1723518	Wade Amphibolite	amphibolite	693969	6314663	53	1740	10.58	2.48	0.1417	0.511709	-18.1	-5.9	3	This study
1723520	Wade Amphibolite	amphibolite	693886	6314693	53	1740	9.18	2.4	0.1583	0.511971	-13	-4.5	3.2	This study
1723520 (dup)	Wade Amphibolite	amphibolite	693886	6314693	53	1740	9.37	2.41	0.1557	0.511953	-13.4	-4.3	3.1	This study
2008371082	undifferentiated	granite	657541	6376815	53	1735	17.2	2.86	0.1004	0.511132	-29.4	-8	2.7	Fraser *et al.*, 2010
1721027	undifferentiated	granite	691278	6317937	53	1735	23.41	2.97	0.0769	0.51072	-37.4	-10.8	2.7	Goodwin, 2010
1721028	Wade Amphibolite	amphibolite	690177	6319074	53	1733	111.37	15.59	0.0846	0.51091	-33.7	-8.8	2.6	This study
1723516	undifferentiated	granite	691694	6312302	53	1730	29.24	3.64	0.0753	0.51086	-34.7	-7.8	2.5	This study
1723526	Wade Amphibolite	gabbro	693824	6313228	53	1730	175.03	22.69	0.0784	0.510846	-35	-8.8	2.6	This study

a $^{143}Nd/^{144}Nd$ CHUR(0) = 0.512638, $^{147}Sm/^{144}Nd$ CHUR(0) = 0.1966.
b T_{DM} calculated using the single stage model of Goldstein *et al.* (1984).
^ = 2-stage T_{DM} calculated using 2 stage model of Liew and Hofmann (1988).
$\varepsilon_{Nd(T)}$ calculated at Age (Ma).
dup = duplicate.

Table 3. Sm-Nd data for the Pinbong Suite.

Sample	Unit	Lithology	E	N	Zone	Age (Ma)	Nd (ppm)	Sm (ppm)	$^{147}Sm/^{144}Nd$	$^{143}Nd/^{144}Nd$	$\varepsilon_{Nd(a0)}$	$\varepsilon_{Nd(t)}$	$T_{(DM)}$	Reference
2138652	Colona Gabbro	gabbro	771569	6527778	52	1740	31.68	6.09	0.1163	0.511556	-21.1	-3.2	2.5	This study
2138656	Colona Gabbro	gabbro	771569	6527778	52	1740	20.64	4.94	0.1446	0.511855	-15.3	-3.7	2.8	This study
97CC-15	Middle Camp Granite	granite	666500	6272620	53	1730	98.17	10.81	0.0666	0.51068	-38.2	-9.4	2.5	Neumann (2001)
97CC-31	Middle Camp Granite	granite	675400	6289150	53	1730	110.95	16.68	0.091	0.510859	-34.7	-11.3	2.8	Neumann (2001)
97CC-53	Middle Camp Granite	granite	666960	6273310	53	1730	91.18	10.21	0.0678	0.510703	-37.7	-9.2	2.5	Neumann (2001)
884-MC3	Middle Camp Granite	granite	–	–	–	1730	33.46	5.15	0.0931	0.511418	-23.8	-0.8	2.2	K. Stewart, unpublished data
884-MC4	Middle Camp Granite	granite	–	–	–	1730	55.53	9.83	0.1071	0.511440	-23.4	-3.5	2.4	K. Stewart, unpublished data
884-MC5	Middle Camp Granite	granite	–	–	–	1730	48.67	8.07	0.1017	0.511511	-22.0	-0.9	2.2	K. Stewart, unpublished data
884-MC6	Middle Camp Granite	granite	–	–	–	1730	50.98	8.81	0.1060	0.511510	-22.0	-1.9	2.3	K. Stewart, unpublished data
2074175	Pinbong Suite	granite	661912	6277255	53	1725	94.29	15.84	0.1016	0.510984	-32.3	-11.3	2.9	This study
2074184	Pinbong Suite	granite	618747	6347601	53	1720	58.1	12.49	0.13	0.511287	-26.3	-11.7	3.4	This study
2074184 (dup)	Pinbong Suite	granite	618747	6347601	53	1720	60.69	10.75	0.1071	0.51129	-26.3	-6.6	2.6	This study
2065398	Carappee Granite	granite	617597	6300451	53	1720	36.15	7.35	0.1229	0.511305	-26	-9.8	3.1	This study
2065399	Carappee Granite	granite	618645	6301711	53	1720	34.63	6.99	0.122	0.511291	-26.3	-9.9	3.1	This study
2065400	Carappee Granite	granite	617529	6303274	53	1720	43.62	9.15	0.1268	0.511373	-24.7	-9.3	3.1	This study
2065401	Carappee Granite	granite	616845	6300100	53	1720	55.97	10.73	0.1159	0.511267	-26.7	-9	2.9	This study
2000363004	Paxton Granite	granite	454511	6602407	53	1720	66.55	10.53	0.0956	0.511273	-26.6	-4.3	2.4	Budd and Skirrow (2007)
200363007A	Paton Granite	granite	454677	6602701	53	1720	64.87	10.71	0.0998	0.511312	-25.9	-4.5	2.4	Budd and Skirrow (2007)
200363008B	Paton Granite	granite	454701	6602759	53	1720	42.3	6.5	0.0926	0.511176	-28.5	-5.6	2.4	Budd and Skirrow (2007)
2000363005D	Paton Granite	granite	454912	6602702	53	1720	60.2	9.63	0.0967	0.511288	-26.3	-4.3	2.4	Budd and Skirrow (2007)
2074179	Pinbong Suite	granite	582288	6381741	53	1720	70.57	9.07	0.0777	0.510967	-32.6	-6.4	2.4	This study
2074177	Pinbong Suite	granite	638204	6272415	53	1720	10.93	3.37	0.1865	0.512172	-9.1	-6.9	2.7^	This study
2138658	Undifferentiated mafic (Lzp_1)	gabbro	505329	6772847	53	1720	14.15	3.4	0.1454	0.511781	-16.7	-5.4	3	This study
2138659	Undifferentiated mafic (Lzp_1)	gabbro	505329	6772847	53	1720	9.01	2.19	0.1467	0.511831	-15.7	-4.7	3	This study

a $^{143}Nd/^{144}Nd$ CHUR(0) = 0.512638, $^{147}Sm/^{144}Nd$ CHUR(0) = 0.1966.
b T_{DM} calculated using the single stage model of Goldstein *et al.* (1984).
^ = 2-stage T_{DM} calculated using 2 stage model of Liew and Hofmann (1988).
$\varepsilon_{Nd(T)}$ calculated at Age (Ma).
dup = duplicate.

Table 4. Sm-Nd data for the Moody Suite.

	Sample	Unit	Lithology	E	N	Zone	Age (Ma)	Nd (ppm)	Sm (ppm)	$^{147}Sm/^{144}Nd$	$^{143}Nd/^{144}Nd$	$\varepsilon_{Nd(0)}$[a]	$\varepsilon_{Nd(t)}$[b]	$T_{(DM)}$	Reference
Moody Suite	2138800	Yunta Well Leucogranite	granite	593166	6206547	53	1700	8.22	2.15	0.1582	0.511822	-15.9	-7.6	3.6	This study
	2138802	Yunta Well Leucogranite	granite	600783	6211339	53	1700	3.86	1.04	0.1624	0.512024	-12	-4.5	3.3	This study
	2138803	Moreenia Monzogranite	monzogranite	591059	6219435	53	1700	67.54	12.34	0.1104	0.511252	-27	-8.3	2.8	This study
	2138807	Moreenia Monzogranite	monzogranite	581079	6217709	53	1700	125.04	15.85	0.0766	0.511017	-31.6	-5.5	2.4	This study
	2138785	Uranno Microgranite	granite	583712	6208848	53	1700	83.73	12.63	0.0912	0.511175	-28.5	-5.6	2.4	This study
	2138783	Chinmina Monzonite	monzonite	577816	6199822	53	1700	67.53	13.64	0.1221	0.511396	-24.2	-8	2.9	This study
	2138791	Chinmina Monzonite	granite	581431	6205769	53	1700	147.52	19.82	0.0812	0.511011	-31.7	-6.6	2.4	This study
	2138782	?Moody Suite	granite	606702	6211550	53	1700	43.22	6.39	0.0895	0.510921	-33.5	-10.2	2.7	This study
	2138789	?Uranno Microgranite	granite	584924	6205289	53	1700	79.71	16.1	0.1221	0.511341	-25.3	-9.1	3	This study
	2138809	?Uranno Microgranite	granite	586571	6214994	53	1700	14.29	2.78	0.1178	0.51126	-26.9	-9.7	3	This study

a $^{143}Nd/^{144}Nd$ CHUR(0) = 0.512638, $^{147}Sm/^{144}Nd$ CHUR(0) = 0.1966.
b T_{DM} calculated using the single stage model of Goldstein *et al.* (1984).
^ = 2-stage T_{DM} calculated using 2 stage model of Liew and Hofmann (1988).
$\varepsilon_{Nd(T)}$ calculated at Age (Ma).
dup = duplicate.

MAJOR, TRACE AND RARE EARTH ELEMENT GEOCHEMISTRY

Moola Suite

The Moola Suite ranges in composition from granite, syenite, monzonite, monzodiorite and gabbro (Fig. 18a). On classification diagrams of Frost (2001) the Moola Suite can be broadly classified as magnesian, alkalic to calc-alkalic and metaluminous, with the majority of analyses from the Burkitt Granite (Figs 18b-c). Samples with >70 wt% SiO_2 transgress into the ferroan field of the Fe* diagram (Fig. 18b) and spread across all fields on the MALI diagram (Fig. 18c), affecting the Gluepot Granite, Wortham Granite and unnamed Moola Suite granites. The Moola Suite defines fractionation trends for CaO, MgO, P_2O_5, TiO_2 and Fe_2O_{3T} with increasing SiO_2, while Al_2O_3, Na_2O and K_2O display inflections around 57 wt% SiO_2 (Fig. 19). The Moola Suite is generally LREE-enriched relative to HREE and displays negative Nb, Ti and Sr anomalies, and negative P anomalies for less silicic rocks on primitive mantle-normalised trace element diagrams (Figs 20 and 21).

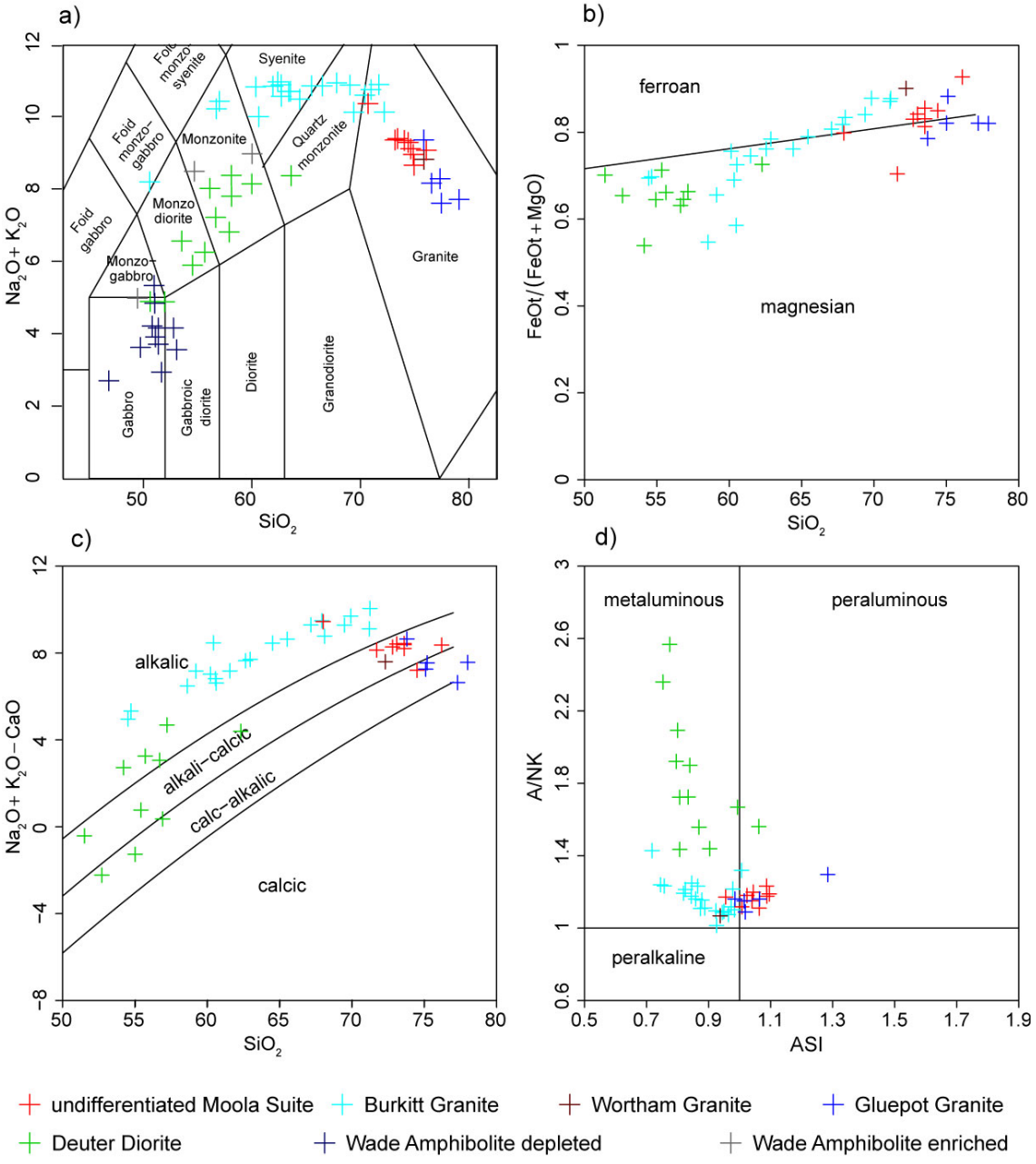

Figure 18. Classification diagrams for Moola Suite. (a) Total alkali silica diagram, (Middlemost, 1994). **(b)** Fe* vs SiO_2 diagram (Frost, 2001). Fe* = $FeO^{tot}/(FeO^{tot} + MgO)$. **(c)** Modified Alkali-Lime Index (MALI), (Frost, 2001). **(d)** Aluminium Saturation Index (ASI), (Frost, 2001).

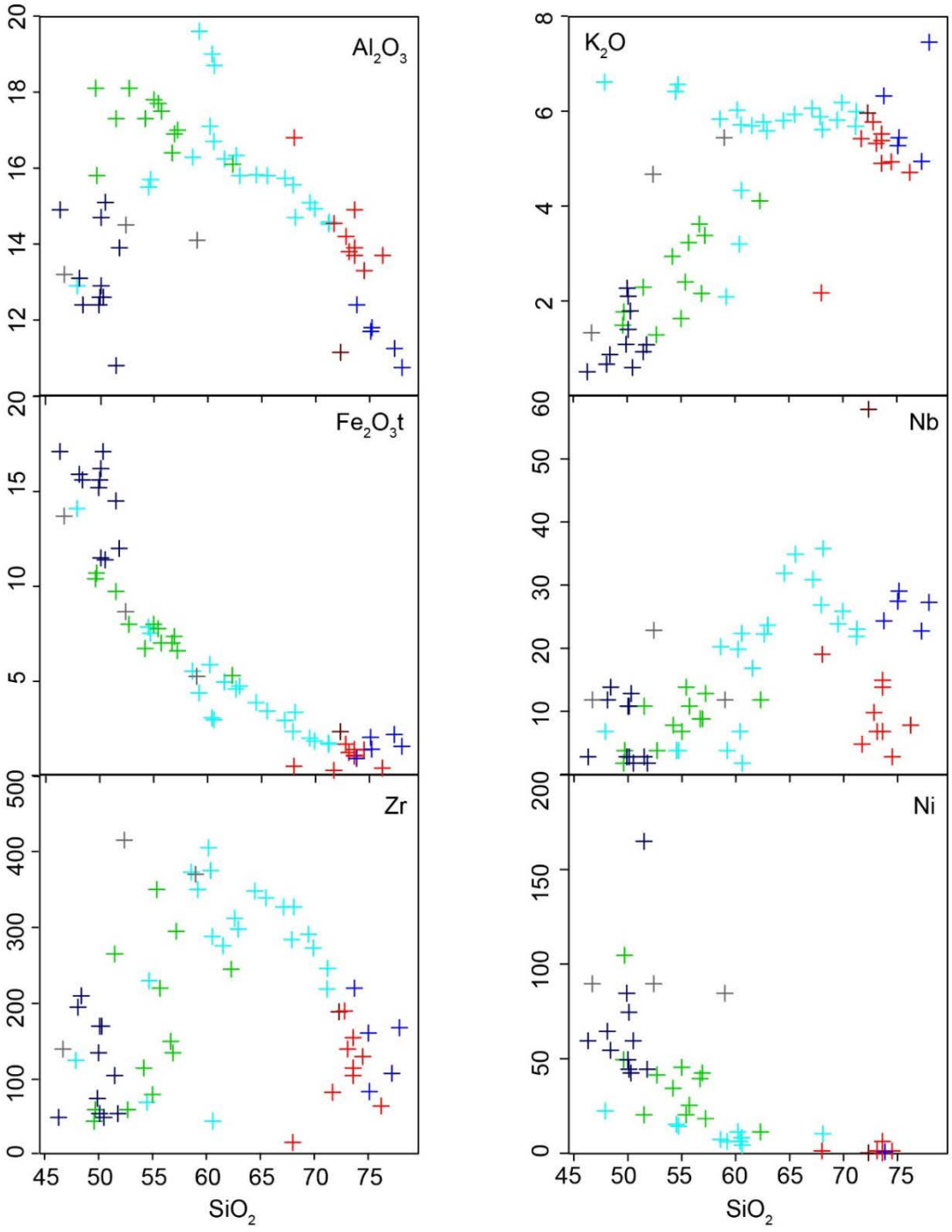

Figure 19. Selected major and trace element bivariate diagrams for Moola Suite. Symbols as per Figure 18.

Undifferentiated granites of the Moola Suite from the area west and southwest of Iron Duke are weakly peraluminous (ASI between 1.0 and 1.1), highly silicic with SiO_2 >70 wt% and depleted in all major elements except K_2O, indicating that these granites are the most fractionated rocks of the Moola Suite (Fig. 19). Trace element abundances for La, Ce, Nb and Th vary (Fig. 19). Primitive mantle-normalised trace element diagrams display strong negative anomalies for Nb, Ti and P, and strong positive U and Th anomalies, resulting in patterns similar to the Burkitt Granite (Fig. 20). REE patterns are generally smooth, except for two samples of undifferentiated Moola Suite granites which display irregular REE patterns (Fig. 21), and exhibit LREE enrichment relative the HREE ($(La/Yb)_N$ = 19.92–131.50). Most samples display weak negative Eu anomalies (Eu/Eu* = 0.69–0.91).

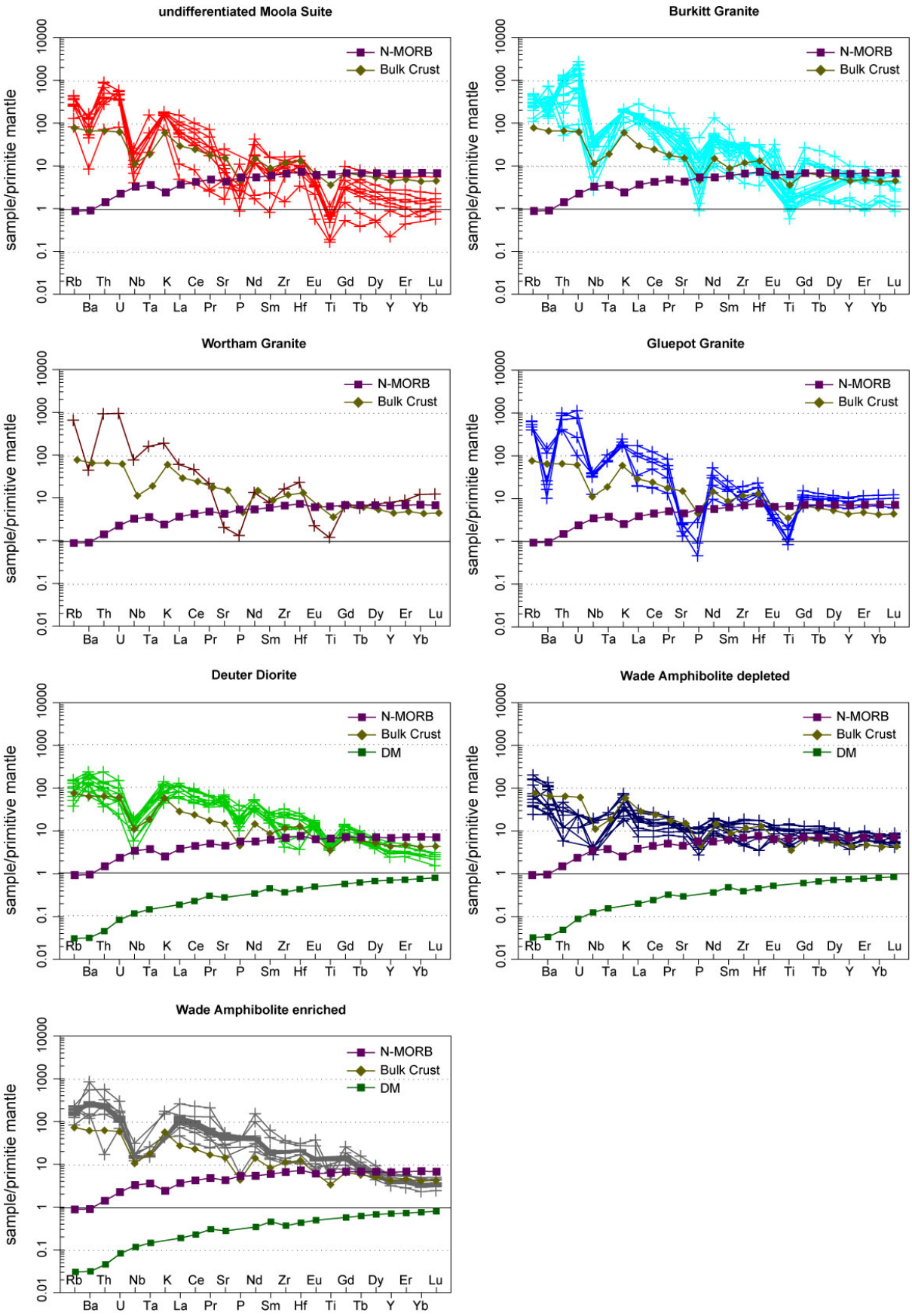

Figure 20. Trace element plots for Moola Suite, normalised to primitive mantle (values from Sun and McDonough (1989)). N-MORB (normal mid-ocean ridge basalt) values from Sun and McDonough (1989). Bulk crust values from Rudnick and Gao (2003). DM (depleted mantle) values from Taylor and McLennan (1985). For symbology see Figure 19.

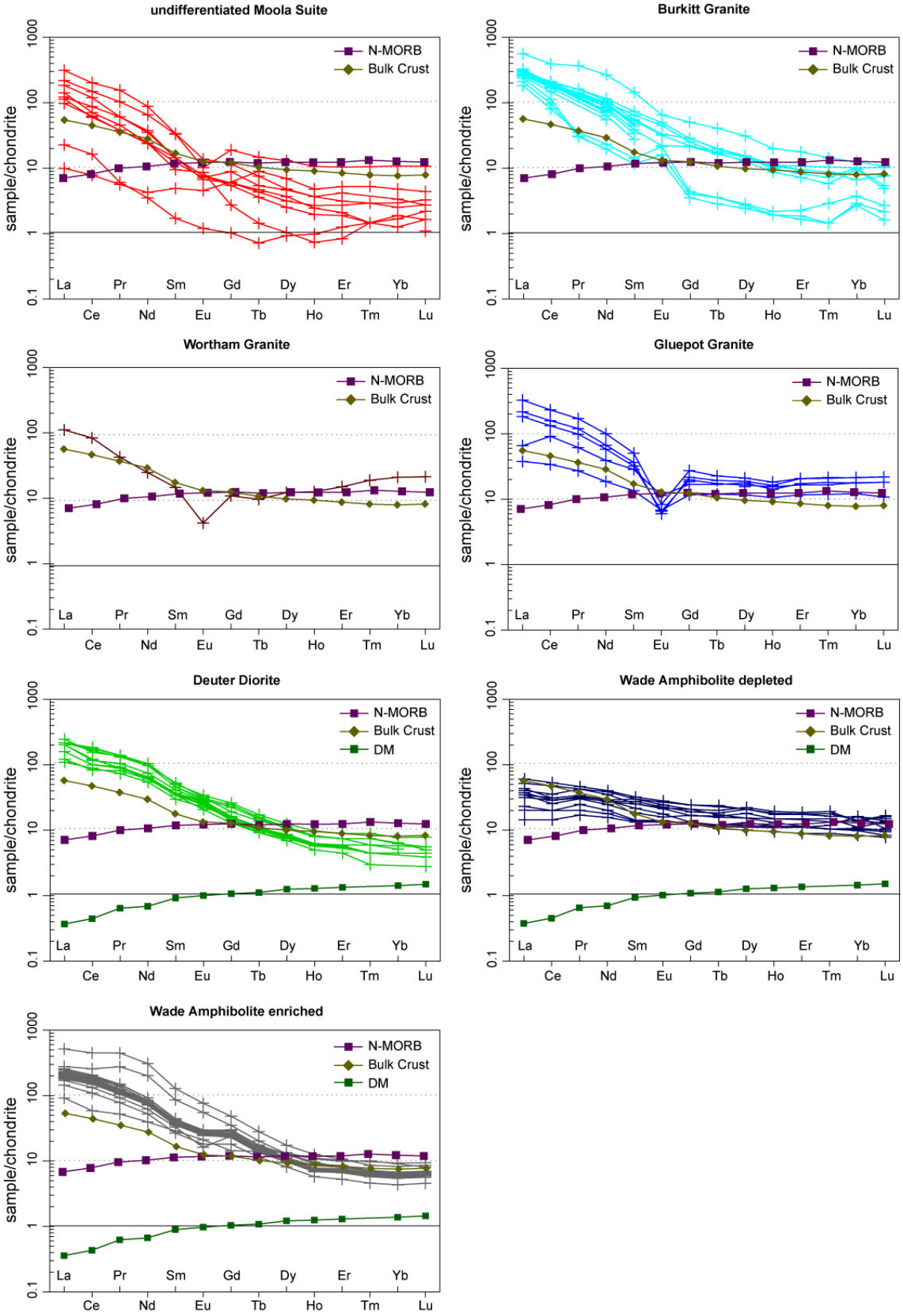

Figure 21. REE plots for Moola Suite, normalised to chondrite (values from (Taylor and McLennan, 1985)). N-MORB (normal mid-ocean ridge basalt) values from Sun and McDonough (1989). Bulk crust values from Rudnick and Gao (2003). DM (depleted mantle) values from Taylor and McLennan (1985). For symbology see Figure 19.

BURKITT GRANITE

The Burkitt Granite is magnesian to ferroan, alkalic and metaluminous (ASI = 0.6–1.0) syenite, quartz monzonite and granite, which is reflected by broad silica values ranging from 58.6–71.24 wt% (Fig. 18). It is characterised by elevated values for Na_2O+K_2O (9.8–10.8 wt%) and high field strength elements (HFSE) such as Nb, Zr, Y and LREE (Figs 19 and 21).

The Burkitt Granite forms linear trends for most major and trace elements (Fig. 19) with increasing fractionation indicating plagioclase, hornblende, biotite, K-feldspar and apatite were the main fractionating phases. Inflections occur at approximately 65 wt% silica for Nb, Th, Zr, Ce and La on trace element variation diagrams (Fig. 19). Strong negative Nb, Ti and P anomalies are present on primitive mantle-normalised trace element diagrams (Fig. 20). The Burkitt Granite displays smooth REE patterns with either slightly negative or distinctly positive Eu anomalies (Eu/Eu* 0.77–2.7) (Fig. 21).

WORTHAM GRANITE

Only one geochemical analysis exists for the Wortham Granite. This sample is a metaluminous and ferroan granite of alkali-calcic composition (Fig. 18). It has a high silica content (SiO_2 = 72.3 wt%) and is characterised by low Al_2O_3 and high Y and Nb compared with other Moola Suite granites (Fig. 19). The Wortham Granite sample has a REE pattern that is distinct from the undefined Moola Suite granites and Burkitt Granite, but is similar to the Glue Pot Granite (Fig. 21).The Wortham Granite is HREE enriched [$(La/Yb)_N$ = 5.6] and a has an obvious negative Eu anomaly (Eu/Eu* = 0.33) (Fig. 21).

GLUEPOT GRANITE

The Gluepot Granite is a predominantly magnesian, alkali-calcic to calc-alkalic, peraluminous granite (Fig. 18). This granite is also characterised by low Al_2O_3 and high K_2O, Nb and Y compared with undefined Moola Suite granites of comparible silica contents (Fig. 19). Normalised trace element diagrams for the Gluepot Granite are similar to undefined Moola Suite granites, characterised by negative Ba, Nb, Sr, P and Ti anomales (Fig. 20). REE patterns, however, are distinct and show a HREE-enrichment [$(La/Yb)_N$ = 3.3–16.1] when compared to the Burkitt Granite and unnamed Moola Suite granites. Eu anomalies are moderately to distinctly negative (Eu/Eu* = 0.21–0.54) (Fig. 21).

DEUTER DIORITE

The Deuter Diorite is a calc-alkaline to alkalic, magnesian and metaluminous monzodiorite to monzonite (Fig. 18). SiO_2 values range from 49.6–62.3 wt%. Al_2O_3, CaO, P_2O_5, MgO, TiO_2 and Fe_2O_{3T} define negative trends with increasing silica (Fig. 19), which is consistent with fractionation of the main mineral phases in Deuter Diorite e.g. plagioclase, K-feldspar, quartz, hornblende and biotite. K_2O and Na_2O increase with increasing silica. Trace element abundances are variable and elements such as Nb and Zr increase with increasing silica (Fig. 19). The Deuter Diorite displays strong negative Nb anomalies and moderate negative Ti and P anomalies on primitive mantle-normalised trace element diagrams (Fig. 20). REE profiles are steep and smooth, with enrichment in the LREE relative to the HREE [$(La/Yb)_N$ = 11.6–37.1)] (Fig. 21).

WADE AMPHIBOLITE

The Wade Amphibolite consists of two geochemical groups; depleted amphibolite, with a low $(La/Yb)_N$ value, and enriched amphibolite, with a high $(La/Yb)_N$ value. The depleted Wade Amphibolite crops out 5.7 km southeast of Burkitt Hill, 12.7 km south of Iron Knob (Cooyerdoo Hill), 7.5 km and 5.8 km northwest of Iron Duke and 6.6 km southwest of Iron Duke (Fig. 4). It also occurs in form of a dolerite xenolith within the Deuter Diorite in DDH LED001 (drillhole 229988) in the interval 595.0–603.0 m. The enriched Wade Amphibolite crops out ~7.5 km northwest of Iron Duke and 4.3 km southwest of Iron Duke (Fig. 4). It is also intersected in RDD002 (drillhole 229989) ~15 km southwest of Iron Knob.

The depleted Wade Amphibolite includes tholeiitic (Fig. 22) gabbro, gabbroic diorite, and monzogabbro with narrow range of SiO_2 values from 48.1–51.8 wt% (Fig. 18). Samples of this

depleted amphibolite display primitive geochemical signatures that include enrichments in CaO, MgO, Fe_2O_{3T}, TiO_2, Ni, Cr and Yb (Figs 18 and 19). Primitive mantle-normalised trace element patterns are relatively flat with moderate troughs in Nb, P, Hf and Ti and peaks in large ion lithophile elements (Rb, Ba and K; Fig. 20). REE profiles are distinct from all other mafic Moola Suite rocks: they are almost flat with only slight enrichments in La compared to Yb [$(La/Yb)_N$ = 1.4–3.6] (Fig. 21). LREE are slightly more enriched than typical E-MORB values, while MREE and HREE values are similar (Fig. 21).

The enriched Wade Amphibolite samples are calc-alkaline (Fig. 22) and metaluminous (ASI = ~0.7) gabbros and monzonites. Major and trace element abundances are similar to Deuter Diorite (Fig. 18). The enriched Wade Amphibolite is notably characterised by high $(La/Yb)_N$ ratios (10.8–66.4; typically ~35) which is reflected by steep REE profiles with LREE enrichment (Fig. 21). Eu anomalies are almost absent (Eu/Eu* = ~0.9).

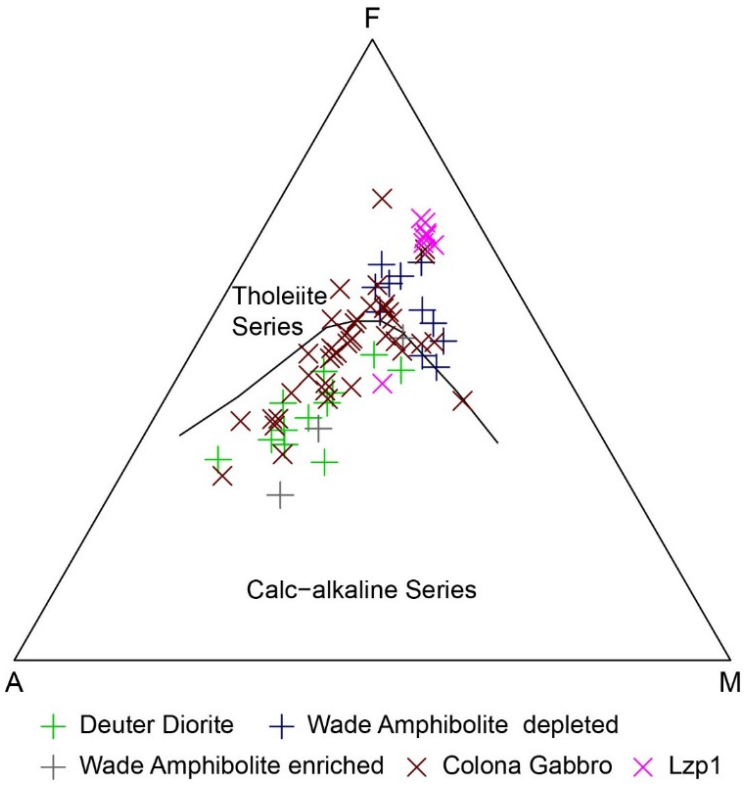

Figure 22. AFM classification diagram for mafic rocks of the Moola and Pinbong suites.

Pinbong Suite

The Pinbong Suite is predominantly granitic in composition, with SiO_2 values typically greater than 68 wt%, but also contains quartz monzonite and monzonite (Fig. 23). Mafic to intermediate intrusives range from peridotitic-gabbroic rocks to granodiorites (Fig. 22). Granitic rocks are mostly peraluminous to lesser metaluminous, while the gabbroic rocks are metaluminous and enriched in alkalis. Granitic rocks are largely magnesian, alkali-calcic and peraluminous (Fig. 23). The Pinbong Suite displays fractionation trends for CaO, MgO, TiO_2 and Fe_2O_{3T} with increasing silica (Fig. 24). Na_2O and K_2O display much scatter on bivariate diagrams against silica (Fig. 24), suggesting mobility of these elements due to alteration. In general, the Pinbong Suite displays negative anomalies for Ba, Nb, P and Ti on primitive mantle-normalised trace element diagrams (Fig. 25), and shows enrichments in LREE (Fig. 26).

Undifferentiated Pinbong Suite granites have high silica contents (67.4–77.5 wt% SiO_2), high K_2O, and low Al_2O_3, CaO, MgO, Fe_2O_{3T}, TiO_2 and P_2O_5 abundances (Fig. 24). These granites display strong negative Ti, Nb, Sr and P anomalies on primitive mantle-normalised trace element diagrams (Fig. 25). They have very steep REE profiles due to enrichment in LREE relative to HREE

[$(La/Yb)_N$ vales of 64–158] and increasing depletion in HREE (Fig. 26). Several granites, however, are characterised by a higher abundance of HREE with $(La/Yb)_N$ values between 4.8 and 23 resulting in relatively flat HREE profiles. All undifferentiated Pinbong Suite granites have strong negative Eu anomalies (Eu/Eu* 0.24–0.56).

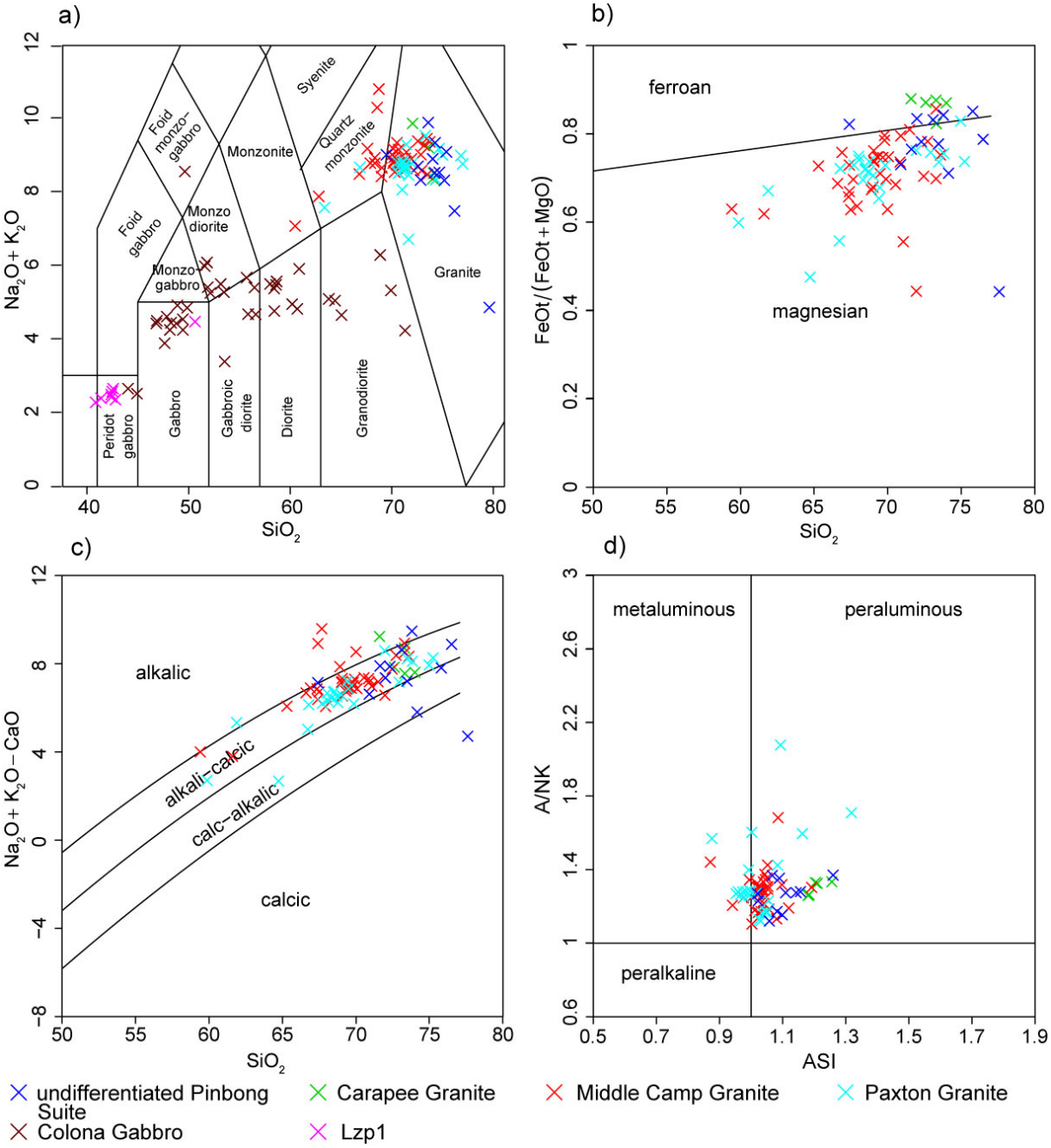

Figure 23. Classification diagrams for Pinbong Suite. (a) Total alkali silica diagram, (Middlemost, 1994). **(b)** Fe* vs SiO_2 diagram (Frost, 2001). Fe* = $FeO^{tot}/(FeO^{tot}$ + MgO). **(c)** Modified Alkali-Lime Index (MALI), (Frost, 2001). **(d)** Aluminium Saturation Index (ALI), (Frost, 2001).

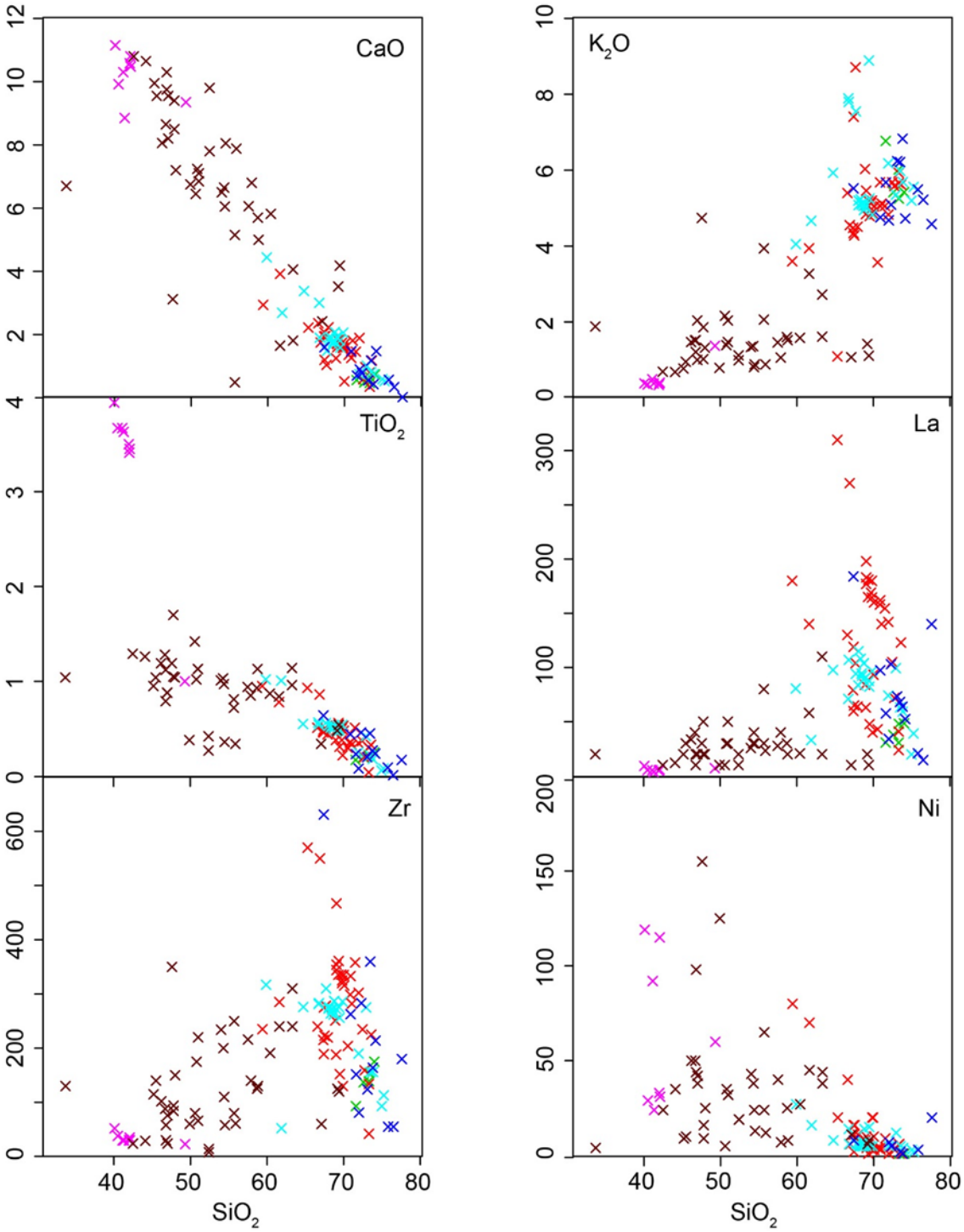

Figure 24. Selected major and trace element bivariate diagrams for Pinbong Suite. For symbology see Figure 23.

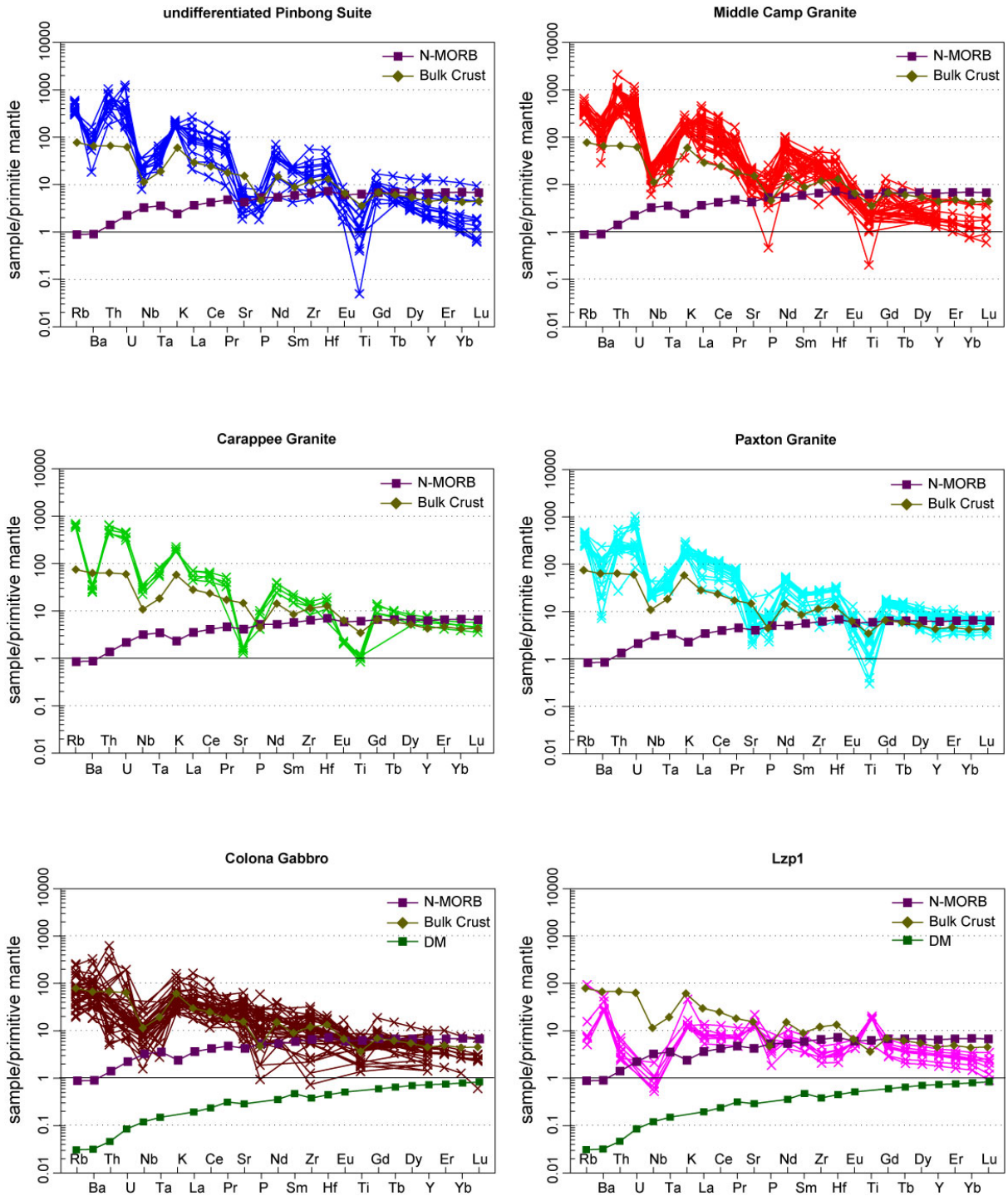

Figure 25. Trace element plots for Pinbong Suite, normalised to primitive mantle (values from Sun and McDonough (1989)). N-MORB (normal mid-ocean ridge basalt) values from Sun and McDonough (1989). Bulk crust values from Rudnick and Gao (2003). DM (depleted mantle) values from Taylor and McLennan (1985).For symbology see Figure 23.

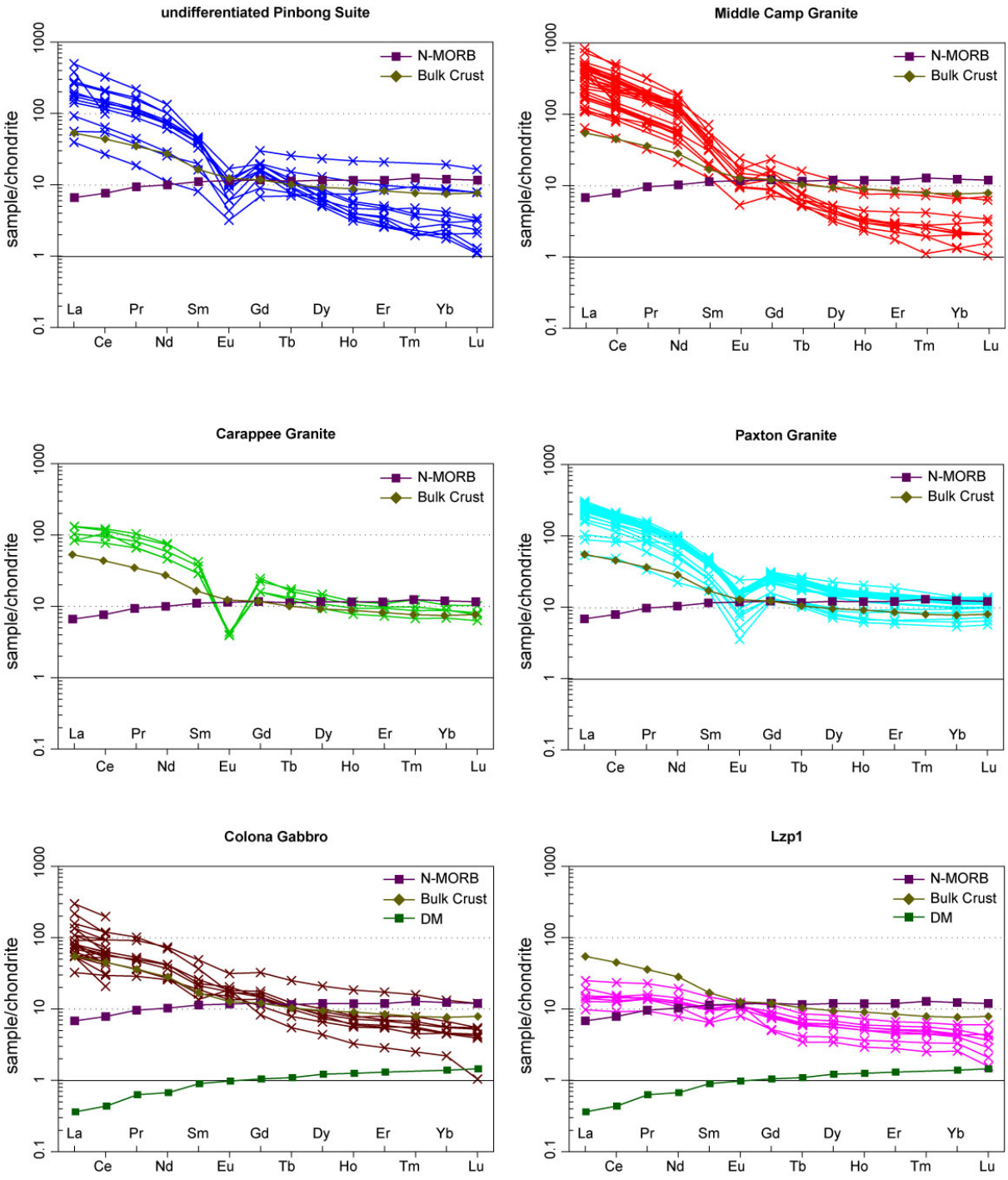

Figure 26. REE plots for Pinbong Suite, normalised to chondrite (values from (Taylor and McLennan, 1985)). N-MORB (normal mid-ocean ridge basalt) values from Sun and McDonough (1989). Bulk crust values from Rudnick and Gao (2003). DM (depleted mantle) values from Taylor and McLennan (1985). For symbology see Figure 23.

MIDDLE CAMP GRANITE

The Middle Camp Granite plots predominantly as granite to lesser quartz monzonite and monzonite on a TAS classification diagram (Fig. 23a). It is classified as magnesian, alkali-calcic and peraluminous (Fig 23b-d). It is an intermediate to high silica granite (59.4–76.5 wt% SiO_2) with high Al_2O_3, P_2O_5 and Na_2O abundances relative to other Pinbong Suite granites. More mafic end members (SiO_2 <65 wt%) have elevated CaO, MgO, TiO_2 and Fe_2O_{3T} contents (Fig. 24). The Middle Camp Granite displays decreases in Al_2O_3, CaO, MgO, P_2O_5, TiO_2 and Fe_2O_{3T} with increasing silica, indicating the fractionating mineral phases were biotite, plagioclase, K-feldspar, apatite and titanite.

The Middle Camp Granite displays high abundances of trace elements such as La, Ce, Th and Zr relative to other Pinbong Suite granites (Fig. 24). Ni and Cr are elevated in the more mafic end members. Primitive mantle-normalised trace element plots are characterised by negative Nb, P and Ti anomalies and positive Th anomalies (Fig. 25). The Middle Camp Granite displays steep REE profiles ($(La/Yb)_N$ = 18–375) and Eu anomalies are moderately negative (Eu/Eu* = 0.45–0.81; Fig. 26).

CARAPPEE GRANITE

The Carappee Granite is a high silica and peraluminous granite (Fig. 23). It plots exclusively in the ferroan field on Fig. 23b; however this may be due to high silica influencing its FeO-MgO contents. It is predominantly alkali-calcic on the MALI diagram (Fig. 23c).

The Carappee Granite has relatively high K_2O contents, moderate Al_2O_3 and P_2O_5 contents and low abundances of CaO, TiO_2 and Fe_2O_{3T}. (Fig. 24). It is enriched in Nb and Y, and depleted in La, Ce, Ba, Zr and Th compared to other high silica Pinbong Suite granites (Fig. 24). Primitive mantle-normalised trace element patterns are characterised by negative Ba, Nb, Sr and Ti anomalies (Fig. 25). The REE signature for the Carappee Granite is charaterised by strong negative Eu anomalies (Eu/Eu* = 0.12–0.20) and relatively flat LREE and HREE patterns (Fig. 26), with $(La/Yb)_N$ = 10.07–15.78.

PAXTON GRANITE

The Paxton Granite has a wide range of silica values of 59.8–75.2 wt% and is predominantly magnesian, alkali-calcic and metaluminous to peraluminous (Fig. 23). Samples of the Paxton Granite define crystallisation trends for Al_2O_3, CaO, P_2O_5, Fe_2O_{3T}, TiO_2 and MgO (Fig. 24). Other major and trace elements show values similar to those of the Middle Camp Granite and undifferentiated granites of the Pinbong Suite with comparable silica contents (Fig. 24). Trace element patterns are characterised by strong negative Nb and Ti anomalies on primitive mantle-normalised trace element diagrams (Fig. 25). Rare earth element patterns are fractionated with strong LREE enrichment relative to HREE (Fig. 26). The Paxton Granite samples display strong negative Eu anomalies (Fig. 26) indicating fractionation of plagioclase.

COLONA GABBRO

The Colona Gabbro includes metaluminous to weakly peraluminous, tholeiitic to calc-alkaline gabbros to granodiorites (Figs 22 and 23). The Colona Gabbro forms fractionation trends for major elements such as CaO, MgO, P_2O_5 and Fe_2O_{3T} with increasing silica (Fig. 24).

In general, the Colona Gabbro is characterised by low trace element abundances for La, Ce, Nb, U and Th, while Cr and Ni are enriched (Fig. 24).

Primitive mantle-normalised trace element patterns for the Colona Gabbro are characterised by negative Nb anomalies and some samples display distinctly negative P anomalies (Fig. 25). The Colona Gabbro displays significant variation in trace element abundances compared with Lzp_1 (Fig. 25), for example. These variations may be a reflection of different batches of melts and trace element patterns closely resemble a lower (mafic) crustal composition. LREE are moderately enriched relative to HREE [$(La/Yb)_N$ 5.1–30.3] and Eu anomalies are weakly negative to strongly positive (Fig. 26) (Eu/Eu* = 0.79–1.75). LREE abundances are similar to those of the depleted

Wade Amphibolite, however, the Colona Gabbro is more depleted in HREE suggesting a garnet-dominant source region.

UNNAMED MAFICS OF THE PINBONG SUITE (MAP SYMBOL Lzp_1)

Lzp_1 samples range from predominantly tholeiitic gabbros to rare calc-alkaline gabbro (Figs 22 and 23). The majority of Lzp_1 are high Mg-Ti gabbros (MgO >6 wt%; TiO_2 >4 wt% and SiO_2 <52 wt%), with high Fe_2O_{3T} and CaO contents (Fig. 24). Al_2O_3, K_2O, P_2O_5 and Na_2O contents are lower than those of the Colona Gabbro (Fig. 24). Lzp_1 samples are enriched in Fe_2O_{3T} and TiO_2 in comparison to the Wade Amphibolite samples at comparable MgO contents. Lzp_1 is also enriched in Cr and Ni, and depleted in HFSE (Zr, Nb, Th and U) and REE (Fig. 25).

Primitive mantle-normalised trace element plots for Lzp_1 are characterised by low Th, U and Nb contents (close to primitive mantle values) and positive Ti anomalies are observed (Fig. 25). REE profiles are moderately flat, with slight LREE enrichments relative to HREE (Fig. 26) [$(La/Yb)_N$ = 3–8]. Lzp_1 is also characterised by positive to no Eu anomalies (Eu/Eu* = 0.95–1.97). Lzp_1 contains the most REE-depleted samples compared to all other mafic units in the Peter Pan Supersuite (Fig. 26).

Primitive mantle-normalised trace element patterns of Lzp_1 differ from Wade Amphibolite, namely by positive Ti anomalies and depletions in most trace elements (Figs 25 and 26). REE patterns are also unique; overall Lzp_1 display greater REE depletion compared with other mafic units of the Peter Pan Supersuite, although LREE are enriched relative to HREE, and display positive to no Eu anomalies (Fig. 26).

Moody Suite

The Moody Suite is predominantly granitic to monzonitic in composition, with silica values ranging from 55.6 to 77.4 wt% (Fig. 27). It is predominantly ferroan, calc-alkalic to alkali-calcic and predominantly peraluminous (Fig 27). The Moody Suite displays fractionation trends for P_2O_5, Fe_2O_{3T}, and La with increasing SiO_2 (Fig. 28). Na_2O and Th have a scattered distribution on bivariate diagrams against SiO_2, suggesting mobility of these elements due to alteration (Fig. 28). In general, the Moody Suite displays negative anomalies for Ba, Nb, P and Ti on primitive mantle-normalised trace element diagrams (Fig. 29), and shows neutral to negative Eu anomalies and flat to steep REE patterns with enrichment in LREE relative to HREE (Fig. 30).

YUNTA WELL LEUCOGRANITE

The Yunta Well Leucogranite has a very narrow silica abundance ranging from 72.2–75.4 wt% (Fig. 27). It can be classified as a magnesian and ferroan, alkali-calcic peraluminous granite on the Frost (2001) classification diagrams (Fig. 27a-d). The Yunta Well Leucoranite is characterised by high Na_2O and low Fe_2O_{3T}, MgO, TiO_2, CaO and moderate to low P_2O_5 and K_2O. P_2O_5 and K_2O lie on separate trends to the other Moody Suite granites (Fig. 28). The Yunta Well Leucogranite is also characterised by low REE (Ce and La), Y, Zr, Th and Ba (Fig. 28). On a primitive mantle-normalised trace element diagram, the Yunta Well Leucogranite displays strong negative anomalies for Ba, Nb, Sr and Ti (Fig. 29). REE patterns are distinctive for the Yunta Well Leucogranite compared with the rest of the Moody Suite (Fig. 30). LREE abundances are similar to N-MORB values and MREE and HREE are similar to bulk crust (Fig. 30). REE profiles are almost flat or show a slight decline in HREE compared to LREE [Eu/Eu* = 0.99–1.07; $(La/Yb)_N$ = 1.98–4.78], with only one sample displaying a negative Eu anomaly (Eu/Eu* = 0.28).

MOREENIA MONZOGRANITE

The Moreenia Monzogranite is an intermediate silica (66.–72.7 wt% SiO_2) granite to lesser quartz monzonite (Fig. 27a). It is classified as ferroan, alkali-calcic and predominantly peraluminous (Fig. 27b-d). The Moreenia Monzogranite plots between the Chinmina Monzonite and Yunta Well Leucogranite on major and trace element bivariate diagrams against SiO_2 (Fig. 28). Major elements such as CaO, TiO_2 and Fe_2O_{3T} display a decrease with degree of fractionation. Primitive mantle-normalised trace element patterns display negative Nb, P and Ti anomalies (Fig. 29). The Moreenia Monzogranite is a relatively fractionated phase of the Moody Suite with $(La/Yb)_N$ values

ranging between 21.84–55.26 and Eu/Eu* values of 0.25–0.70. LREE are enriched relative to HREE and negative Eu anomalies are moderate (Fig. 30).

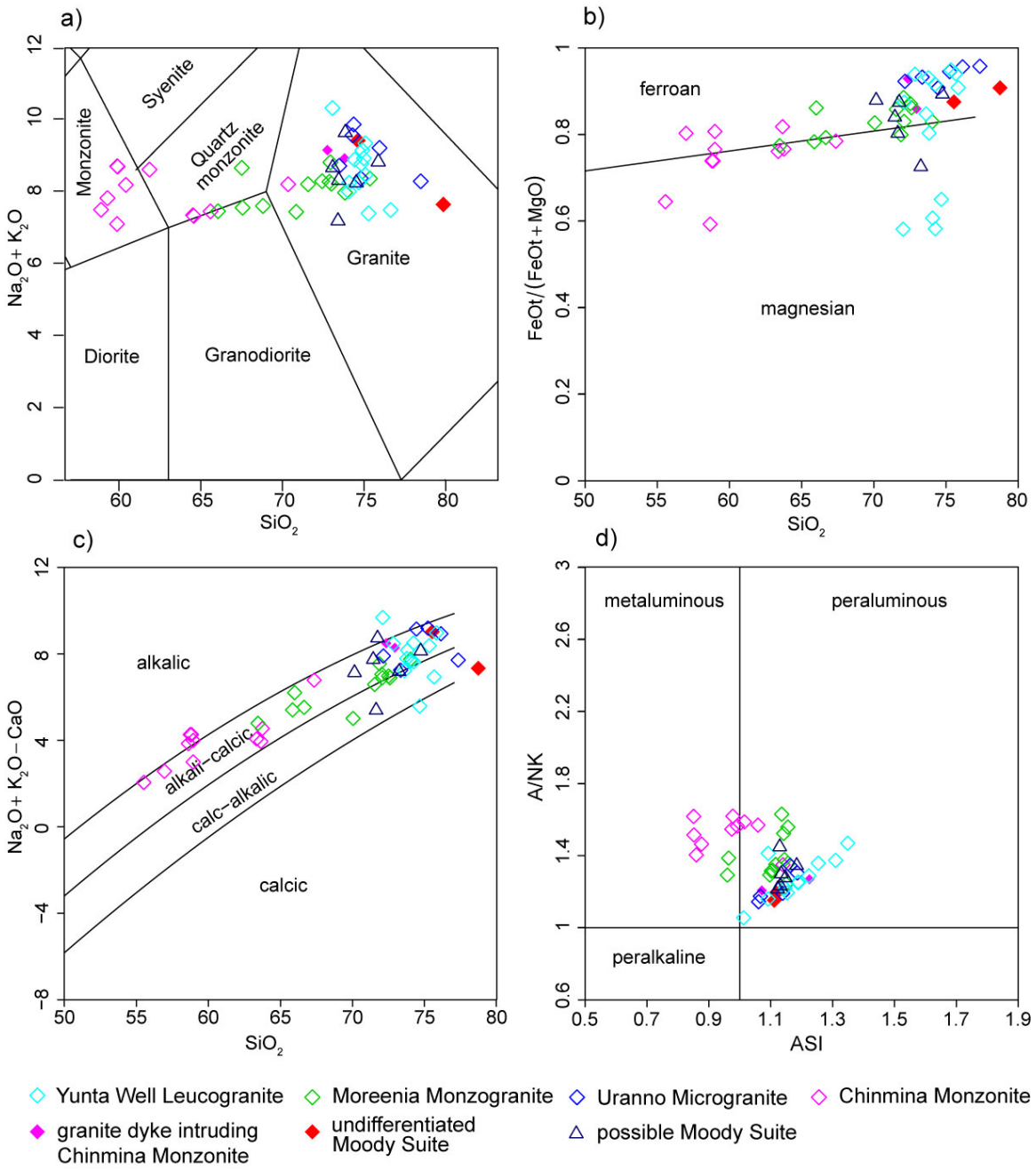

Figure 27. Classification diagrams for Moody Suite. (a) Total alkali silica diagram, (Middlemost, 1994). **(b)** Fe* vs SiO2 diagram (Frost, 2001). Fe* = $FeO^{tot}/(FeO^{tot} + MgO)$. **(c)** Modified Alkali-Lime Index (MALI), (Frost, 2001). **(d)** Aluminium Saturation Index (ALI), (Frost, 2001).

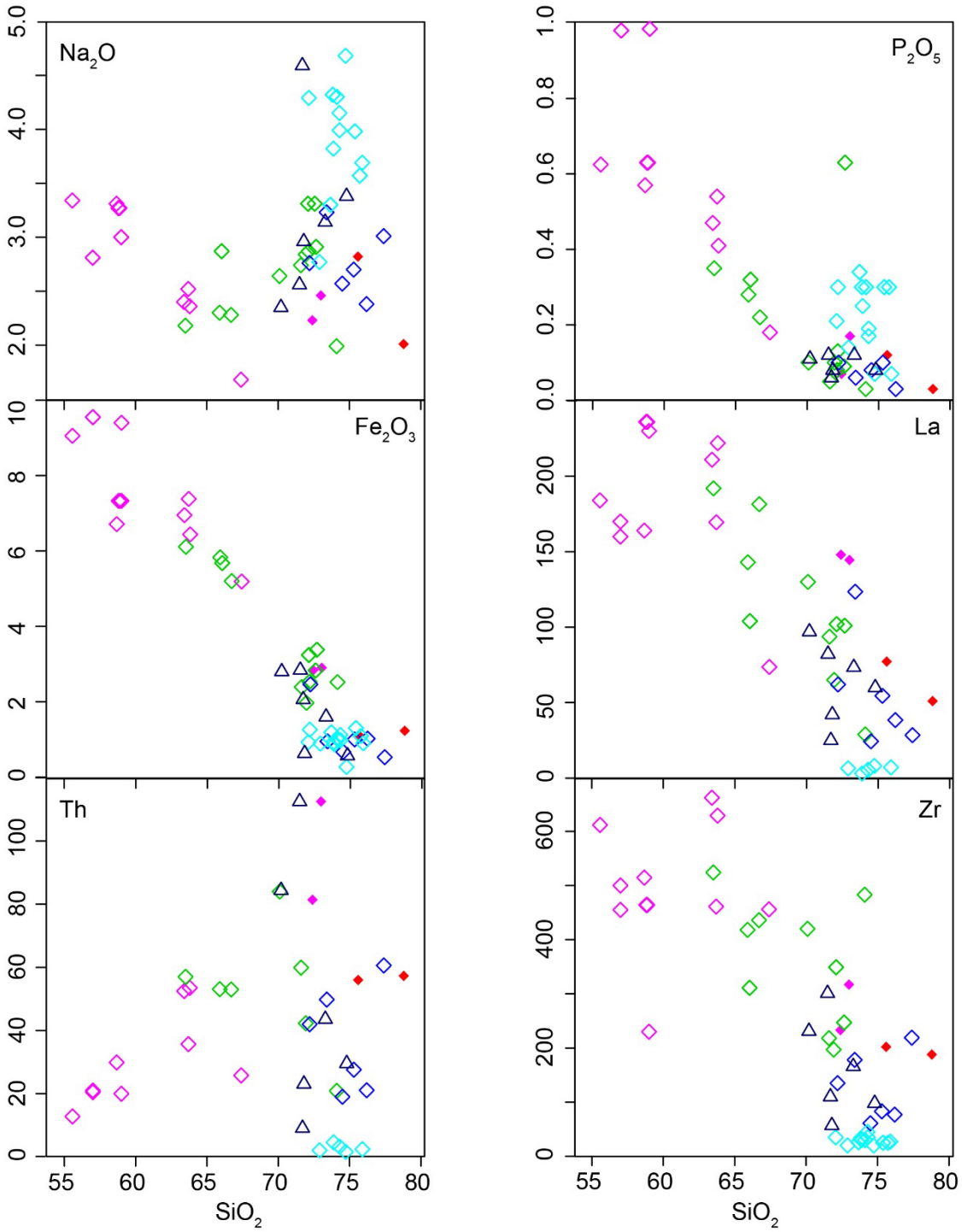

Figure 28. Selected major and trace element bivariate diagrams for Moody Suite. For symbology see Figure 27.

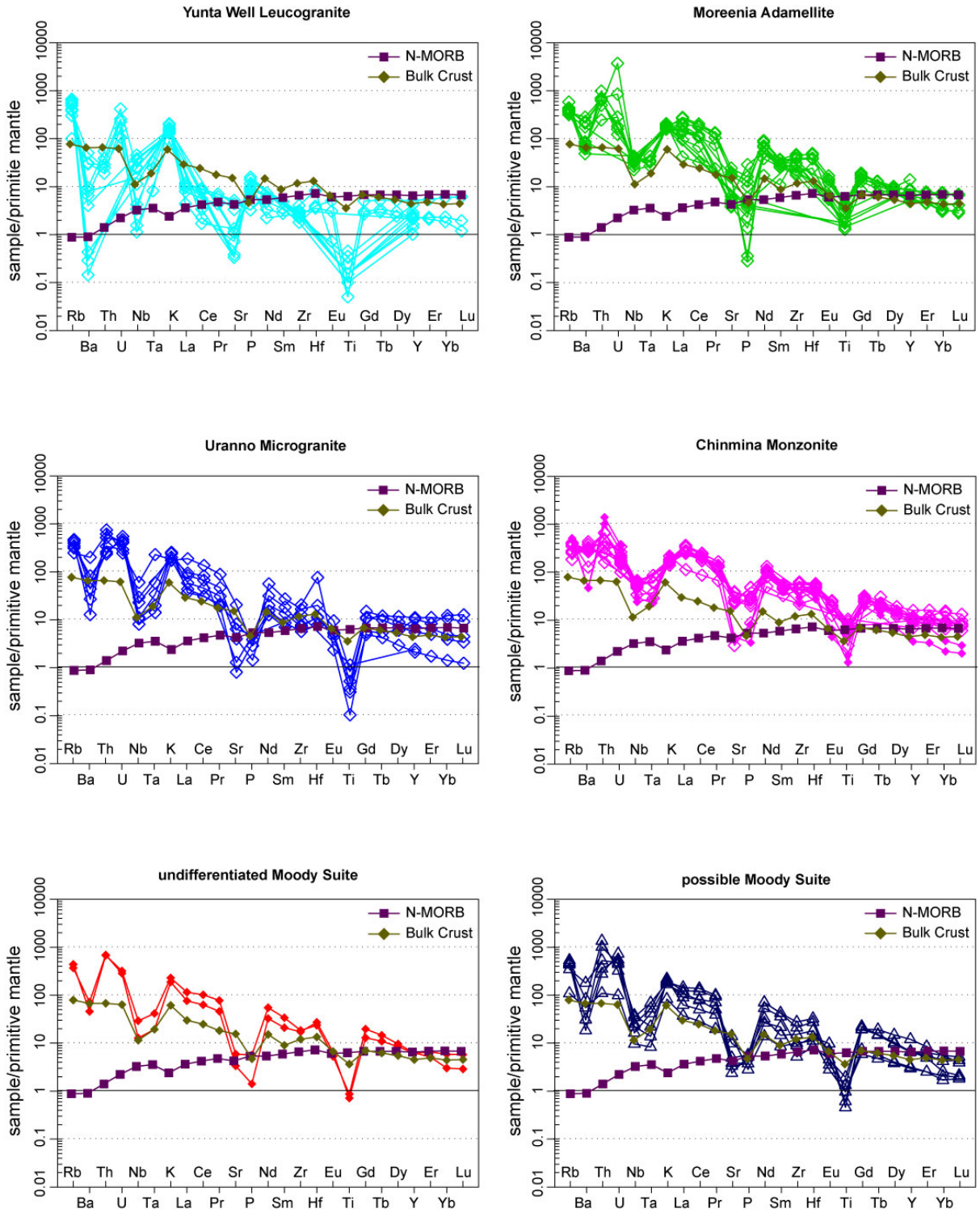

Figure 29. Trace element plots for Moody Suite, normalised to primitive mantle (values from Sun and McDonough (1989)). N-MORB (normal mid-ocean ridge basalt) values from Sun and McDonough (1989). Bulk crust values from Rudnick and Gao (2003). DM (depleted mantle) values from Taylor and McLennan (1985). For symbology see Figure 28.

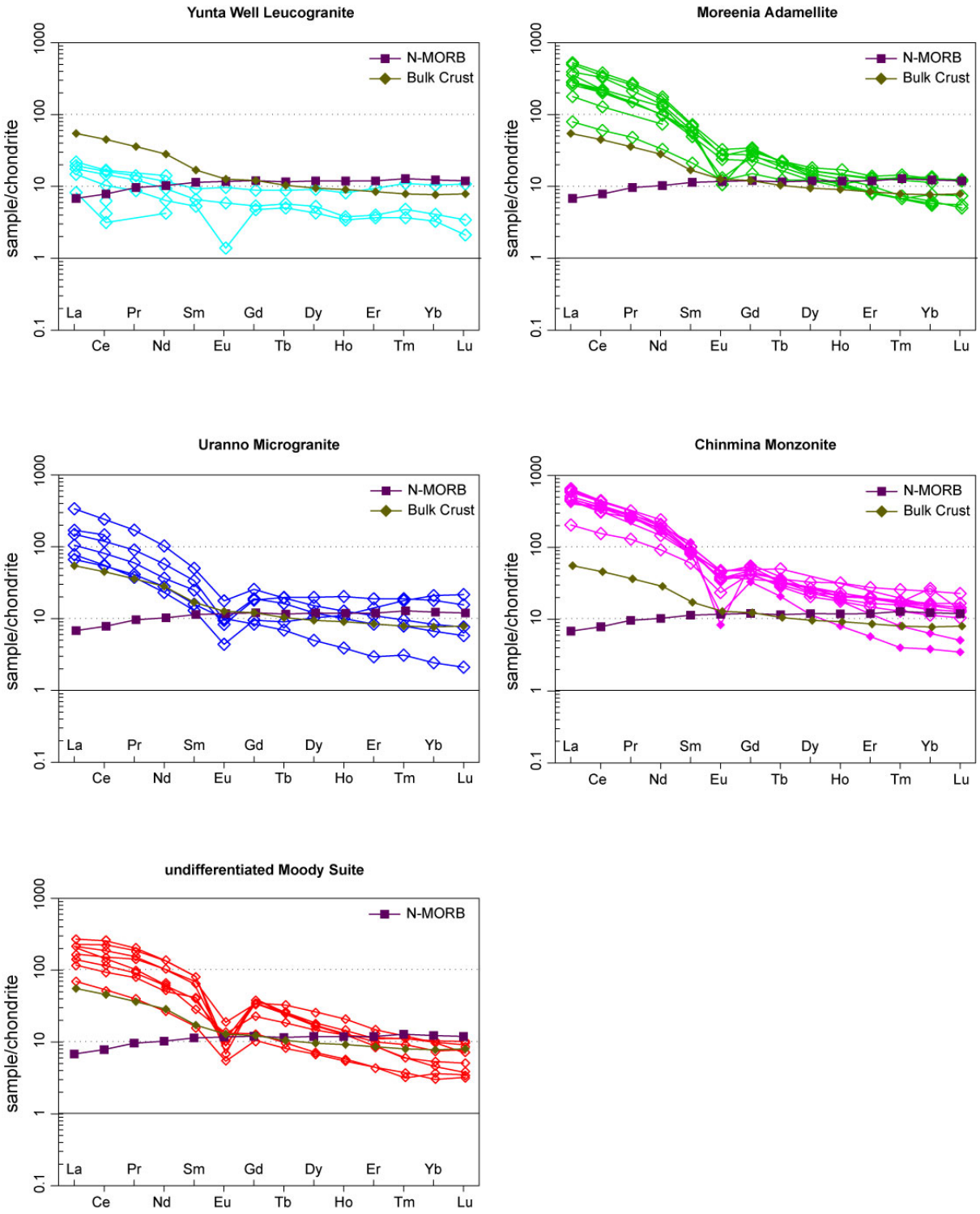

Figure 30. REE plots for Moody Suite, normalised to chondrite (values from (Taylor and McLennan, 1985)). N-MORB (normal mid-ocean ridge basalt) values from Sun and McDonough (1989). Bulk crust values from Rudnick and Gao (2003). DM (depleted mantle) values from Taylor and McLennan (1985). For symbology see Figure 25.

URANNO MICROGRANITE

The Uranno Microgranite is a high silica (SiO_2 72.2–77.4 wt%), ferroan, alkali-calcic, peraluminous granite (Fig. 27). It is characterised by low MgO, P_2O_5 and Fe_2O_{3T} contents (Fig. 28). While silica values are the comparable to the Yunta Well Leucogranite, the Uranno Microgranite has lower Na_2O and P_2O_5, and higher La, Ce, Th, Zr, Yb and Ba (Fig. 28). Trace element patterns are generally similar to other Moody Suite samples, however the Uranno Microgranite has negative Ba and Ti anomalies more pronounced than the Moreenia Monzogranite but less pronounced than the Yunta Well Leucogranite (Fig. 29). REE abundances and patterns are similar to the Moreenia Monzogranite except two samples are HREE enriched [$(La/Yb)_N$ = 3.94–6.2], and one sample is HREE depleted with no Eu anomaly (Eu/Eu* = 0.87; Fig. 30).

CHINMINA MONZONITE

The Chinmina Monzonite ranges from monzonite to quartz monzonite, and is ferroan to magnesian, alkali-calcic and predominantly metaluminous (Fig. 27). It has low SiO_2 (55.6–59 wt% SiO_2), high Al_2O_3, CaO, TiO_2, Fe_2O_{3T}, P_2O_5 and MgO (Fig. 28). Decreasing CaO, Al_2O_3, Fe_2O_{3T}, TiO_2 and increasing K_2O with increasing silica (Fig. 28) suggest the main fractionating phases were hornblende, titanite and microcline. The Chinmina Monzonite also displays enrichments in Ba, La, Ce, Zr, Nb and Y compared to the other Moody Suite granites (Fig. 28). On N-MORB normalised trace element diagrams the Chinmina Monzonite exhibits moderate negative Nb and Ti anomalies (Fig. 29). Chondrite normalised REE patterns for the Chinmina Monzonite are relatively steep, with enrichment in LREE relative to HREE ($(La/Yb)_N$ = 35.01–46.51) and slight negative Eu anomalies (Eu/Eu* = 0.65–0.68) (Fig. 30).

Granitic dykes intruding the Chinmina Monzonite have high SiO_2 contents (72.4 and 73 wt%), and are ferroan, calc-alkalic to alkali-calcic and peraluminous (Fig. 27). Major element abundances overlap with other felsic units of the Moody Suite (Fig. 28). La, Ce and Th are enriched compared to other Moody Suite granites with similar silica contents, while other trace elements are similar (Fig. 28). Normalised trace element patterns are distinct from the Chinmina Monzonite but appear similar to Uranno Microgranite, with negative Ba, Nb, Sr, P and Ti anomalies (Fig. 29). REE patterns, however, are unique in the granite dykes samples, with very steep profiles ($(La/Yb)_N$ = 67.31–114.15) and extremely negative Eu anomalies (Eu/Eu* = 0.1–0.23), indicating this phase is the most fractionated in the Moody Suite (Fig. 30).

SM-ND ISOTOPE GEOCHEMISTRY

Moola Suite

$^{143}Nd/^{144}Nd$ ratios for all Moola Suite granites range from 0.510720–0.511132 and $^{147}Sm/^{144}Nd$ ratios from 0.0753–0.1004. T_{DM} ages for the granites are 2.5 and 2.7 Ga with moderately evolved $\varepsilon_{Nd(1735)}$ values of -6.8 to -3.6 (Fig. 31).

$^{143}Nd/^{144}Nd$ ratios for Burkitt Granite range from 0.510485–0.511063 and $^{147}Sm/^{144}Nd$ ratios from 0.0849–0.0932. Nd values are very evolved and vary significantly for the Burkitt Granite, with $\varepsilon_{Nd(1740\ Ma)}$ = -17.1 to -7.7. The most evolved sample (-17.1) has the oldest T_{DM} and lowest $^{143}Nd/^{144}Nd$ and $^{147}Sm/^{144}Nd$ ratios. T_{DM} ages for the Burkitt Granite range from 2.6 to 3.1 Ga.

The Wortham Granite has a $^{143}Nd/^{144}Nd$ of 0.511565 and $^{147}Sm/^{144}Nd$ ratio of 0.1136. $\varepsilon_{Nd(1740\ Ma)}$ = -2.4 with a T_{DM} of 2.4 Ga.

The Deuter Diorite has a $^{143}Nd/^{144}Nd$ ratio of 0.511307 and $^{147}Sm/^{144}Nd$ ratio of 0.1024, $\varepsilon_{Nd(1740\ Ma)}$ = -4.9 and T_{DM} of 2.5 Ga. $^{143}Nd/^{144}Nd$ ratios and $^{147}Sm/^{144}Nd$ ratios are low (0.510846–0.510910 and 0.0784–0.0846 respectively).

$\varepsilon_{Nd(1730\ Ma)}$ values for enriched Wade Amphibolite are considerably evolved, with values of -8.8 and -8.7 and with T_{DM} ages of 2.6 Ga (Goodwin, 2010). The depleted Wade Amphibolite has the highest $^{143}Nd/^{144}Nd$ ratios (0.511953–0.512320) and $^{147}Sm/^{144}Nd$ ratios (0.1557–0.1671) of the Moola Suite. Apart from one sample with the most negative $\varepsilon_{Nd(1740\ Ma)}$ value (-4.3), depleted Wade

Amphibolite is more juvenile than Deuter Diorite and enriched Wade Amphibolite, with $\varepsilon_{Nd(1740\ Ma)}$ values of -1.2 to 0.4 and T_{DM} of 2.7 Ga to 3.1 Ga for the more evolved sample.

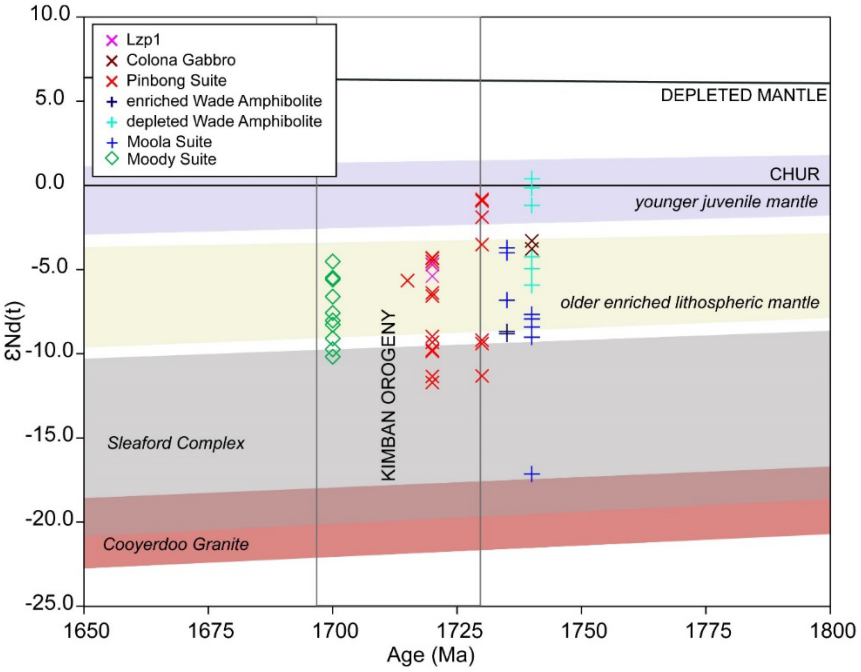

Figure 31. Sm-Nd isotope evolution diagram for Peter Pan Supersuite. Mantle and crustal reservoirs are also shown, illustrating the heterogeneous mantle identified by Schaefer (1998) in addition to Archean basement of the Gawler Craton, the Sleaford Complex and Cooyerdoo Granite.

Pinbong Suite

Pinbong Suite granites have $^{143}Nd/^{144}Nd$ ratios that range from 0.510967–0.512172 and $^{147}Sm/^{144}Nd$ ratios that range from 0.0777–0.1300. $\varepsilon_{Nd(1730\ Ma)}$ range from -11.7 to -6.6. The most evolved granites (-11.7 to -11.4 and -6.6 to -6.4) are from Peter Pan Platforms, Ferns Quarry and Bascombe Rocks.

The Middle Camp Granite has a wide range of $^{143}Nd/^{144}Nd$ ratios, $^{147}Sm/^{144}Nd$ ratios and $\varepsilon_{Nd(1730\ Ma)}$ values. Similarly to other Pinbong Suite granites, these form two broad groupings: evolved $^{143}Nd/^{144}Nd$ ratios = 0.510680–0.510859, $^{147}Sm/^{144}Nd$ ratios = 0.0666–0.0910, $\varepsilon_{Nd(1730\ Ma)}$ = -11.8 to -9.2 and T_{DM} 2.5–2.8 Ga; and juvenile $^{143}Nd/^{144}Nd$ ratios = 0.511418–0.511511, $^{147}Sm/^{144}Nd$ ratios = 0.0931–0.1071, $\varepsilon_{Nd(1730\ Ma)}$ = -3.5 to -0.8 and T_{DM} 2.2–2.4 Ga. The evolved Middle Camp Granite are from Mindrow Creek, Minbrie Springs and Middle Camp Ruins; the samples of juvenile Middle Camp Granite are unpublished data from K. Stewart, and the location of these samples is unknown.

The Carappee Granite has a narrow distribution of Sm-Nd isotope ratios ($^{143}Nd/^{144}Nd$ ratios = 0.511267–0.511373; and $^{147}Sm/^{144}Nd$ ratios = 0.1159–0.1268). Corresponding $\varepsilon_{Nd(1730\ Ma)}$ values are also narrow (-9.8 to -9.0) and evolved. T_{DM} ages for Carappee Granite range from 2.9–3.1 Ga.

The Paxton Granite has $^{143}Nd/^{144}Nd$ ratios = 0.511176–0.511312 and $^{147}Sm/^{144}Nd$ ratios = 0.0926–0.10998. Paxton Granite has $\varepsilon_{Nd(1720\ Ma)}$ values ranging from -5.7 to -4.3. T_{DM} ages for the Paxton Granite are relatively young and consistently around 2.4 Ga. These values are within the range of the Middle Camp Granite but are considerably more juvenile compared to the Burkitt Granite.

The Colona Gabbro has $^{143}Nd/^{144}Nd$ = 0.511556–0.511855 and $^{147}Sm/^{144}Nd$ ratios = 0.1163–0.1446). $\varepsilon_{Nd(1730\ Ma)}$ values are -3.8 and -3.4 which are relatively evolved but in the range of depleted Wade Amphibolite amphibolites. T_{DM} ages for Colona Gabbro are 2.8 and 2.5 Ga.

Sm-Nd isotope ratios for Lzp_1 are $^{143}Nd/^{144}Nd$ = 0.511781 and 0.511831 and $^{147}Sm/^{144}Nd$ ratios are 0.1454– 0.1467. $\varepsilon_{Nd(1730\ Ma)}$ values are -5.3 and -4.6 which are more evolved than Colona Gabbro and depleted Wade Amphibolite amphibolites, suggesting an enriched mantle source region. T_{DM} ages for Lzp_1 are 3.0 Ga.

Moody Suite

The Moody Suite has $^{143}Nd/^{144}Nd$ ratios that range from 0.511011–0.512024 and $^{147}Sm/^{144}Nd$ ratios that range from 0.0766–0.1624. $\varepsilon_{Nd(1700\ Ma)}$ range from -10.2 to -4.5, and TDM ages from 3.6–2.4 Ga, with the Yunta Well Leucogranite being the most evolved formation in the Moody Suite.

The Yunta Well Leucogranite has $^{143}Nd/^{144}Nd$ = 0.511822–0.512172; and $^{147}Sm/^{144}Nd$ ratios = 0.1582– 0.1624. $\varepsilon_{Nd(1700\ Ma)}$ values are -7.6 and -4.5 and T_{DM} ages are 3.6 and 3.3 Ga.

The Moreenia Monzogranite has variable Sm-Nd isotope compositions with $^{143}Nd/^{144}Nd$ ratios of 0.511017–0.511252 and $^{147}Sm/^{144}Nd$ ratios = 0.0766– 0.1104. $\varepsilon_{Nd(1700\ Ma)}$ values are -8.3 and -5.5. T_{DM} ages for the Moreenia Monzogranite are 2.8 and 2.4 Ga.

One sample of Uranno Microgranite from the recognised outcrop area was analysed for Sm-Nd isotopes, as well as two samples from other locations also interpreted to be part of the Uranno Microgranite. The Uranno Microgranite has $^{143}Nd/^{144}Nd$ of 0.511175; while the possible Uranno Microgranite samples have $^{143}Nd/^{144}Nd$ ratios of 0.511260–0.511341. $^{147}Sm/^{144}Nd$ ratios also vary, with Uranno Microgranite having a $^{147}Sm/^{144}Nd$ ratio of 0.0912, while the possible Uranno Microgranite samples have much more evolved $^{147}Sm/^{144}Nd$ ratios of 0.1178–0.1221. $\varepsilon_{Nd(1730\ Ma)}$ values are correspondingly evolved for the possible Uranno Microgranite samples with values of -9.7 and -9.1 and T_{DM} ages are older at 3.0 Ga. This contrasts to the less evolved value of -5.6 for the Uranno Microgranite and younger T_{DM} ages 2.4 Ga.

The Chinmina Monzonite has $^{143}Nd/^{144}Nd$ ratios of 0.511011 and 0.511396 and $^{147}Sm/^{144}Nd$ ratios of 0.0812 and 0.1221. $\varepsilon_{Nd(1700\ Ma)}$ values are evolved and range from -8.0 to -6.6, however T_{DM} ages for Chinmina Monzonite are 2.9 and 2.4 Ga.

GEOCHEMICAL AND ISOTOPIC EVOLUTION: SOURCE REGION CONSTRAINTS

GRANITES

The three magmatic phases of the Peter Pan Supersuite correlate to different stages of the Kimban Orogeny: early- to syn-orogenic granites in the Moola Suite, syn-orogenic granites in the Pinbong Suite and late-orogenic granites in the Moody Suite. While the Moola and Pinbong suites represent distinct periods of intrusion spatially and temporally, geochemically they are very similar, suggesting these two suites were derived from similar source regions. The Moody Suite represents a distinct source region.

Moola and Pinbong Suites

While mineralogically variable, the Moola and Pinbong Suite granites range from magnesian to ferroan, alkali to alkali-calcic and metaluminous to peraluminous, although the majority of samples are magnesian, alkali-calcic and peraluminous. The unit that stands out significantly is the Burkitt Granite of the Moola Suite, which is a syenite, predominantly ferroan but transitions to magnesian with increasing silica, and is exclusively alkalic and metaluminous (Figs 18 and 23).

Granites with magnesian, alkali-calcic and peraluminous compositions are typically interpreted to be syn-orogenic (Frost *et al.*, 2001). The low Fe/(Fe+Mg) ratio of the Moola and Pinbong suites suggests that they were derived from a hydrous oxidising magma, and their broad range of aluminium saturation index (ASI) values suggests that they were derived from a compositionally variable source (Frost *et al.*, 2001).

The interpretation of a variable source region of the Moola and Pinbong suites is supported by a wide variation in Sm-Nd isotopic values, with $\varepsilon_{Nd(1740\ Ma)}$ of the Moola Suite ranging from -17.1 to -2.4, and $\varepsilon_{Nd(1730\ Ma)}$ of the Pinbong Suite ranging from -11.7 to -4.3. Sm-Nd isotopic values of the more evolved granites of the Moola and Pinbong suites overlap with the isotopic values of the Neoarchaean to earliest Paleoproterozoic Sleaford Complex and Mesoarchaean Cooyerdoo Granite (Fig. 31), suggesting that these units are likely to be the source for the Moola and Pinbong suites. Many granites of the Moola and Pinbong suites have Sm-Nd values which are more juvenile than the Sleaford Complex and Cooyerdoo Granite basement (Fig. 31), suggesting that these granites have a mixed mantle and crustal input. The variability in the Sm-Nd isotopic characteristics and source region is likely to reflect varying depths of crustal melting, varying degrees of mixing of mantle and crustal material, and variability in crustal composition.

The unique geochemical signature of the Burkitt Granite may be a reflection both of a distinct source region for this granite, and a greater degree of fractionation of the parent magma. Sm-Nd values are very evolved for the Burkitt Granite, with $\varepsilon_{Nd(1740\ Ma)}$ = -17.1 to -7.7, and suggest a source region similar to the Mesoarchaean Cooyerdoo Granite. The high silica and alkalic composition of the Burkitt Granite suggest that it is highly fractionated, and a metaluminous composition is consistent with the crystallisation of calcic minerals such as hornblende (Frost *et al.*, 2001).

Moody Suite

The Moody Suite is peraluminous and calc-alkalic to alkali-calcic and, unlike the Moola and Pinbong suites, is predominantly ferroan. Although this geochemical signature is often interpreted to be typical of A-type granites in anorogenic and extensional settings (Whalen *et al.*, 1987, Eby, 1992), the fact that the 1710–1700 Ma crystallisation ages of the Moody Suite overlap with 1740–1690 Ma metamorphic ages of the Kimban Orogeny (Fig. 2) indicates that the Moody Suite is syn-tectonic. The ferroan composition implies these granites are the product of an iron-rich melt derived from a reduced, tholeiitic or mildly alkalic, mafic igneous source (Frost *et al.*, 2001).

Geochemically, the Moody Suite are more homogeneous and less variability is observed in Sm-Nd isotope compositions than the Moola and Pinbong suites, with $\varepsilon_{Nd(1700\ Ma)}$ ranging from -10.2 to -4.5 (Fig. 20), suggesting a more homogenous source region. These isotopic values are also consistent with some degree of incorporation of material of the Paleoproterozoic Hutchison Group into the melt source of the Moody Suite, which has $\varepsilon_{Nd(1790\ Ma)}$ ranging from -10.91 to -3.51 (Szpunar *et al.*, 2011). This interpretation is consistent with the presence of xenoliths of the Hutchison Group within the Moody Suite and the intrusive contact relationship between the Moody Suite and Hutchison Group.

DIORITES, AMPHIBOLITES AND GABBROS

Mafic phases of the Peter Pan Supersuite are contained within the Moola and Pinbong Suites. As observed in the granites, despite temporal and spatial differentiation, these mafic rocks fall into two broad groups: depleted, tholeiitic amphibolites and gabbros; and enriched, calc-alkaline diorites, amphibolites and gabbros. The depleted amphibolites and gabbros are typically hornblende-plagioclase-clinopyroxene-bearing while the enriched mafic rocks are plagioclase-hornblende-quartz-biotite-titanite-bearing. These two distinct geochemical signatures suggest that the mafic rocks of the Peter Pan Supersuite were derived from melting of a heterogeneous mantle source region. The trace element signatures of the mafic rocks suggest that this mantle source is likely to have been enriched by an earlier magmatic or tectonic event, such as mantle metasomatism or subduction, affecting large ion lithophile and high field strength elements.

The depleted, tholeiitic amphibolites of the Wade Amphibolite and unnamed gabbros of the Pinbong Suite (Lzp_1) are interpreted to have been derived from shallow melts of an asthenospheric source region (younger juvenile mantle) during lithospheric extension (Fig. 20).

Although the depleted tholeiitic amphibolites of the Wade Amphibolite have juvenile Sm-Nd isotopic compositions, with $\varepsilon_{Nd(1740\ Ma)}$ = -1.2 to 0.4, some of the depleted tholeiitc gabbros of the

Pinbong Suite have relatively evolved Nd signatures (~-5.9 to -4.6; Fig. 20). These evolved Nd signatures are coupled with older T_{DM} ages of 3.1–3.0 Ga and, while attributed to the younger juvenile mantle reservoir, reflect the presence of an older lithospheric component in both northern Eyre Peninsula and northern Gawler Craton. The overall geochemical signature for the depleted tholeiitic amphibolites and gabbros is comparable with mantle source regions; for example HFSE and most REE trend towards N-MORB and depleted mantle values (Figs 20–21, 25–26), suggesting that only the Sm-Nd ratios have been perturbed. Some degree of crustal contamination would be one explanation for this signature; however to modify the Sm and Ti abundances large amounts of crustal material are required which is at odds with the low silica content and overall primitive signature of the intrusions. Alternatively, these characteristics (relatively primitive trace element, REE abundances coupled with evolved Sm-Nd isotopic data) may also represent mantle enrichment which can be achieved by subduction of the continental crust into the upper mantle or by progressive enrichment of a previously depleted lithospheric mantle either by continuous melt percolation or specific enrichment events (Schaefer, 1998).

These geochemical signatures contrast markedly to the enriched calc-alkaline amphibolites of the Wade Amphibolite, which have very evolved Nd signatures (~-9; Fig. 20) and steeper trace element and REE patterns indicative of lower crustal (mafic) material (Figs 20–21), suggesting an enriched lithospheric mantle source. The Colona Gabbro displays a similar trace element and REE signature (Figs 25–26); however it has higher $\varepsilon_{Nd(1740\ Ma)}$ values (-3.8 and -3.4) compared with the amphibolites and gabbros of the Pinbong Suite (Fig. 20). Despite these differences the processes which enrich lithospheric mantle remain the same, the main difference lies in the age and longevity of such an enriched lithospheric mantle.

Schaefer (1998) identified a heterogeneous mantle source region in the mid-Paleoproterozoic responsible for producing two geochemically and isotopically distinct groups of dolerites c. 1810 Ma. He suggested that an older, enriched lithospheric mantle reservoir, enriched in incompatible elements and relatively depleted in compatible elements, produced the isotopically evolved dolerites, while a younger, juvenile mantle produced dolerites with primitive signatures. The dolerites derived from the enriched lithospheric mantle source show trace element patterns similar to that of the continental crust, however, Schaefer (1998) determined this signature was a reflection of mantle source characteristics due to presence of enriched lithospheric mantle beneath continental crust. The geochemical signatures observed in the mafic rocks of the Peter Pan Supersuite are very similar to those observed in the mid-Proterozoic mafic intrusives, suggesting the two mantle sources identified by Schaefer were still present and resampled during the 1750–1700 Ma intrusive event.

SUMMARY

The 1745–1700 Ma time period coincides with the c. 1740–1690 Ma Kimban Orogeny, when widespread, predominantly felsic intrusive magmatism and minor mafic magmatism occurred throughout most of the Gawler Craton. Three suites of magmatic rocks have been distinguished during this time period: the Moola Suite (1745–1735 Ma), the Pinbong Suite (1735–1700 Ma) and the Moody Suite (1710–1700 Ma).

The Moola Suite and Pinbong Suite share many geochemical similarities with granites derived from heterogeneous source regions and mafic rocks derived from at least two mantle source regions: and older, enriched lithospheric mantle and a younger, enriched mantle. Signatures for the Moola and Pinbong Suite granites are consistent with granites generated in orogenic settings. Likely source areas for the Moola and Pinbong suite granites are the Sleaford Complex and Cooyerdoo Granite. The mafic rocks are interpreted to have been generated during episodes of lithospheric extension and lithospheric thinning during the orogeny, and represent a heterogeneous mantle source region, most likely modified by earlier metasomatism or subduction events. The Moody Suite contains ferroan granites derived from an iron-enriched Hutchison Group source region.

ACKNOWLEDGEMENTS

David Bruce, University of Adelaide, is thanked for carrying out the Sm–Nd isotope analysis. Betina Bendall and Adrian Fabris are thanked for providing some of the rock photos used in this report. Mario Werner and Wayne Cowley are thanked for providing constructive reviews of this report.

REFERENCES

Allen, S. R., McPhie, J., Ferris, G. and Simpson, C. 2008. Evolution and architecture of a large felsic igneous province in western Laurentia: The 1.6 Ga Gawler Range Volcanics, South Australia. *Journal of Volcanology and Geothermal Research*, 172, pp. 132-147.

Benbow, M. C., 1993. Tallaringa Map Sheet, SH 53-5, Explanatory Notes. *1:250 000 Geological Series*, Department of Mines and Energy, South Australia, Adelaide.

Budd, A. R., 2006. The Tarcoola Goldfield of the Central Gawler Gold Province, and the Hiltaba Association Granites, Gawler Craton, South Australia. PhD Thesis, Department of Earth and Marine Sciences, Australian National University, Canberra.

Budd, A. R. and Fraser, G. 2004. Geological relationships and 40Ar/39Ar age constraints on gold mineralisation at Tarcoola, central Gawler gold province, South Australia. *Australian Journal of Earth Sciences*, 51, pp. 685-699.

Chalmers, N., 2009. Geodynamic evolution of the St Peter Suite, Gawler Craton, South Australia: stratigraphic, geochemical and isotopic investigation. BSc Masters Thesis, Monash University, Clayton.

Coin, C. D. A., 1976. A study of the Precambrian rocks in the vicinity of Tumby Bay, South Australia. PhD Thesis, University of Adelaide, Adelaide.

Conor, C. H. H., 1995. *Moonta-Wallaroo Region. An interpretation of the geology of the Maitland and Wallaroo 1:100 000 sheet areas*. Open file envelope 8886, Department of Primary Industries and Resources, South Australia, Adelaide.

Cowley, W. M., Conor, C. and Zang, W., 2003. New and revised Proterozoic stratigraphic units on northern Yorke Peninsula. *MESA Journal*, 29, pp. 46-58. Department of Primary Industries and Resources, South Australia, Adelaide.

Cowley, W. M., McAvaney, S. O. and Wade, C. E., 2017. Abandonment of Lincoln Complex nomenclature, Gawler Craton, South Australia. *MESA Journal*, 82, pp. 4-14. Department of State Development, Adelaide.

Daly, S. and Fanning, C. M. 1993. Archaean. In Drexel, J. F., Preiss, V. W. and Parker, A. J. (Eds.), *The Geology of South Australia. Vol. 1, The Precambrian,* South Australia. Geological Survey. Bulletin 54, pp 33-50.

Daly, S. J. 1993. Tarcoola Formation. In Drexel, J. F., Preiss, W. V. and Parker, A. J. (Eds.), *The geology of South Australia; Volume 1, The Precambrian,* Geological Survey of South Australia, pp 68–69.

Daly, S. J., Tonkin, D. G., Purvis, A. C. and Shi, Z., 1994. *Colona drilling program*. Open file envelope 8768, Mines and Energy, South Australia, Adelaide.

Dawson, J., 2016. Characterising magmatis suites in the western Gawler Craton: geochemical and geochronological constraints. B. Sc. (Honours) Thesis, Department of Geology and Geophysics, University of Adelaide, Adelaide.

Dutch, R., 2009. Reworking the Gawler Craton: metamorphic and geochronologic constraints on Palaeoproterozoic rezctivation of the southern Gawler Craton, Australia. PhD. Thesis, Department of Geology and Geophysics, University of Adelaide, Adelaide.

Dutch, R., Hand, M. and Kinny, P. D. 2008. High-grade Palaeoproterozoic reworking in the southeastern Gawler Craton, South Australia. *Australian Journal of Earth Sciences*, 55, pp. 1063-1081.

Eby, G. N. 1992. Chemical subdivision of the A-type granitoids: Petrogenetic and tectonic implications. *Geology*, 20, pp. 641-644.

Fanning, C. M., 1997. *Geochronological synthesis of southern Australia. Part II: The Gawler Craton. Preliminary draft prepared for The Gawler Craton Excursion, 21-26 September, 1997*. Open file envelope 8918, Department of Mines and Energy, South Australia, Adelaide

Fanning, C. M., Flint, R. B., Parker, A. J., Ludwig, K. R. and Blissett, A. H. 1988. Refined Proterozoic evolution of the Gawler Craton, South Australia, through U-Pb zircon geochronology. *Precambrian Research*, 40-41, pp. 363-386.

Fanning, C. M., Reid, A. J. and Teale, G. S., 2007. *A Geochronological Framework for the Gawler Craton, South Australia*, Bulletin 55, Primary Industries and Resources, South Australia, Adelaide.

Finlay, J., 1993. Structural interpretation of the Mount Woods Inlier. BSc Honours Thesis, Monash University, Clayton.

Flint, R. B., Fanning, C. M. and Rankin, L. R. 1988. Carappee Granite of central Eyre Peninsula. *Geological Survey of South Australia. Quarterly Geological Notes*, 105, pp. 2-6.

Fraser, G. and Lyons, P. 2006. Timing of Mesoproterozoic tectonic activity in the north-western Gawler Craton constrained by $^{40}Ar/^{39}Ar$ geochronology. *Precambrian Research*, 151, pp. 160-184.

Fraser, G., McAvaney, S., Neumann, N., Szpunar, M. and Reid, A. 2010. Discovery of early Mesoarchaean crust in the eastern Gawler Craton, South Australia. *Precambrian Research*, 179, pp. 1-21.

Fraser, G. and Neumann, N., 2010. New SHRIMP U-Pb zircon ages from the Gawler Craton and Curnamona Province, South Australia, 2008 - 2010. Geoscience Australia 2010/16.

Fraser, G., Reid, A. J. and Stern, R. A. 2012. Timing of deformation and exhumation across the Karari Shear Zone, north-western Gawler Craton, South Australia. *Australian Journal of Earth Sciences*, 59, pp. 1-24.

Fraser, G., Skirrow, R. and Holm, O. 2007. Mesoproterozoic gold prospects in the central Gawler Craton, South Australia: geology, alteration, fluids and timing. *Economic Geology*, 102, pp. 1511-1539.

Frost, B. R., Barnes, C. G., Collins, W. J., Arculus, R. J., Ellis, D. J. and Frost, C. D. 2001. A Geochemical Classification for Granitic Rocks. *Journal of Petrology*, 42, pp. 2033-2048.

Goldstein, S. L., Onions, R. K. and Hamilton, P. J. 1984. A Sm-Nd Isotopic Study of Atmospheric Dusts and Particulates from Major River Systems. *Earth and Planetary Science Letters*, 70, pp. 221-236.

Goodwin, S., 2010. Geochemical and isotopic investigation into the tectonic setting of Mesoarchaean and Palaeoproterozoic granitoid suites within the eastern Gawler Craton, South Australia. BSc Honours Thesis, Department of Geology and Geophysics, Adelaide University, Adelaide.

Halpin, J. A. and Reid, A. J. 2016. Earliest Paleoproterozoic high-grade metamorphism and orogenesis in the Gawler Craton, South Australia: The southern cousin in the Rae family? *Precambrian Research*, 276, pp. 123–144.

Hand, M., Bendall, B. R. and Sandiford, M., 1995. Metamorphic evidence for Palaeoproterozoic oblique convergence in the eastern Gawler Craton. Australian Geological Convention, Geological Society of Australia. Abstracts, 40, pp. 59.

Hand, M., Reid, A. J. and Jagodzinski. 2007. Tectonic framework and evolution of the Gawler Craton, South Australia. *Economic Geology*, 102, pp. 1377-1395.

Hoek, J. D. and Schaefer, B. F. 1998. Palaeoproterozoic Kimban mobile belt, Eyre Peninsula: timing and significance of felsic and mafic magmatism and deformation. *Australian Journal of Earth Sciences*, 45, pp. 305-313.

Hopper, D. J., 2001. Crustal evolution of Palaeo- to Mesoproterozoic rocks in the Peake and Denison Ranges, South Australia. PhD Thesis, University of Queensland, Brisbane, Australia.

Howard, K. E., Hand, M., Barovich, K., Payne, J. L. and Belousova, E. 2011a. U-Pb, Lu-Hf and Sm-Nd isotopic contstraints on provenance and depositional timing of metasedimentary rocks in the western Gawler Craton: implications for Proterozoic reconstruction models. *Precambrian Research*, 184, pp. 43-62.

Howard, K. E., Hand, M., Barovich, K., Payne, J. L., Cutts, K. A. and Belousova, E. 2011b. U-Pb zircon, zircon Hf and whole-rock Sm-Nd isotopic constraints on the evolution of Palaeoproterozoic rocks in the northern Gawler Craton. *Australian Journal of Earth Sciences*, 58, pp. 615-638.

Jagodzinski, E. A., 2005, *Compilation of SHRIMP U-Pb geochronological data, Olympic Domain, Gawler Craton, South Australia, 2001-2003*. Geoscience Australia Record 2005/20.

Jagodzinski, E. A., Black, L., Frew, R. A., Foudoulis, C., Reid, A., Payne, J. L., Zang, W. and Schwarz, M., 2006, *Compilation of SHRIMP U-Pb geochronological data for the Gawler Craton, South Australia 2005-2006*. Primary Industries and Resources South Australia, Report book 2006/20, Adelaide.

Jagodzinski, E. A. and McAvaney, S. O., 2017, *SHRIMP U-Pb geochronology data for northern Eyre Peninsula, 2014 - 2015*. Report book 2016/001, Department of State Development, South Australia, Adelaide.

Jagodzinski, E. A. and Reid, A. 2010. New zircon and monazite geochronology using SHRIMP and LA-ICPMS, from recent GOMA drilling, on samples from the northern Gawler Craton. In Korsch, R. J. and Kositcin, N. (Eds.), *GOMA (Gawler Craton-Officer Basin-Musgrave Province-Amadeus Basin) Seismic and MT Workshop 2010. Geoscience Australia, Record 2010/39,* pp 108-117.

Jagodzinski, E. A., Reid, A., Chalmers, N., Swain, G. M., Frew, R. A. and Foudoulis, C., 2007, *Compilation of SHRIMP U-Pb geochronological data for the Gawler Craton, South Australia, 2007*. Primary Industries and Resources, South Australia. Report book 2007/21, Adelaide.

Jagodzinski, E. A., Reid, A., Crowley, J., McAvaney, S. and Wade, C., 2016. Precise zircon U-Pb dating of a Mesoproterozoic silicic large igneous province: the Gawler Range Volcanics and Benagerie Volcanic Suite, South Australia*., Australian Earth Science Convention*, Geological Society of Australia, Adelaide, South Australia, oral presentation.

Jagodzinski, E. A., Reid, A. J. and Hand, M., 2012, *SHRIMP U-Pb geochronology of Archaean to Palaeoproterozoic rocks from southern Eyre Peninsula*. Report book 2012/00015, Department of Manufacturing, Trade, Innovation, Resources and Energy, South Australia, Adelaide.

Lane, K., 2011. Metamorphic and geochronological constraints on the evolution of the Kalinjala Shear Zone, Eyre Peninsula. BSc. Hons. Thesis, Department of Geology and Geophysics, University of Adelaide, Adelaide.

Lane, K., Jagodzinski, E. A., Dutch, R., Reid, A. J. and Hand, M. 2015. Age constraints on the timing of iron ore mineralisation in the southeastern Gawler Craton. *Australian Journal of Earth Sciences*, 62, pp. 55-75.

Liew, T. C. and Hofmann, A. W. 1988. Precambrian crustal components, plutonic associations, plate environment of the Hercynian Fold Belt of central Europe: Indications from a Nd and Sr isotopic study. *Contributions to Mineralogy and Petrology*, 98, pp. 129-138.

McAvaney, S. 2012. The Cooyerdoo Granite: Palaeo- and Mesoarchaean basement of the Gawler Craton. *MESA Journal*, 65, pp. 31-40.

McAvaney, S. O. and Jagodzinski, E. J., 2012, *Geochronology and geochemistry of a Kimban diorite, drill hole LED001, Lake Gilles, eastern Gawler Craton*. Report book 2012/00010, Department for Manufacturing, Innovation, Trade, Resources and Energy, South Australia, Adelaide.

McAvaney, S. O. and Reid, A., 2008, *The Corunna Conglomerate, Gawler Craton: a review of the sedimentology and new U-Pb zircon geochronology*. Report book Report book 2008/003, Department of Primary Industries and Resources. South Australia, Adelaide.

McAvaney, S. O., Wade, C. E. and Jagodzinski, E. J., 2016a. Tip Top and Wertigo granites, c. 1775 Ma magmatism on northeastern Eyre Peninsula. *MESA Journal*, 80, pp. 63-76. Department of State Development, South Australia, Adelaide.

McAvaney, S. O., Werner, M., Jagodzinski, E. A. and Crowley, J., 2017, *High precision CA-TIMS geochronology of the Palaeoproterozoic Gluepot Granite*. Report book RB2016/00027, Department of State Development, Adelaide.

McAvaney, S. O., Werner, M. X., Pawley, M. J. and Krapf, C. B. E., 2016b, *Geology of the Six Mile Hill 1:75 000 Map Sheet, Mineral Systems Drilling Program*. Department of State Development, South Australia. Report book 2016/00016, Adelaide.

McFarlane, C. R. M. 2006. Palaeoproterozoic evolution of the Challenger Au deposit, South Australia, from monazite geochronology *Journal of Metamorphic Geology*, 24, pp. 75-87.

Middlemost, E. A. K. 1994. Naming materials in the magma/igneous rock system. *Earth Science Reviews*, 37, pp. 215-224.

Mortimer, G. E., Cooper, J. A. and Oliver, R. L. 1988. The geochemical evolution of Proterozoic granitoids near Port Lincoln in the Gawler orogenic domain of South Australia. *Precambrian Research*, 40/41, pp. 387-406.

Parker, A. J., 1980. The Kalinjala Mylonite Zone, eastern Eyre Peninsula. *Quaternary Geological Notes*, 76, pp. 6-11. Geological Survey of South Australia, Adelaide.

Parker, A. J., 1993. *Kimban Orogeny*, In J. F. Drexel, W. V. Preiss and A. J. Parker (Eds.), *The geology of South Australia, Volume 1, The Precambrian*, Bulletin 54. Geological Survey of South Australia, Adelaide. pp. 71-81.

Parker, A. J. and Fanning, C. M., 1998. WHYALLA Map Sheet, SI53-8, Explanatory Notes. *South Australia Geological Atlas 1:250 000 series*, Geological Survey of South Australia, Adelaide.

Parker, A. J., Fanning, C. M. and Flint, R. B., 1981, *Archaean–Middle Proterozoic geology of the southern Gawler Craton, South Australia*. Report book 81/91, Department of State Development, Adelaide.

Parker, A. J., Fanning, C. M. and Flint, R. B. 1985. Geology. In Twidale, C. R., Tyler, M. J. and Davies, M. (Eds.), *Natural History of Eyre Peninsula,* Royal Society of South Australia.

Payne, J. L., Barovich, K. and Hand, M. 2006. Provenance of metasedimentary rocks in the northern Gawler Craton, Australia: Implications for Palaeoproterozoic reconstructions. *Precam. Res.*, 148, pp. 275-291.

Payne, J. L., Ferris, G., Barovich, K. M. and Hand, M. 2010. Pitfalls of classifying ancient magmatic suites with tectonic discrimination diagrams: An example from the Paleoproterozoic Tunkillia Suite, southern Australia. *Precambrian Research*, 177, pp. 227-240.

Payne, J. L., Hand, M., Barovich, K. and Wade, B. P. 2008. Temporal constraints on the timing of high-grade metamorphism in the northern Gawler Craton: implications for assembly of the Australian Proterozoic. *Australian Journal of Earth Sciences*, 55, pp. 623-640.

Rankin, L. R., Flint, R. B. and Fanning, C. M., 1990, *Palaeoproterozoic Nuyts Volcanics of the western Gawler Craton*. Report book 90/00060, Deptartment of Primary Industries and Resources South Australia, Adelaide.

Reid, A., 2007, *Geochronology of the Gawler Craton, South Australia*. Primary Industries and Resources, South Australia. Report book 2007/15, Adelaide.

Reid, A. and Fabris, A. J. 2015. Influence of pre-existing low metamorphic grade sedimentary successions on the distribution of iron oxide-copper-gold mineralisation in the Olympic Cu-Au Province, Gawler Craton. *Economic Geology*, 110, pp. 2147-2157.

Reid, A. and Hand, M. 2012. Mesoarchaean to Mesoproterozoic evolution of the southern Gawler Craton, South Australia. *Episodes*, 35, pp. 216-225.

Reid, A., Hand, M., Jagodzinski, E. J., Kelsey, D. E. and Pearson, N. 2008a. Palaeoproterozoic orogenesis in the southeastern Gawler Craton, South Australia. *Australian Journal of Earth Sciences*, 55, pp. 449-471.

Reid, A. and Jagodzinski, E. A., 2011, *PACE Geochronology: Results of collaborative geochronology projects 2009-2010*. Report book 2011/003, Department of Primary Industries and Resources, South Australia, Adelaide.

Reid, A. and Jagodzinski, E. A., 2012, *PACE Geochronology: Results of collaborative geochronology projects 2011-12*. Report book 2012/12, Adelaide.

Reid, A., Vassallo, J., Wilson, C. and Fanning, C. M., 2007, *Timing of the Kimban Orogeny on southern Eyre Peninsula*. Report book 2007/005, Department of Primary Industries and Resources, South Australia, Adelaide.

Reid, A. J., 2015, *Zircon U-Pb geochronology from selected Palaeoproterozoic igneous rocks of the Gawler Craton by laser ablation inductively coupled plasma mass spectrometry* Report book 2015/00025, Department of State Development, Adelaide.

Reid, A. J., Jagodzinski, E. J., Fraser, G., L and Pawley, M. J. 2014. SHRIMP U-Pb age constraints on the tectonics of the Neoarchean to early Palaeoproterozoic transition within the Mulgathing Complex, Gawler Craton, South Australia. *Precambrian Research*, 250, pp. 27-49.

Reid, A. J., McAvaney, S. O. and Fraser, G. L. 2008b. Nature of the Kimban Orogeny across northern Eyre Peninsula. *MESA Journal*, 51, pp. 25-34.

Reid, A. J., Pawley, M. J., Jagodzinski, E. J. and Dutch, R. A., 2016, *Magmatic processes of the St Peter Suite, Gawler Craton: new U-Pb geochronological data and field observations*. Report book 2016/00012, Department of State Development, South Australia, Adelaide.

Rudnick, R. L. and Gao, S. 2003. Composition of the continental crust. In Rudnick, R. L. (Ed.) *The crust. Treatise on Geochemistry. Volume 3,* Elsevier, pp 1-64.

Rutland, R. W. R., Parker, A. J., Pitt, G. M., Preiss, V. W. and B, M. 1981. The Precambrian of South Australia. In Hunter, D. R. (Ed.) *Precambrian of the Southern Hemisphere,* Developments in Precambrian Geology Series 2, Elsevier, Amsterdam, pp 309-360.

Schaefer, B. F., 1998. Insights into Proterozoic tectonics from the southern Eyre Peninsula, South Australia. PhD Thesis, University of Adelaide, Adelaide.

Schwarz, M. P., 1999. Definition of the Moody Suite, southern Gawler Craton. *MESA Journal*, 13, pp. 39-44. Primary Industries and Resources, South Australia, Adelaide.

Schwarz, M. P. 2003. *LINCOLN, South Australia, sheet SI 53-11*, Geological Atlas 1:250 000 Series - Explanatory Notes, Primary Industries and Resources South Australia,

Stewart, J. R., 2010. Integrated structural geology and geophysical analysis of crustal-scale shear zones in the Gawler Craton, South Australia. Thesis, Monash University, Clayton.

Stewart, K. and Foden, J., 2003, *Mesoproterozoic granites of South Australia*. Report book 2003/15, Primary Industries and Resources, South Australia, Adelaide.

Sun, S. S. and McDonough, W. F. 1989. Chemical and isotopic systematics of oceanic basalts: implications for mantle composition and processes. In Saunders, A. D. and Norry, M. J. (Eds.), *Magmatism in ocean basins,* Geological Society of London Special Publication 42, pp 313-345.

Sunthe Uranium Pty. Ltd., 2011. *EL3594 Mosely Nobs. Second partial surrender report at licence expiry/renewal, for the period 5/7/2006 to 4/7/2011*. Open file envelope 12246, Department for Manufacturing, Innovation, Trade, Resources and Energy, Adelaide

Swain, G. M., Barovich, K., Hand, M., Ferris, G. and Schwarz, M. 2008. Petrogenesis of the St Peter Suite, southern Australia: Arc magmatism and Proterozoic crustal growth iof the Southern Australian Craton. *Precambrian Research*, 166, pp. 283-296.

Swain, G. M., Hand, M., Teasdale, J., Rutherford, L. and Clark, C. 2005a. Age constraints on terrane-scale shear zones in the Gawler Craton, southern Australia. *Precambrian Research*, 139, pp. 164-180.

Swain, G. M., Woodhouse, A., Hand, M., Barovich, K., Schwarz, M. and Fanning, C. M. 2005b. Provenance and tectonic development of the late Archaean Gawler Craton, Australia; U-Pb zircon, geochemical and Sm-Nd isotopic implications. *Precambrian Research*, 141, pp. 106-136.

Symington, N. J., Weinberg, R. F., Hasalová, P., Wolfram, L. C., Raveggi, M. and Armstrong, R. A. 2014. Multiple intrusions and remelting-remobilization events in a magmatic arc: The St Peter Suite, South Australia. *GSA Bulletin*, 126, pp. 1200-1218.

Szpunar, M. and Fraser, G., 2010, *Age of deposition and provenance of Palaeoproterozoic basins on north-eastern Eyre Peninsula: constraints from SHRIMP U-Pb geochronology*. Report book 2010/00008, Department of Primary Industries and Resources, South Australia, Adelaide.

Szpunar, M., Hand, M., Barovich, K. and Jagodzinski, E. J. 2011. Isotopic and geochemical constraints on the Palaeoproterozoic Hutchison Group, southern Australia: Implications for Palaeoproterozoic reconstructions. *Precambrian Research*, 187, pp. 99-126.

Taylor, S. R. and McLennan, S. M. 1985. *The Continental Crust: Its composition and evolution*, Blackwell Scientific Publications,

Teasdale, J., 1997. The interpretive geology and tectonothermal evolution of the western Gawler Craton. PhD Thesis, University of Adelaide, Adelaide.

Thomson, B. P. c., 1980. Geological map of South Australia Map Sheet, *Geological Atlas of South Australia, 1:1 000 000 series*. South Australia. Geological Survey,

Vassallo, J. J. and Wilson, C. J. L. 2002. Palaeoproterozoic regional-scale non-coaxial deformation: an example from eastern Eyre Peninsula, South Australia. *Journal of Structural Geology*, 24, pp. 1-24.

Wade, B. P., Barovich, K., Hand, M., Scrimgeour, I. R. and Close, D. F. 2006. Evidence for early Mesoproterozoic arc-related magmatism in the Musgrave Block, central Australia: implications for Proterozoic crustal growth and tectonic reconstructions of Australia. *Journal of Geology*, 114, pp. 43-63.

Wade, C. E. and McAvaney, S. O., 2017, *Neoarchaean to earliest Palaeoproterozoic magmatism in the southern Gawler Craton; petrogenesis of the Carpa Granite and Minbrie Gneiss*. Report book 2016/00019, Department of State Development, South Australia, Adelaide.

Webb, A. W., Thomson, B. P., Blissett, A. H., Daly, S. J., Flint, R. B. and Parker, A. J. 1986. Geochronology of the Gawler Craton, South Australia. *Australian Journal of Earth Sciences*, 33, pp. 119-143.

Whalen, J. B., Currie, K. L. and Chappell, B. W. 1987. A-type granites: geochemical characteristics, discrimination and petrogenesis. *Contributions to Mineralogy and Petrology*, 95, pp. 407-419.

APPENDIX I. STRATIGRAPHIC DEFINITIONS

PETER PAN SUPERSUITE (NEW NAME)

Derivation of name

Named after Peter Pan Dam, Eyre Peninsula (579375mE, 6381995mN, GDA94, Zone 53).

Distribution

Peter Pan Supersuite is widely distributed throughout the Gawler Craton. Outcrops occur predominantly on central and northeastern Eyre Peninsula, but the Supersuite also occurs in the eastern Gawler Craton, the Tarcoola area in the central Gawler Craton, the Peake and Denison Inliers, Coober Pedy Ridge and Yoolperlinna Inlier in the northern Gawler Craton, and the Fowler Domain in the western Gawler Craton.

Daughter units

Moola Suite (new name), Pinbong Suite (new name) and Moody Suite (change to previous definition).

Type locality

Refer to daughter units.

Lithology

Undeformed, weakly foliated, gneissic to migmatitic mafic to felsic alkaline intrusives, including gabbro, gabbroic diorite, monzogabbro, monzodiorite, monzonite, syenite, quartz monzonite, granodiorite and granite.

Relationships

The Peter Pan Supersuite contains igneous rocks intruded during the c.1745–1690 Ma Kimban Orogeny. Some parts of the Peter Pan Supersuite are undeformed, or have a magmatic fabric typically aligned with the regional Kimban structural grain. Other parts of the Peter Pan Supersuite are deformed, ranging from a weak foliation to a migmatite. On Eyre Peninsula some parts of the Peter Pan Supersuite are observed structurally interleaved and folded with the Sleaford Complex and Hutchison Group.

The Peter Pan Supersuite intrudes an Archean to Paleoproterozoic basement, including the Sleaford Complex, Hutchison Group, Broadview Schist and Moonabie Formation. It is locally unconformably overlain by the Paleoproterozoic Corunna Conglomerate and Tarcoola Formation and intruded by the Gawler Range Volcanics.

Age

Magmatic ages of the Peter Pan Supersuite range from 1745 to 1700 Ma.

Comments

The name Peter Pan Supersuite is introduced to describe magmatism between 1750–1700 Ma associated with the Kimban Orogeny, replacing (in part) the now obsolete term Lincoln Complex (Cowley *et al.*, 2017).

MOOLA SUITE (NEW NAME)

Derivation of name

Named after Moola Homestead, ~40 km west-southwest of Whyalla, Eyre Peninsula (702915mE, 6333270mN, GDA94, Zone 53).

Distribution

The Moola Suite occurs extensively across the Gawler Craton, on northeastern Eyre Peninsula in the southern Gawler Craton, the Olympic Domain in the eastern Gawler Craton, the Peake and Denison Inliers and Yoolperlunna Inlier in the northern Gawler Craton, and the Fowler Domain in the western Gawler Craton.

Outcrops of the Moola Suite are largely limited to northeastern Eyre Peninsula, where the Burkitt Granite, Wortham Granite, Glue Pot Granite and Wade Amphibolite are exposed. Notable outcrops of unnamed granite, dolerite and amphibolite belonging to the Moola Suite also occur on Eyre Peninsula west of Lake Gilles (Fraser and Neumann, 2010), at Refuge Rocks (Fanning *et al.*, 2007) and west of Iron Duke (Goodwin, 2010, Reid and Jagodzinski, 2011). The Deuter Diorite is intersected in drillhole LED001 east of Lake Gilles, and unnamed granites are intersected in drillholes at the Moola Prospect (Reid and Jagodzinski, 2011). In the eastern Gawler Craton the Moola Suite an unnamed granite of the Moola Suite is intersected at the Vulcan Prospect (Reid and Jagodzinski, 2012). In the northern Gawler Craton a c. 1740 Ma trondhjemite cropping out at Lagoon Hills in the Peake and Denison inliers is assigned to the Moola Suite (Hopper, 2001), as well as a granite gneiss with a poorly constrained protolith age of 1740 ± 31 Ma in the Yoolperlinna Inlier. Intrusion of the Moola Suite is contemporaneous with c. 1745 Ma felsic volcanism and deposition of clastic and iron-rich sediments at Spring Hill in the Peake and Denison inliers (Fanning *et al.*, 2007).

Parent

Peter Pan Supersuite.

Daughter units

Wortham Granite (new name)
Burkitt Granite (change to previous usage)
Gluepot Granite (new name)
Deuter Diorite (new name)
Wade Amphibolite (new name)

Type locality

See daughter units for type localities.

Lithology

The suite is dominated by undeformed to weakly foliated granites, but also includes hornblende-bearing syenite, garnet-bearing leucogneiss, diorite, dolerite and amphibolite.

Relationships

The Moola Suite was intruded immediately preceding and during the earliest part of the 1740–1690 Ma Kimban Orogeny. It ranges from undeformed to weakly to moderately foliated.

Moola Suite intrudes Archean to Paleoproterozoic basement, including the Minbrie Gneiss at Refuge Rocks, the Hutchison Group ~12 km south-southwest of Uno Homestead, and the Moonabie Formation at Southeast Mount Whyalla, and is inferred to intrude the Broadview Schist.

It is unconformably overlain by the Corunna Conglomerate west of the Baxter Range and is intruded by dykes and veins of the Gawler Range Volcanics in the Baxter Range in LED 001 (drillhole 229988).

Age

The Moola Suite ranges in age from 1745–1735 Ma.

BURKITT GRANITE (CHANGE TO PREVIOUS USAGE)

Derivation of name

Named after Burkitt Hill, 12 km northwest of Iron Knob, Corunna Station, Eyre Peninsula (690255mE, 6382088mN, GDA94, Zone 53). Name first used in Dalgarno *et al.* (1968), but never defined.

Distribution

Burkitt Granite occurs on Corunna Station on northeastern Eyre Peninsula, in the southern Gawler Craton. It crops out as tors and scattered platform exposures mostly extending 9 km south, 2.5 km north and 4.5 km in width along the Iron Knob-Yardea Road. Small isolated outcrops are also located approximately 1.7 km west-southwest of West End Hill in the Baxter Range. The Burkitt Granite is characterised by a pronounced magnetic high in TMI imagery, with planar margins presumably modified by faulting. In extends 15 km to the south of known outcrop in the subsurface, intersected in RDD002 (drillhole 229989).

Parent

Moola Suite.

Type locality

Outcrop of large tors directly south of Iron Knob – Yardea Road, ~11.5 km west from Corunna Station, comprising the area extending 100 m radially from the point 689045mE, 6385491mN, GDA94, Zone 53.

Lithology

The Burkitt Granite is a medium- to coarse-grained, orange-pink, slightly porphyritic K-feldspar-quartz-plagioclase-hornblende-magnetite granite. Lath-shaped K-feldspar phenocrysts are up to 25 mm in length, and sit within an equigranular groundmass of medium- to coarse-grained K-feldspar, quartz and plagioclase, with hornblende and magnetite, and accessory sphene, monazite and zircon. The pluton is largely unfoliated, but locally contains a magmatic foliation orientated north-northwest, defined by the alignment of K-feldspar phenocrysts.

Relationships

The Burkitt Granite is interpreted to intrude an Archean to earliest Paleoproterozoic basement comprising the Cooyerdoo Granite and Sleaford Complex, and is unconformably overlain by the c. 1680 Ma Corunna Conglomerate.

Age

Magmatic age 1755 ± 19 Ma and 1742 ± 42 Ma (Fraser and Neumann, 2010).

WORTHAM GRANITE (NEW NAME)

Derivation of name

Named after Wortham Dam, Roopena Station, ~30 northwest of Whyalla, Eyre Peninsula (720514mE, 6371445mN, GDA94, Zone 53).

Distribution

The Wortham Granite is exposed as low outcrops and subcrops in the vicinity of Wortham Dam on Roopena Station, north-eastern Eyre Peninsula. It is exposed as low outcrops and subcrop extending over an area approximately 500 m x 400 m wide, ~3 km southwest of Wortham Dam to the west of the Roopena Fault Zone. In the subsurface the Wortham Granite may be defined by a magnetic high trending north-northwest ~750 m wide and with a linear extent of ~8 km. Isolated outcrops of a similar granite occur 3.5 km north of Wortham Dam within the Roopena Fault Zone, which may be part of or equivalent to the Wortham Granite.

Parent

Moola Suite.

Type locality

Low outcrops located ~10 km south-southwest of Roopena Homestead, Roopena Station, Eyre Peninsula, comprising the area extending 100 m radially from the point 719075mE, 6368945mN, GDA94, Zone 53.

Lithology

The Wortham Granite is a pink medium-grained equigranular granite composed of K-feldspar, quartz, plagioclase, biotite and tourmaline. It contains a weak foliation formed during the Kimban Orogeny.

Relationships

Although no contacts are observed, the Wortham Granite is inferred to intrude the Broadview Schist which crops out in close proximity to the granite.

Age

Magmatic age 1747 ± 13 Ma (Jagodzinski and McAvaney, 2017).

DEUTER DIORITE (NEW NAME)

Derivation of name

Named after Deuter Paddock, Corunna Station, ~23 km west of Iron Knob, Eyre Peninsula (678115mE, 6374685mN, GDA94, Zone 53).

Distribution

The Deuter Diorite occurs on Corunna Station, northeastern Eyre Peninsula, in the southern Gawler Craton. It does not crop out, and is intersected only in drillhole DDH LED001. The pluton can be traced on magnetic imagery spanning 9 x 2.5 km, elongate in a north-south direction.

Parent

Moola Suite.

Type locality

Diamond drillhole DDH LED001 (229988), 680450mE, 6381003mN, GDA94, Zone 53, within the interval 518.8–595 m.

Lithology

The Deuter Diorite is an intermediate pluton comprising granodiorite, diorite and gabbroic phases (McAvaney and Jagodzinski, 2012). The pluton is dominated by an equigranular medium- to coarse-grained diorite, quartz diorite to quartz-monzonite composed of plagioclase, hornblende, biotite and minor quartz ± clinopyroxene ± k-feldspar, with accessory magnetite, apatite and titanite. The equigranular diorite has sharp contacts with a porphyritic diorite phase (324.50–327.45 m), composed of plagioclase phenocrysts up to 4 mm long in a fine-grained groundmass of plagioclase and granular hornblende with minor interstitial biotite, quartz, potassium feldspar, titanite, apatite and oxide. Equigranular diorite is interlayered with and intruded by a medium- to coarse-grained equigranular granodioritic phase (72.50–137.40 m), composed of plagioclase, k-feldspar, quartz, hornblende and biotite, which has an intrusive contact with the equigranular diorite. A gabbroic phase (417.0–420.0 m) has a gradational contact with the equigranular diorite and is composed of medium-grained equigranular pyroxene and plagioclase. The Deuter Diorite is largely undeformed, but for local mylonite development at ~338 m.

Relationships

The Deuter Diorite contains xenoliths of quartzofeldspathic metasediment at 87.50–91.60 m, amphibolite schist at 83.3–85.0 m and a dolerite at 595–603 m, presumed to be indicative of the host rock of the intrusion. The quartzofeldspathic metasediment has a maximum depositional age of 1855 ± 6 Ma, and is presumably part of the Hutchison Group ((McAvaney and Jagodzinski, 2012). The dolerite is part of the Wade Amphibolite. The Deuter Diorite is intruded by dacite, andesite and basalt dykes of the Gawler Range Volcanics (McAvaney and Jagodzinski, 2012).

Age

Magmatic age 1742 ± 6 Ma (McAvaney and Jagodzinski, 2012).

GLUEPOT GRANITE (NEW NAME)

Derivation of name

Named after Gluepot Dam, Roopena Station, ~15 km northwest of Whyalla, Eyre Peninsula (726417mE, 6353277mN, GDA94, Zone 53).

Distribution

The Gluepot Granite occurs on Roopena Station on northeastern Eyre Peninsula, in the southern Gawler Craton. It is a discrete pluton approximately 25 km long and 6 km wide from Angle Dam to Wild Dog Hill, defined by an elliptical magnetic high in regional TMI imagery. The Gluepot Granite is poorly exposed and dominated by subcrop and deeply weathered granite, with isolated platform exposures and rare granite hills and tors.

Parent

Moola Suite.

Type locality

The type locality for the Gluepot Granite is the small hill with prominent granite tors ~1.3 km north-northwest of Whyalla Dam, Roopena Station, where porphyritic granite can be observed. It comprises the area extending 100 m radially from the point 725210mE, 6367995N, GDA94, Zone 53. A reference locality for gneissic phase of the Gluepot Granite is ~1.7 km NW of Speck Dam,

comprising the area extending 100 m radially from the point 724686mE, 6365829mN, GDA94, Zone 53.

Lithology

The Gluepot Granite is a heterogeneous granite comprising coarse-grained porphyritic granite, medium-grained equigranular granite, as well as late stage pegmatite and aplite phases, and local fabric development. The pluton is dominated by a coarse-grained porphyritic phase composed of large pink tabular to rounded k-feldspar phenocrysts up to 60 mm in diameter, often with Rapakivi rims, in a groundmass of medium- to coarse-grained plagioclase and potassium feldspar, subrounded quartz, biotite, and minor tourmaline.

Along its eastern margin adjacent to its contact with the Moonabie Formation, the pluton contains late stage pegmatite and aplite phases, and is associated with voluminous massive quartz and quartz-tourmaline rock. Pegmatite is composed of very coarse-grained K-feldspar, plagioclase, quartz and tourmaline and is observed intruding the granite as dykes and veins. Aplite is fine-grained and equigranular, and composed of a granular intergrowth of sericitised feldspar and quartz with interstitial tourmaline. The porphyritic granite is also cross-cut by microgranite and aplite dykes of various trends.

A quartz-phyric rhyolite plug approximately 10 m wide within the Moonabie Formation at SE Mount Whyalla, proximal to a pegmatitic margin of the granite, is inferred to be part of the same intrusion. It is composed of round quartz phenocrysts up to 5 mm in diameter and white feldspar phenocrysts up to 3 mm in diameter in a pink fine-grained flow-banded groundmass

The Gluepot Granite also contains minor phases of equigranular k-feldspar-plagioclase-quartz-biotite-tourmaline granite. Localised fabric development within the equigranular granite phase is observed along the western margin of a south-southeast-trending microgranite dyke. The deformed granite is characterised by aligned ovoid quartz crystals (3–5 mm in size) that are elongate parallel to the strike of the microgranite dyke.

Relationships

The Gluepot Granite is observed to intrude the Moonabie Formation 4 km east of Mindrow Dam. At Southeast Mount Whyalla an intrusive contact can be observed between both a pegmatitic phase of the Gluepot Granite and the Moonabie Formation, and a quartz-phyric rhyolite plug equated with the Gluepot Granite.

Age

The Gluepot Granite yielded a CA-TIMS age of 1740 ± 0.6 Ma (McAvaney *et al.*, 2017). A quartz-phyric rhyolite plug intruding the Moonabie Formation at southeast of Mount Whyalla is interpreted to be genetically related to the Gluepot Granite and has a magmatic age of 1752 ± 10 Ma (Fraser and Neumann, 2010).

WADE AMPHIBOLITE (NEW NAME)

Derivation of name

Named after Wade Dam, Uno Station, Eyre Peninsula (662928mE, 6385259mN, GDA94, Zone 53).

Distribution

The Wade Amphibolite occurs as isolated outcrops and subcrops on northeastern Eyre Peninsula on Cooyerdoo, Shirrocoe and Gilles Downs and Corunna stations. Notable outcrops occur in on the northern shore of Lake Gilles and to the west of Iron Duke.

The Wade Amphibolite contains two geochemical groups; an enriched phase and a depleted phase. The depleted Wade Amphibolite crops out 5.7 km southeast of Burkitt Hill, 12.7 km south of Iron Knob (Cooyerdoo Hill), 7.5 km and 5.8 km northwest of Iron Duke and 6.6 km southwest of Iron Duke. It also occurs in form of a dolerite xenolith within the Deuter Diorite in DDH LED001 (drillhole 229988) in the interval 595.0–603.0 m. The enriched Wade Amphibolite crops out ~7.5 km northwest of Iron Duke and 4.3 km southwest of Iron Duke. It is also intersected RDD002 (drillhole 229989) ~15 km southwest of Iron Knob between 308.2–316.4 m, 317.2–379.0 m and 413.0–417.5 m.

Type locality

Small hill 2.1 km south of Lake Gilles Paddock, northern shore of Lake Gilles, Corunna Station, Eyre Peninsula, comprising the area extending 100 m radially from the point 675808mE, 6384534mN, GDA94, Zone 53.

Lithology

The Wade Amphibolite is a fine- to coarse-grained amphibolite composed of hornblende, clinopyroxene, plagioclase, biotite ± K-feldspar ± quartz, with accessory apatite and titanite. The amphibolite ranges from massive recrystallised to gneissic, with alternating hornblende-rich and plagioclase-rich laminae.

Parent

Moola Suite.

Relationships

On the northern shore of Lake Gilles, on Corunna Station, the Wade Amphibolite is observed to intrude c. 2520 Ma leucogranite gneiss of the Sleaford Complex as north-northwest-trending dykes parallel to the regional Kimban structural grain (Reid *et al.*, 2008b). In the vicinity of Iron Duke contact relationships are not exposed, but it is inferred to intrude the c. 3150 Ma Cooyerdoo Granite and Sleaford Complex. In LED001 the Wade Amphibolite occurs as a dolerite xenolith within the Deuter Diorite (McAvaney and Jagodzinski, 2012).

Age

An amphibolite from the Wade Amphibolite from west of Iron Duke yielded a magmatic age of 1736 ± 4 Ma, within error of the age obtained for an unnamed granite of the Moola Suite cropping out within 2 km of the gabbro, which yielded an age of 1737±5 Ma (Reid and Jagodzinski, 2011).

PINBONG SUITE (NEW NAME)

Derivation of name

Named after Little Pinbong Rockhole, northern Eyre Peninsula (544042mE, 6366761mN, GDA94 Zone 53).

Distribution

The Pinbong Suite is the most widespread suite in the Peter Pan Supersuite, occurring on central and southern Eyre Peninsula in the southern Gawler Craton, the Olympic Domain in the eastern Gawler Craton, Coober Pedy Ridge in the northern Gawler Craton and in the central Gawler Craton.

The most extensive outcrops of the Pinbong Suite are on central Eyre Peninsula, including the Middle Camp Granite in the Cleve Hills, the Carappee Granite ~35 km southwest of Kimba, and unnamed occurrences at Poverty Corner, Little Pinbong Rockhole, Peter Pan Platforms, Bascombe Rocks and Fern Quarry. In addition, an unnamed feldspar-quartz-muscovite granite

crops out in the Cleve Hills 2.5 km north and 5 km west of Cleve (map symbol Lzp_2). In central Eyre Peninsula the Pinbong Suite is also intersected in drillholes at the Bungalow Prospect 15 km north-northwest of Cowell in drillholes DDH BUDD 23 (drillhole 255924), DDH BUDD 28 (drillhole 255925) and DDH BUDD 168 (drillhole 277601) (Reid and Jagodzinski, 2011), and in WDDH01 (drillhole 270096) between 649.91–734.40 m at Moseley Nobs, ~35 km north-northwest of Kimba. On southern Eyre Peninsula the Pinbong Suite occurs in outcrop at Seal Point on Flinders Island, at Redbanks, and Cape Carnot (Jagodzinski *et al.*, 2007).

In the eastern Gawler Craton dolerites of the Pinbong Suite are intersected in drillhole DDH RD 160 (681735 mE 6630758 mN) in the Olympic Dam deposit. In the central Gawler Craton the Pinbong Suite is represented by the Paxton Granite, which crops out in the Tarcoola Goldfields, and is intersected in the subsurface at the Perseverance Deposit in drillholes GP078D (drillhole 235049), GP004D (drillhole 207047) and GP028RD (drillhole 235002) (Budd and Fraser, 2004). In the northern Gawler Craton gabbro of the Pinbong Suite is intersected in drillhole DD89LR 22 (drillhole 134168) at the Mount Brady Prospect, Coober Pedy Ridge. In the western Gawler Craton granite, granodiorite and diorite of the Pinbong Suite crops out on the shores of Lake Anthony (Dawson, 2016), and in the Fowler Domain the Colona Gabbro is intersected in drillholes in near Colona Homestead (Daly *et al.*, 1994).

Parent

Peter Pan Supersuite.

Daughter units

Middle Camp Granite (change to previous usage)
Carappee Granite (change to previous definition)
Colona Gabbro (new name)
Paxton Granite (change to previous definition).

Type locality

Refer to daughter units for type localities.

Lithology

The Pinbong Suite is dominated by equigranular foliated, gneissic and migmatitic quartz-feldspar-biotite granite which is generally more plagioclase-rich and biotite-rich compared to the Moola Suite. The suite also contains K-feldspar megacrystic granite, feldspar-quartz-muscovite granite, hornblende-biotite-titanite monzogranite, syenogranite, gabbro and dolerite.

Relationships

The Pinbong Suite was intruded during the 1740–1690 Ma Kimban Orogeny. It varies from weakly foliated to migmatitic. The Pinbong Suite intrudes the Sleaford Complex at Peter Pan Platforms, intrudes the Miltalie Gneiss at Bascombe Rocks, and intrudes the Hutchison Group at Middle Camp and at Poornamookinie Creek, Cleve Hills.

Age

The Pinbong Suite ranges in age from 1735–1700 Ma.

MIDDLE CAMP GRANITE (CHANGE TO PREVIOUS USAGE)

Derivation of name

Named after Middle Camp Homestead, Cleve Hills, central Eyre Peninsula (666465mE, 6272807mN, GDA94, Zone 53). The name was first used by Rutland *et al.* (1981), but was never formally defined.

Distribution

Middle Camp Granite occurs in the Cleve Hills on central Eyre Peninsula, in the Gawler Craton. It crops out approximately 9.5 km west of Cowell on Eyre Peninsula, as a pluton extending 3.5 km across and ~11 km long trending north-northeast.

Parent

Pinbong Suite.

Type locality

Granite outcrops along the track west-northwest of Ullabidinie Reservoir, Middle Camp Station comprising the area extending 100 m radially from the point (669770mE, 6274656mN, GDA94, Zone 53) are here designated as the type locality.

Lithology

The Middle Camp Granite is a fine- to medium-grained, equigranular quartz-k feldspar-plagioclase-biotite foliated granite. The granite is intruded by late-stage aplitic veins and dykes which are subparallel or at a low angle to the foliation in the granite. Both the granite and aplite are ptygmatically folded with axes subparallel to the foliation.

Relationships

The Middle Camp Granite intrudes c. 2000 Ma Warrow Quartzite and the c. 2520–2420 Ma Minbrie Gneiss (Parker *et al.*, 1981), although contacts have been modified by deformation during the Kimban Orogeny.

Age

The Middle Camp Granite has yielded magmatic ages ranging from 1736 ± 6 Ma (Fraser and Neumann, 2010) to 1726 ± 7 Ma (Fanning *et al.* 2007).

CARAPPEE GRANITE (CHANGE TO PREVIOUS DEFINITION)

The Carappee Granite, as defined in Flint *et al.* (1988), is here assigned to the Pinbong Suite.

COLONA GABBRO (NEW NAME)

Derivation of name

Named after Colona Homestead, northwestern South Australia (790428mE, 6497324mN, GDA94, Zone 52).

Distribution

Colona Gabbro is found in approximately 20 drillholes around the Colona Homestead, Fowler Domain, Gawler Craton.

DH number	DH name	Interval (depth from) m	Interval (depth to) m
137274	COL 2	78	80
137290	COL 15	90	96
137291	COL 16	55	56
137292	COL 16D	55	64.25
137293	COL 17	52	54
137297	COL 20D	40	47.5
137298	COL 21	24	28
137299	COL 21D	27.55	52.07
137301	COL 23	64	66
137301	COL 23	64	68
137302	COL 24	38	40
137304	COL 25D	48	62
137305	COL 26	70	74
137311	COL 31	24	26
137312	COL 32	56	60
137313	COL 33	76	78
137320	COL 40	94	96
137323	COL 43D	52	69
137324	COL 44D	52	71.7

Parent

Pinbong Suite.

Type locality

Diamond drillhole COL 43D (DH number 137323), 771569mE, 6527778mN, GDA94, Zone 52, in the interval 52–69 m.

Lithology

The Colona Gabbro comprises layered intermediate to mafic intrusive rocks including granodiorite, tonalite and hornblende gabbros. Complex intermingling and mixing textures between the intermediate to mafic rocks indicate that they are comagmatic (Teasdale, 1997). The body in drill holes Colona 43D and Colona 45D preserves apparent layered cumulate textures, with hornblende-rich gabbroic layers and plagioclase-rich dioritic layers (Daly *et al.*, 1994). The Colona Gabbro has been deformed by amphibolite facies metamorphism and weak to strong tectonic fabrics (Daly *et al.*, 1994).

Relationships

Basement to the Colona Gabbro has not been intersected in drillholes.

Age

The Colona Gabbro has yielded magmatic ages ranging from 1739 ± 6 Ma (Reid, 2015) to 1729 ± 7 Ma (Fanning *et al.*, 2007). Given that these two ages are within error they are interpreted to represent a single unimodal population, and the magmatic age of the Colona Gabbro is estimated at c. 1735 Ma.

PAXTON GRANITE (CHANGE TO PREVIOUS DEFINITION)

The Paxton Granite, as defined in Budd and Fraser (2004), is here assigned to the Pinbong Suite.

MOODY SUITE (CHANGE TO PREVIOUS DEFINITION)

The Moody Suite, as defined in Schwarz (1999), is here assigned to the Peter Pan Supersuite.

MOREENIA MONZOGRANITE (CHANGE TO PREVIOUS USAGE)

Given that the term Adamellite is no longer in common usage, the name Moreenia Adamellite has been replaced by Moreenia Monzogranite.

APPENDIX II. NEW GEOCHEMICAL DATA FOR THE PETER PAN SUPERSUITE

Double-click Appendix_II.xlsx in the Attachments panel to open